Regulation of Toll-like receptor expression
by glucocorticoid-induced leucine zipper and p38 MAPK
in human endothelial cells

Dissertation

zur Erlangung des Grades

des Doktors der Naturwissenschaften

der Naturwissenschaftlich-Technischen Fakultät III

Chemie, Pharmazie, Bio- und Werkstoffwissenschaften

der Universität des Saarlandes

von

Dipl.-Biol. Kerstin Hirschfelder

Saarbrücken

2010

Tag des Kolloquiums: 20.09.2010

Dekan: Prof. Dr.-Ing. Stefan Diebels

Berichterstatter: Prof. Dr. Alexandra K. Kiemer

     Prof. Dr. Markus Hoth

Vorsitz: Prof. Dr. Rolf W. Hartmann

Akad. Mitarbeiterin: Dr. Britta Diesel

Erklärung

Hiermit versichere ich an Eides statt, dass ich die vorliegende Arbeit selbständig und ohne Benutzung anderer als der angegebenen Hilfsmittel angefertigt habe. Die aus anderen Quellen oder indirekt übernommenen Daten und Konzepte sind unter Angabe der Quelle gekennzeichnet.

Die Arbeit wurde bisher weder im In- noch im Ausland in gleicher oder ähnlicher Form in einem Verfahren zur Erlangung eines akademischen Grades vorgelegt.

Saarbrücken, Mai 2010   ……………………………………

                                       (Kerstin Hirschfelder)

Contents

Abbreviations

A	ampere
amp	ampicilline
ANP	atrial natriuretic peptide
AP-1	activator protein 1
APS	ammonium persulfate
ATP	adenosin-5'-triphosphate
BHQ1	black hole quencher 1
bp	base pair
BSA	bovine serum albumine
cDNA	complementary DNA
Co	control
DMSO	dimethyl sulfoxide
DNA	desoxyribonucleic acid
DNase	desoxyribonuclease
dNTP	desoxynucleosidtriphosphate
ds	double stranded
DTT	dithiothreitol
EDTA	ethylenediamine-N,N,N,N'-tetra acid
EGTA	ethylene glycol tetraacetic acid
EMSA	electrophoretic mobility shift assay
f	femto (10^{-15})
FACS	fluorescence activated cell sorting
FAM	6-carboxy-fluorescein
FCS	fetal calf serum
g	gram
GFP	green fluorescent protein
GILZ	glucocorticoid-induced leucine zipper
h	hour
HDL	high density lipoprotein
HUVEC	human umbilical vein endothelial cells
IFN	interferon
IκB	inhibitory protein kappa B

kDa	kilodalton
L	liter
LB	Luria-Bertani
LDL	low density lipoprotein
LPS	lipopolysaccharide
m	mili (10^{-3})
M	molar
MAPK	mitogen-activated protein kinase
MCP-1	monocyte chemoattractant protein 1
min	minute
mRNA	messenger ribonucleic acid
MyD88	myeloid differentiation factor 88
µ	micro (10^{-6})
n	nano (10^{-9})
NF-κB	nuclear factor kappa B
PAGE	polyacrylamide gel electrophoresis
PBS	phosphate buffered saline
PBS^{+}	phosphate buffered saline with calcium and magnesium ions
PBST	phosphate buffered saline with Tween 20
PCR	polymerase chain reaction
%	per cent
PMSF	phenylmethylsulfonyl fluoride
RNA	ribonucleic acid
RNase	ribonuclease
R-PE	R-phycoerythrin
rpm	rotation per minutes
RT	reverse transcriptase
SDS	sodium dodecyl sulfate
sec	second
SEM	standard error of mean
ss	single stranded
TBE	Tris-boric acid-EDTA buffer
TE	Tris-EDTA buffer
TEMED	N,N,N',N'-tetramethyl ethylenediamine
TLR	toll-like receptor

TNF-α	tumor necrosis factor alpha
U	unit
UV	ultra violet
V	volt
[v/v]	volume per volume
[w/v]	weight per volume
xg	fold gravitational force
YFP	yellow fluorescent protein

Abstract

Inflammatory actions in the pathophysiology of atherosclerosis are characterized by an activation of the endothelium as well as an increased expression of Toll-like receptor (TLR) 2. Aim of this work was to decipher the roles of glucocorticoid-induced leucine zipper (GILZ) and p38 mitogen-activated protein kinase (MAPK) in endothelial TLR expression. A pronounced constitutive expression of the anti-inflammatory mediator GILZ was found in human umbilical vein endothelial cells (HUVEC), which was downregulated under inflammatory conditions. This GILZ downregulation paralleled by TLR2 upregulation was confirmed in human atherosclerotic vessels. Mechanistic examinations showed that GILZ decay led to a nuclear translocation and activation of the transcription factor NF-κB resulting in upregulation of TLR2 expression. Pharmacological inhibition of p38 MAPK as well as overexpression of dominant negative p38α MAPK showed a positive involvement of p38 MAPK in inflammatory TLR2 expression. This p38 MAPK-mediated action, however, was independent of GILZ. Taken together, this work provides evidence for a role of GILZ and p38 MAPK in the regulation of inflammatory TLR expression in human endothelial cells and provides insides for a better understanding of inflammatory actions in atherosclerosis.

Die Pathophysiologie der chronisch entzündlichen Erkrankung Arteriosklerose ist durch eine Aktivierung des Endothels sowie durch eine erhöhte Expression des Toll-like Rezeptors (TLR) 2 charakterisiert. Ziel dieser Arbeit war, eine mögliche Beteiligung des Glucocorticoid-induzierten Leucin Zippers (GILZ) sowie der p38 Mitogen-aktivierten Proteinkinase (MAPK) bezüglich der Regulation der endothelialen TLR Expression zu untersuchen. In Endothelzellen, isoliert aus humanen Nabelschnurvenen (human umbilical vein endothelial cells, HUVEC), wurde eine konstitutive Expression des anti-inflammatorischen Mediators GILZ nachgewiesen, die durch inflammatorischen Stimulus erniedrigt wurde. Diese verringerte GILZ Expression bei gleichzeitiger Induktion von TLR2 konnte in humanen arteriosklerotischen Gefäßen bestätigt werden. Mechanistische Untersuchungen zeigten, dass die Abwesenheit von GILZ zu einer nukleären

Translokation sowie zu einer Aktivierung des Transkriptionsfaktors NF-κB führt, die wiederum eine Erhöhung der TLR2 Expression zur Folge hat. Für p38 MAPK wurde durch pharmakologische Inhibierung sowie Überexpression dominant negativer p38α MAPK ebenfalls eine Beteiligung an der Expression von TLR2 gezeigt, die zudem unabhängig von GILZ war. Zusammenfassend zeigt diese Arbeit, dass sowohl GILZ als auch p38 MAPK eine Rolle in der Expression von TLR2 humanen Endothelzellen spielen und trägt daher zu einem besseren Verständnis der entzündlichen Prozesse in der Arteriosklerose bei.

1. Introduction

1.1   Atherosclerosis

1.1.1 Overview

Atherosclerosis is an inflammatory cardiovascular disease, which can lead to myocardial infarctions or strokes. To date, cardiovascular diseases are the main cause of morbidity and death in the Western world (Klingenberg & Hansson, 2009). Atherosclerosis is known to be a complex alteration of medium and large size arteries, which is characterized by endothelial dysfunction and accumulation of lipids and inflammatory cells in the vascular wall (Roy *et al.*, 2009). Herein, the inflammatory activation of endothelial cells plays a central role (Erridge, 2008). Identified risk factors are environmental factors, such as Western high-fat diet, smoking and lack of exercise, but also factors with a genetic component, such as elevated levels of low-density lipoproteins (LDL), elevated blood pressure, diabetes, or obesity (Lusis, 2000).

1.1.2 Constitution of vessels

The inner cell layer in all vessels is represented by endothelial cells forming a semi-permeable barrier. Medium and large size arterial vessels are in general composed of further three layers: tunica intima, tunica media, and tunica adventitia (dela Paz & D'Amore, 2009). The first layer, the tunica intima, is formed by connective tissue. The tunica media as the second layer consists of smooth muscle cells and connective tissue. The third layer, the tunica adventitia, is formed by connective tissue again. In contrast to veins, arteries exhibit two additional laminae: one between tunica interna and media, which is termed internal elastic lamina, and another one between tunica media and tunica adventitia, which is termed external elastic lamina.

1.1.3 Development of atherosclerotic lesions

The activation of arterial endothelial cells probably *via* oxidized low density lipoproteins (LDL) is suggested as on of the first steps of an atherosclerotic plaque development (Hansson, 2009). This endothelial activation leads to the expression of adhesions molecules, chemokines and cytokines, which results in recruitment of monocytes and to a lesser extent T-cells and their transmigration into the

subendothelial intima (Erridge, 2009; Bevilacqua, 1993) (Figure 1). The monocytes differentiate into macrophages, which take up lipids and cholesterol and become foam cells (Ross, 1993). These foam cells are less able than monocytes or macrophages to move away from the intima. The lesion stage, at which no plaque extends into the vessel wall yet, is termed fatty streak. Over many years, more and more monocytes are recruited, which also become foam cells. Because of their high lipid uptake, they become necrotic and leave crystalline cholesterol and cell debris. In this fashion, the plaque increases and extends into the vessel wall. Smooth muscle cells migrate into the intima and form a protective cap over the lesion (Ross, 1993). At this stage, the plaque is also stabilized by emplacement of collagen and calcium. By that the plaque can keep on growing, which either leads to stenosis or clinical silenence for many years. A further inflammatory event can rupture a vulnerable plaque, which results in formation of a thrombus. This thrombus, in turn, causes myocardial infarctions or strokes (Hansson, 2005).
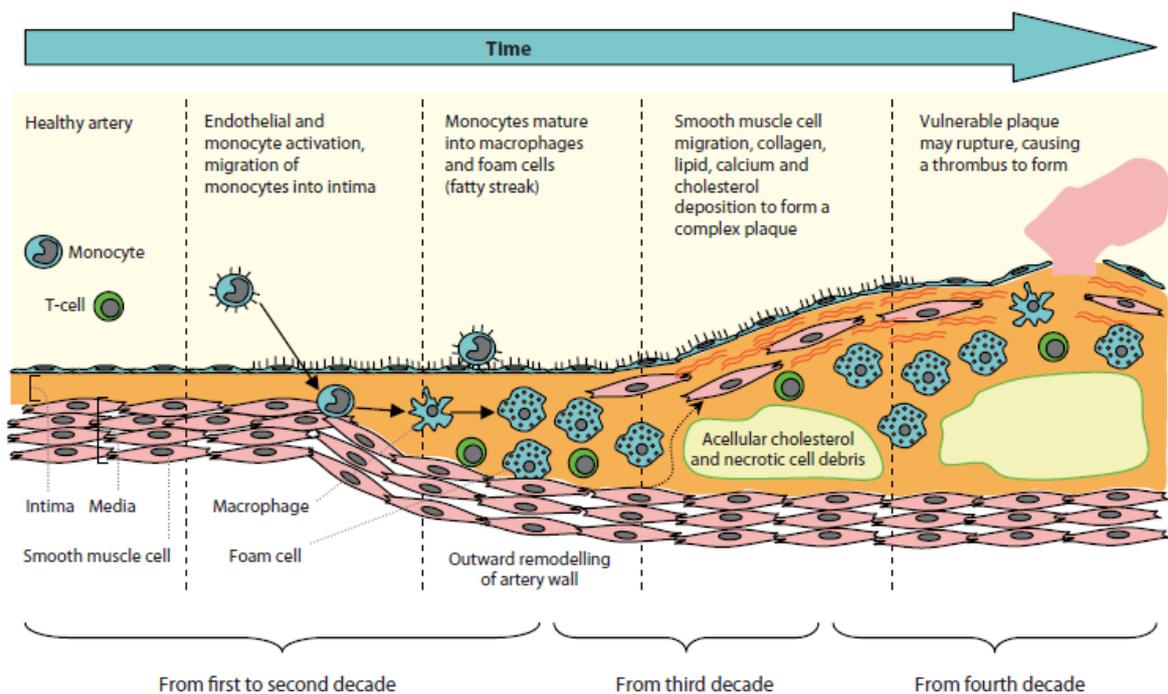
Figure 1: Development of an atherosclerotic plaque. Adapted from Erridge, 2009.

1.2 Toll-like receptors

1.2.1 History

The protein Toll was first described in 1984 as an essential receptor controlling the dorso-ventral polarization in *Drosophila melanogaster* during embryogenesis (Anderson & Nüsslein-Volhard, 1984). Twelve years later, it was found that the Toll receptor also functions in immune responses of the fruit fly (Lemaitre *et al.*, 1996). In 1997, a human homologue of the *Drosophila* Toll protein was identified and termed Toll-like receptor (Medzhitov *et al.*, 1997). Actually, ten human and thirteen mouse TLRs have as yet been identified, which recognize a broad spectrum of ligands (Lundberg & Hansson, 2010). TLRs are extra- and intracellularly expressed in e.g. macrophages, dendritic, epithelial, and endothelial cells. These pattern recognition receptors represent an important system, which alerts the host to numerous pathogens and regulate the activation of both innate and adaptive immunity.

1.2.2 Ligands

As shown in Figure 2, human TLRs recognize a broad spectrum of pathogen-associated molecular patterns (PAMPs), which are characteristic for bacterial and viral pathogens as well as for fungi and protozoa (den Dekker *et al.*, 2010). While TLRs 1, 2, 4, 5, 6 and 10 are located in the outer cell membrane, TLRs 3, 7, 8, 9 function in membranes of endosomal compartments. All TLRs operate as homodimers except for TLR2, which also forms heterodimeric complexes with TLR1 or TLR6 (Lundberg & Hansson, 2010; Kawai & Akira, 2006).
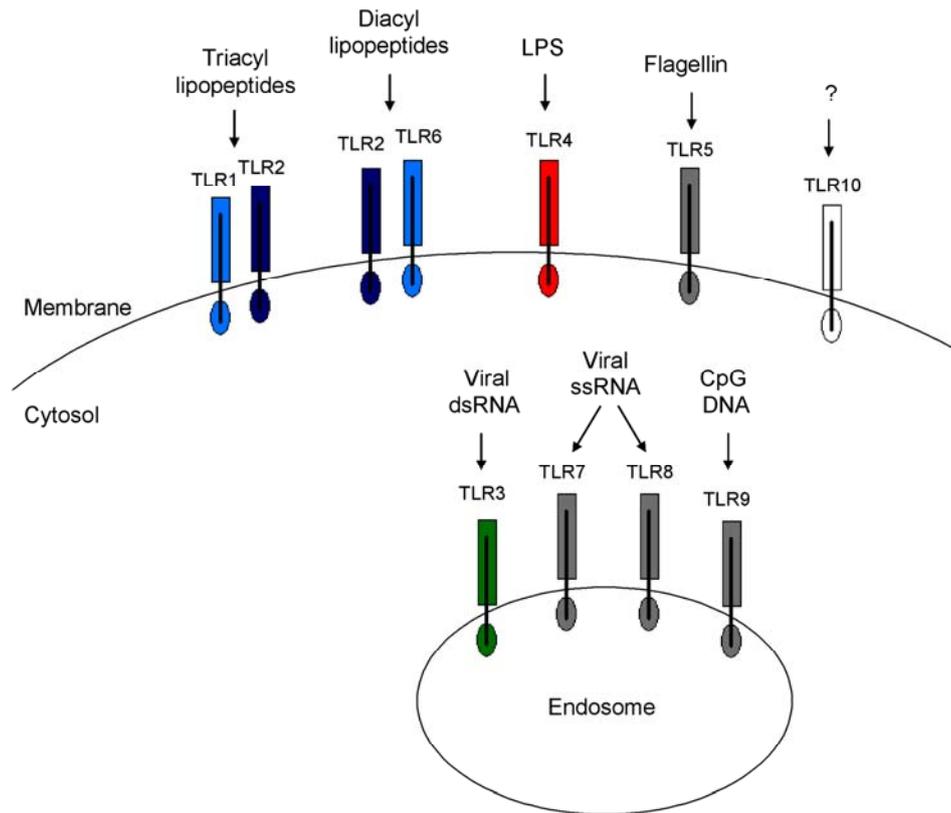
Figure 2: Overview about TLR localisation and ligands. Abbreviations: ds=double stranded, LPS=lipopolysaccharide, ss=single stranded, TLR=toll like receptor.

TLRs 1, 2 and 6

In co-operation with TLR1, TLR2 recognizes triacylated bacterial lipoproteins from Gram-negative bacteria or mycobacteria, as well as the synthetic compound Pam$_3$CSK$_4$. In co-operation with TLR6 diacyl-lipopeptides from Gram-positive bacteria, zymosan from yeast or diacylated mycoplasmal lipopeptides, termed macrophage-activating lipopeptide 2 kDa (MALP-2), are recognized by TLR2 (Lundberg & Hansson, 2010; Kawai & Akira, 2006; Takeuchi *et al.*, 2002). These TLR2 heterodimerisations allow the recognition of the largest number of pathogen structures compared to other TLRs, but do not necessarily lead to a different intracellular signalling (Farhat *et al.*, 2007). TLR2 heterodimers already exist before they recognize ligands, which is in contrast to the ligand-induced heterotypic assembling of TLR2/TLR6 with the scavenger receptor CD36 (Triantafilou *et al.*, 2006). Additionally, a homodimerisation of TLR2 for recognition of lipoteichoic acid

(LTA) has also been described (Beutler, 2004). Because of its large spectrum of ligands, TLR2 plays an especially important role in the defence of pathogens.

TLR4

TLR4 is the receptor for lipopolysaccharide (LPS) from Gram-negative bacteria, but also for other bacterial toxins or viral structures (Lundberg & Hansson, 2010; Björkbacka, 2006). Recently, it has been demonstrated that TLR4 can be part of a heterotrimeric complex containing TLR4, TLR6 and CD36, when oxidized LDL and amyloid-β peptide derived from the proteolytic cleavage of the amyloid precursor protein are recognized by CD36 (Stewart *et al.*, 2010). Besides the recognition of exogenous ligands, TLR4 as well as TLR2 are also suggested to recognize endogenous ligands, which can be found at sites of inflammation, such as stress-inducible heat shock proteins or components of the extracellular matrix (Lundberg & Hansson, 2010).

TLRs 3, 5, 7, 8, 9 and 10

In contrast to TLR2 and TLR4, all other TLRs recognize only one type of pathogen structure. Ligand for TLR3 is viral double-stranded RNA (dsRNA) and for TLR7 as well as TLR8 viral single-stranded RNA (ssRNA). Bacterial flagellin is recognized by TLR5, while hypomethylated CpG motifs of microbial DNA are ligands for TLR9 (Lundberg & Hansson, 2010). For TLR10 no ligand has as yet been identified.

1.2.3 TLR signalling

The recognition and binding of ligands triggers a signal transduction finally leading to an inflammatory reaction including expression of inflammatory cytokines, such as tumor necrosis factor α (TNF-α), interleukins (IL) and interferons (IFN). TLRs represent type 1 transmembrane receptors. The extracellular part consists of leucine rich repeats (LRR), which are responsible for the pattern recognition. In contrast, the intracellular part exhibits a Toll/IL-1 receptor (TIR) signalling domain, which is required for the recruitment of adaptor proteins also containing a TIR domain (Beutler, 2004). The key mediator in TLR-signalling is an adapter molecule termed myeloid differentiation factor 88 (MyD88). TLR signal transduction can be distinguished between MyD88-dependent and -independent. As shown in Figure 3,

all TLRs with the exception of TLR3 share MyD88-dependent signalling, while TLR4 can also signal MyD88-independent (Mitchell *et al.*, 2007; Kawai & Akira, 2006).
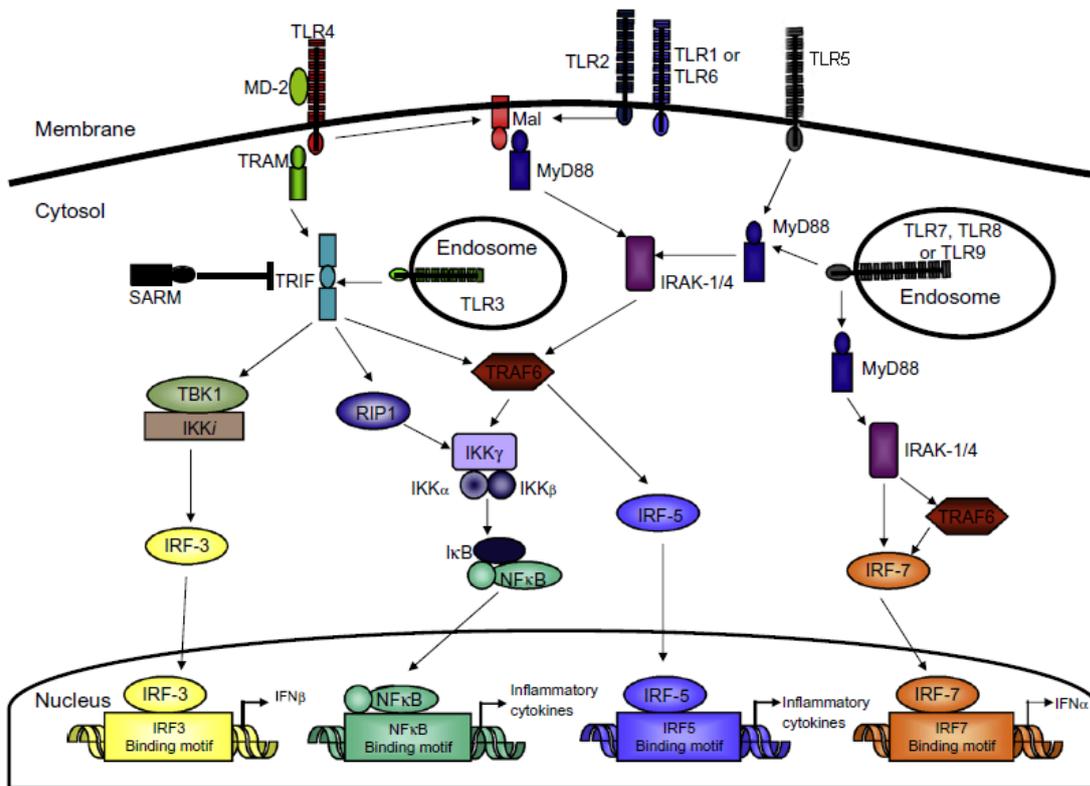
Figure 3: Overview about MyD88-dependent and -independent TLR-signalling. Modified after Jenkins & Mansell, 2010. Abbreviations: IFN=interferon, IκB=inhibitory protein kappa B, IKK= inhibitor kappa B kinase, IRAK=interleukin 1 receptor associated kinase, IRF=interferon-regulatory factor, Mal=MyD88-adapter-like, MyD88=myeloid differentiation factor 88, MD-2=myeloid differentiation factor, NF-κB=nuclear factor kappa B, RIP=receptor-interacting protein, SRAM=sterile alpha and Toll/interleukin 1 receptor motif containing, TAK=transforming growth factor-beta activated kinase, TBK=TRAF family member-associated NF-κB activator binding kinase, TLR=toll-like receptor, TRAF=tumor necrosis factor associated receptor, TRAM=TRIF-related adapter protein, TRIF=Toll/interleukin 1 receptor domain-containing adapter inducing IFN-β.

MyD88-dependent signalling

As shown in Figure 3, TLRs 5, 7, 8 and 9 associate directly with MyD88, while in TLR2 and TLR4 signalling MyD88-adapter-like (Mal, also known as Toll/IL-1 domain-containing adaptor protein (TIRAP)) is necessary for MyD88 recruitment. Through binding to MyD88, members of the IL-1 receptor associated kinase (IRAK) family are recruited. IRAK1 is phosphorylated by IRAK4 and associates subsequently with

tumor necrosis factor receptor associated factor 6 (TRAF6). TRAF6 is ubiquitinylated by itself, which results in the activation of the inhibitor κB kinase (IKK) complex consisting of the IKKs α, β and γ. This leads to the phosphorylation and ubiquitin-mediated degradation of the NF-κB inhibitor IκB, and NF-κB can translocate into the nucleus and induce inflammatory gene expression. Once activated, TRAF6 can also activate a transcription factor termed interferon-regulatory factor 5 (IRF-5), which also induces inflammatory gene expression (Jenkins & Mansell, 2010).

Besides this signalling cascade, the mitogen activated protein kinase (MAPK) cascades can be induced by transforming growth factor (TGF)-beta activated kinase 1 (TAK1), which in turn is activated by TRAF6. Phosphorylation of p38 MAPK and c-Jun NH2-terminal kinase (JNK) *via* TAK1 leads to the activation of the transcription factor activator protein 1 (AP-1) and inflammatory gene expression (Hong-Geller *et al.*, 2008; Kawai & Akira, 2006).

In plasmacytoid dendritic cells, TLRs 7, 8 and 9 signalling has been described to activate IRF-7 downstream to TRAF6 leading to IRF-7 nuclear translocation and expression of IFN-γ (Jenkins & Mansell, 2010).

MyD88-independent signalling

MyD88-independent signalling shares the TIR domain-containing adapter inducing IFN-β (TRIF) (Figure 3). In contrast to TLR3 signalling, TLR4 signalling additionally needs the TRIF-related adapter protein (TRAM) as well as the association of TLR4 with the myeloid differentiation protein 2 (MD-2). After ligand recognition, two different TRIF-dependent pathways are known. One pathway leads to TRIF/TRAF6 and/or TRIF/receptor-interacting protein 1 (RIP1) interaction, which results in the activation and nuclear translocation of NF-κB *via* the IKK complex. In addition, TRIF/TRAF6 can further activate IRF-5. The second pathway activates the TRAF family member-associated NF-κB activator (TANK)-binding kinase 1 (TBK1), which interacts with IKK-*i*. This kinase phosphorylates the transcription factor IRF-3 leading to nuclear translocation and activation of IFN-β transcription (Jenkins & Mansell, 2010).

A negative regulation of TLR3 signalling is facilitated by the adapter molecule sterile alpha and TIR motif containing (SARM) *via* inhibition of TRIF (Jenkins & Mansell, 2010).

1.3   TLRs and atherosclerosis

TLRs seem to play an important role in the development of atherosclerosis (Erridge, 2008; Björkbacka, 2006; Michelsen & Arditi, 2006). Mainly TLR2 and TLR4 are overexpressed in human atherosclerotic lesions of carotid arteries when compared to normal internal mammary arteries (Edfeldt *et al.*, 2002). This TLR overexpression was prevalently observed in endothelial cells and macrophages. In addition, TLR2 and TLR4 overexpression was correlated with nuclear translocation of the NF-κB subunit p65 in the same cells. These results were confirmed by mouse models showing that deletion of TLR2 led to a diminished progression of atherosclerotic lesions (Madan & Amar, 2008; Tobias & Curtiss, 2008; Liu *et al.*, 2008; Mullick *et al.*, 2005), while blood concentrations of the inflammation marker monocyte chemoattractant protein 1 (MCP-1) were diminished (Liu *et al.*, 2008). Similarly, deletion of MyD88, which is necessary for TLR2 signalling, and deletion of TLR4 led to diminished atherosclerosis (Björkbacka *et al.*, 2004; Michelsen *et al.*, 2004). Inversely, stimulation with the TLR2 ligand Pam_3CSK_4 increased the development of atherosclerotic lesions (Schoneveld *et al.*, 2005; Mullick *et al.*, 2005).

As described above, the development of atherosclerosis is dependent on endothelial activation. In mouse models, the absence of TLR2 in both non-bone marrow cells (vascular cells) and bone marrow cells (non-vascular cells) has been observed to contribute to lesion progression (Mullick *et al.*, 2005).

1.4   Importance of the endothelium in inflammatory actions

Under physiological conditions the endothelium exerts many important functions, which are pivotal for biological homeostasis (Sima *et al.*, 2009; Aird, 2007). Besides functions in vascular tone regulation, endothelial cells are involved in anti-inflammatory as well as in anti-coagulative actions. Herein, the expression of surface molecules is limited at a minimum to allow an unobstructed blood flow. Due to its direct contact to the blood, the endothelium represents an important target for numerous inflammatory stimuli and is therefore involved in defence mechanisms. As mentioned above, recognition of pathogens by TLRs leads to a signal cascade inducing the expression of pro-inflammatory cytokines, such as TNF-α, IL-1β and

IFN-γ as well as of other inflammatory mediators (Beutler, 2004). This endothelial cell activation leads to an increased permeability of the endothelium, which allows subendothelial migration of leukocytes.

The endothelium is also involved in the regulation of cholesterol and lipid homeostasis. Under pathophysiological conditions, such as hyperlipidaemia and hyperglycemia, alterations of endothelial functions precede the development of atherosclerotic lesions and manifestation of this inflammatory disease (Sima *et al.*, 2009).

1.5   Tumor necrosis factor α (TNF-α)

1.5.1   Overview

Tumor necrosis factor α (TNF-α) is a potent cytokine expressed mainly by macrophages and monocytes, but also by lymphocytes, fibroblasts, keratinocytes, endothelial and neuronal cells (Wajant *et al.*, 2003; Baud & Karin, 2001). It belongs to a family of peptide mediators consisting of 19 cytokines, such as CD40 or Fas ligand. TNF-α has been characterized to be produced after cell stimulation by pathogen recognition or other inflammatory signals and to exert a large spectrum of bioactivities. Thus, TNF-α influences innate and adaptive immunity, cell proliferation and apoptosis in different cell types such as endothelial cells, monocytes, and smooth muscle cells (Pugin *et al.*, 1995; Heller & Kronke, 1994; Popa *et al.*, 2007).

1.5.2   TNF-α signalling

There are two structurally distinct receptors responsible for the biological activities of TNF-α: TNFR1 and TNFR2. With exception of erythrocytes, all cell types carry these receptors in their membrane (Popa *et al.*, 2007). Binding of TNF-α to TNFR1 results in TNFR1 association with the TNF receptor-associated death domain protein (TRADD). This binding can either result in apoptotic signalling *via* the Fas-associated death domain (FADD) or in pro-inflammatory signalling *via* TRAF2 and RIP, which finally leads to an activation of the transcription factors AP-1 and NF-κB (Popa *et al.*, 2007; Aggarwal, 2003; Karin *et al.*, 1997; Barnes & Karin, 1997). In contrast, TNFR2 is only involved in pro-inflammatory actions *via* TRAF2 (Popa *et al.*, 2007). It has

been supposed, however, that crosstalk of both receptors is important for complete cell response after TNF-α stimulation (Aggarwal, 2003).

1.5.3 TNF-α in atherosclerosis

The production and secretion of TNF-α by activated monocytes and macrophages represents an early event in the development of atherosclerosis, which in turn leads to the activation of endothelial cells. Activated endothelial cells also express TNF-α resulting in the amplification of inflammatory actions. The plasma levels of TNF-α are associated with the degree of early atherosclerosis (Skoog *et al.*, 2002). Therefore, the blockade of TNF-α has been discussed as an emerging therapy for the treatment of atherosclerosis (Klingenberg & Hansson, 2009). This discussion is supported by findings that blockade of TNF-α by monoclonal antibodies led to increased high density lipoprotein (HDL) plasma concentrations, while atherogenic indices were decreased (Popa *et al.*, 2007).

1.6   Glucocorticoid-induced leucine zipper (GILZ)

1.6.1 Overview

The glucocorticoid–induced leucine zipper (GILZ, synonymous TSC22D3) was first described in 1997 as an anti-inflammatory protein inducible by glucocorticoids (D'Adamio *et al.*, 1997). The human GILZ gene encodes a 135 amino acids (aa) protein with a molecular weight of 15 kDa (Cannarile *et al.*, 2001). Because of its heptad repeat of leucine residues in the central leucine zipper (LZ) domain (aa 76-97), GILZ belongs to the leucine zipper family (Landschulz *et al.*, 1988; Alber, 1992). The repeats are necessary to promote homodimerisation of GILZ proteins, by which GILZ becomes functionally active (Figure 4). The N-terminal domain (NTD, aa 1-75) exhibits no obvious DNA-binding sequence, which is in contrast to other leucin zipper family members (Busch & Sassone-Corsi, 1990; Vinson *et al.*, 1989). The C-terminal domain (aa 98-137) offers a region rich in proline (P) and glutamic acid (E; PER). Other GILZ isoforms have been found in murine cells and rat tissues (Bruscoli *et al.*, 2010; Soundararajan *et al.*, 2007). However, the existence of GILZ isoforms has as yet not been confirmed in human tissues.

```
¹MNTEMYQTPMEVAVY
QLHNFSTSFFSSLLGGD
VVSVKLDNSASGASVVA
LDNKIEQAMDLVKNHLM
YAVREEVEV⁷⁶LKEQIRE
LLEKNSQLERENTLL⁹⁸K
TLASPEQLEKFQSRLSP
EEPAPEAPETPETPEAP
GGSAV
```
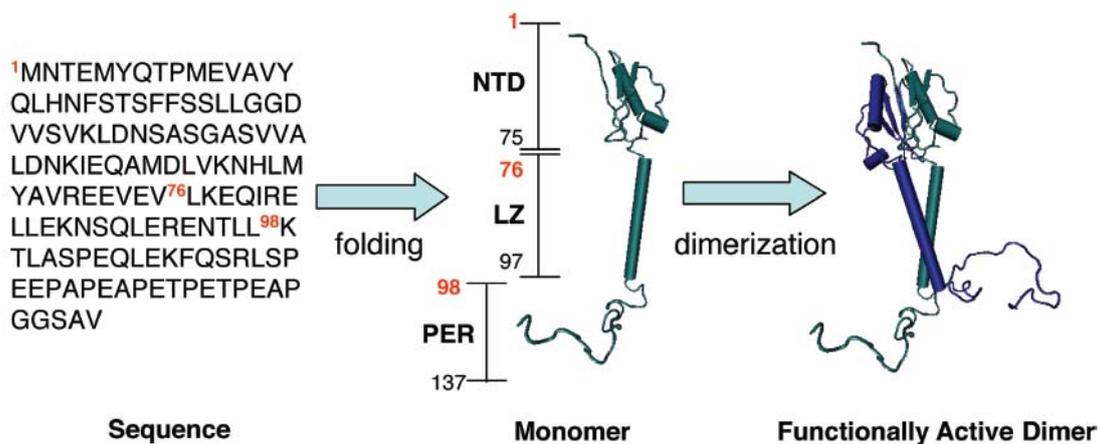
Figure 4: Correlation of GILZ protein sequence and GILZ protein dimerisation. Adapted from Di Marco *et al.*, 2007. Abbreviations: NTD=N-terminal domain, LZ=leucine zipper, PER=proline (P) and glutamic acid (E) region.

1.6.2 GILZ in inflammation

Expression of GILZ has been described in different cell types, such as in human macrophages, T-cells, dendritic cells, mast cells, and human airway epithelial cells (Ayroldi & Riccardi, 2009). However, there are no data for basal expression in endothelial cells as yet. As mentioned above, GILZ induction by glucocorticoids leads to its binding to and inhibition of the transcription factor NF-κB, which subsequently results in a diminished transcription of cytokines (Ayroldi & Riccardi, 2009; Di Marco *et al.*, 2007). The GILZ homodimer additionally interferes with the AP-1 components c-Jun and c-Fos and prevents their binding to DNA (Mittelstadt & Ashwell, 2001). GILZ mRNA as well as protein levels are attenuated by cytokines in cultured epithelial cells (Eddleston *et al.*, 2007). This is confirmed by findings that GILZ is downregulated or even absent in inflammatory diseases, such as chronic rhinosinusitis, Crohn disease, or tuberculosis (Zhang *et al.*, 2009; Berrebi *et al.*, 2003).

1.7 p38 mitogen-activated protein kinase (p38 MAPK)

1.7.1 Overview

The p38 mitogen-activated protein kinase (p38 MAPK) is a member of the MAPK family and exhibits a molecular weight of 38 kDa. MAPKs are expressed in most tissues and are involved in cell proliferation, differentiation, and apoptosis. Four isoforms of p38 MAPK have been identified, which partially exhibit different functions (Zhou *et al.*, 2008; Pramanik *et al.*, 2003): p38α (also known as SAPK2a, RK, CSBPs, Mxi2, Mpk2) (Lee *et al.*, 1994), p38β (SAPK2b) (Jiang *et al.*, 1996; Stein *et al.*, 1997), p38γ (SAPK3) (Li *et al.*, 1996) and p38δ (SAPK4) (Jiang *et al.*, 1997; Wang *et al.*, 1997). The expression levels of the single isoforms are different in monocytes, macrophages, neutrophils, and endothelial cells. The most abundant isoforms in umbilical vein endothelial cells are p38α and p38β (Hale *et al.*, 1999).

1.7.2 Activation of p38 MAPK

All p38 MAPK isoforms share a high sequence homology and the specific phosphorylation motif threonine-glycine-tyrosine (TGY) in the kinase subdomain VIII (Raingeaud *et al.*, 1995). p38 MAPK is phosphorylated by DNA damage, heat, and osmotic shock, as well as by pro-inflammatory stimuli, such as bacterial LPS or cytokines (Kiemer *et al.*, 2002b; Takada & Aggarwal, 2004; Raingeaud *et al.*, 1995; Lee *et al.*, 1994; Weber *et al.*, 2003; Hashimoto *et al.*, 2001). The dual phosphorylation of threonine 180 and tyrosine 182 by pro-inflammatory cytokines, such as TNF-α or IL-1, is performed by upstream kinases termed MAPK-kinases (MKK). MKKs themselfs are phosphorylated by MKK-kinases (MKKK), which are activated by extracellular stimuli (Chen *et al.*, 2001; Herlaar & Brown, 1999). Downstream targets of phosphorylated p38 MAPK are other members of the MAPK family or transcription factors, such as AP-1 resulting in altered gene expression (Chen *et al.*, 2001; Herlaar & Brown, 1999).

1.7.3 Role in inflammation

Members of the MAPK family function in many physiological and pathophysiological processes (Pearson *et al.*, 2001). The p38 MAPK pathway especially has been described as a central regulator of inflammatory actions (Zhang *et al.*, 2007). The

induction of important inflammatory mediators, such as the pro-inflammatory cytokines TNF-α, IL-1β, IL-6 and IL-8, the chemokine MCP-1, the adhesion molecules vascular cell adhesion molecule 1 (VCAM-1) and intercellular adhesion molecule 1 (ICAM-1), as well as cyclooxygenase 2 (COX-2) has been shown to be dependent on p38 MAPK signalling (Zhang *et al.*, 2007). Therefore, inhibition of p38 MAPK represents a pharmacological target in inflammatory diseases (Kumar *et al.*, 2003; Lee *et al.*, 1999)

Over the last years it has become obvious that p38 MAPK regulates the expression of inflammatory proteins also on posttranscriptional level (Khabar, 2005; Kracht & Saklatvala, 2002).

1.8   Monocyte chemoattractant protein 1 (MCP-1)

1.8.1 Overview

Monocyte chemoattractant protein 1 (MCP-1, synonymous CCL2) is a key chemokine regulating the recruitment and migration of monocytes. To date, more than fifty human chemokines and twenty chemokine receptors have been identified (Deshmane *et al.*, 2009). Based on the number and location of the cysteine (C) residues at the N-terminus of the molecules, chemokines can be classified into four subfamilies. MCP-1 is a member of the CC-family and functions as an inflammatory chemokine (Robinson *et al.*, 1989). The expression of chemokine is induced by pro-inflammatory cytokines. Chemokines bind to specific cell surface transmembrane receptors, which are coupled with heterotrimeric G-proteins. The receptor for MCP-1, CCR2, is expressed on macrophages, immature dendritic cells, and lymphocytes (Ruffini *et al.*, 2007). Its presence on endothelial cells has also been described (Gupta *et al.*, 1998). MCP-1 itself is produced by many cell types, e.g. fibroblasts, epithelial cells, monocytes, macrophages, and endothelial cells (Deshmane *et al.*, 2009).

1.8.2 MCP-1 in inflammation

By inflammatory stimulus, such as treatment with TNF-α, MCP-1 is highly upregulated in endothelial cells (Weber *et al.*, 2003; Rollins *et al.*, 1990). Moreover,

MCP-1 expression has been suggested to be a general marker for inflammatory activation of endothelial cells (Szmitko *et al.*, 2003). In addition, there is strong evidence that MCP-1 is overexpressed in atherosclerotic plaques and increased in plasma levels of patients with cardiovascular diseases suggesting an important role of MCP-1 in the development and progression of atherosclerosis (Sima *et al.*, 2009; Niu & Kolattukudy, 2009; Liu *et al.*, 2008; Ikeda *et al.*, 2002).

1.9   Aim of this work

The pathophysiology of the chronic disease atherosclerosis is characterized by increased expression of the pattern recognition receptors TLR2 and TLR4. The mechanisms, however, determining the expression of these TLRs have as yet been unknown. Moreover, there are no data in the literature how the expression of the TLR2 co-receptors TLR1 and TLR6 is regulated.

Due to their physiological character and localisation, endothelial cells are significantly involved in inflammatory processes. The vascular endothelium forms a barrier between the blood as a carrier of circulating pathogens and the interstitium. Therefore, endothelial cells have to be able to recognize pathogens and to trigger a signalling leading to pathogen elimination. To date, the best available model to understand the development and progression of atherosclerosis are endothelial cells isolated from human umbilical vein (HUVEC). They have been characterized to be highly comparable to the *in vivo* situation and are available in sufficient quantity.

Aim of this work was to clarify, whether the anti-inflammatory mediator GILZ as well as the immunoregulatory p38 MAPK are involved in the regulation of endothelial TLR expression.

Concerning the role of these two proteins the following questions had to be answered:

1. Role of GILZ in inflammatory TLR expression
    a) Is GILZ expressed in endothelial cells?
    b) Is GILZ expression regulated under inflammatory conditions?
    c) Does GILZ affect endothelial TLR expression?
    d) Can a link between GILZ and TLR2 be observed in atherosclerotic vessels?
    e) What are the mechanisms involved in GILZ-dependent regulation of TLR expression?

2. Role of p38 MAPK in inflammatory TLR expression

    a) Is p38 MAPK involved in TLR expression?

    b) Which p38 MAPK isoform regulates TLR expression?

    c) Are p38 MAPK-mediated actions connected to GILZ expression?

2. Materials and Methods

2.1   Materials

Endothelial cell growth medium was purchased from Promocell (Heidelberg, Germany), Earle's Medium 199, Ham's 12, fetal calf serum gold (FCS), glutamine, penicilline/streptomycine and trypsine were from (PAA, Cölbe, Germany). Kanamycine, ampicilline, tumor necrosis factor α (TNF-α), dexamethasone, atrial natriuretic peptide (ANP), poly(deoxyinodinic-deoxycytidylic) acid sodium salt (poly(dIdC)), phosphatase inhibitor cockatil I and II were purchased from Sigma (Taufkirchen, Germany). SB203580 was from Jena Bioscience (Jena, Germany), and protease inhibitor was purchased from Roche (Mannheim, Germany). H_2O and TE buffer for molecular biology were obtained from Applichem (Darmstadt, Germany).

The antibody against von Willebrand factor was purchased from AbD Serotec (Wiesbaden, Germany). For Western blot analysis and immunofluorescence anti-GILZ, anti-p65, anti-p50, anti-IκBα, anti-p38 MAPK, and anti-TLR6 antibodies were purchased from SantaCruz (Heidelberg, Germany), anti-cRel, anti-p38 MAPK and anti-p-p38 MAPK antibodies were from CellSignaling (Frankfurt/Main, Germany). The IRdye-labeled secondary antibodies were purchased from LI-COR Biosciences (Bad Homburg, Germany). Alexa Fluor®-labeled secondary antibodies were from Molecular Probes (Invitrogen, Karlsruhe, Germany). Used for flow cytometry anti-TLR1, anti-TLR2, anti-TLR4 antibodies were obtained from eBioscience (San Diego, California, USA). Corresponding isotype controls were from eBioscience (San Diego, California, USA), BD Biosciences (Heidelberg, Germany) and from SantaCruz (Heidelberg, Germany). Biotin and anti-biotin streptavidin were from Jackson ImmunoResearch (Camebridgeshire, UK). The R-PE-labeled secondary antibody was purchased from Rockland (Gilbertsville, USA).

All primers, probes and oligonucleotides were purchased from MWG (Ebersfeld, Germany). siGILZ (siGENOME SMARTpool) and siControl (siGenome) were obtained from Dharmacon (Nidderau, Germany). The plasmid pCR3.1-huGILZ-ORF was a gift from Prof. Dr. Carlo Riccardi, University of Perugia, Italy (Di Marco *et al.*, 2007). pGL4.32[*luc*2P/NF-κB-RE/Hygro] was from Promega (Heidelberg, Germany). pcDNA3-p38α-dn and pcDNA3-p38β2-dn were a gift from Prof. Dr. Jian-Dong Li, University of Rochester Medical Center, USA (Shuto *et al.*, 2001). pcDNA3-huTLR2-YFP was from Prof. Dr. Douglas Golenbock, University of Massachusetts Medical School, USA (Latz *et al.*, 2002).

All other materials were purchased from Sigma (Taufkirchen, Heidelberg), Roth (Karlsruhe, Germany), MP Biomedicals (Heidelberg, Germany), and Merck (Darmstadt, Germany).

2.2   Cell culture

2.2.1 Solutions

PBS (phosphate buffered saline) pH 7.4		PBS (phosphate buffered saline)$^+$	
NaCl	123.2 mM	NaCl	137 mM
Na_2HPO_4	10.4 mM	Na_2HPO_4	8.1 mM
KH_2PO_4	3.16 mM	KH_2PO_4	1.47 mM
in H_2O		KCl	2.68 mM
		$MgCl_2$ x 6 H_2O	0.5 mM
		$CaCl_2$	0.68 mM
		in H_2O	

2.2.2   Human umbilical vein endothelial cells (HUVEC)

Human umbilical vein endothelial cells (HUVEC) were obtained by isolation of endothelial cells from human umbilical veins supplied by the Klinikum Saarbrücken and the Städtisches Klinikum Neunkirchen, Germany. Umbilical cords were postnatally transferred into PBS$^+$ containing 1% [v/v] penicilline (100 U/ml)/streptomycine (100 µg/ml) and 1% [v/v] kanamycine and stored at 4°C up to 10 days prior to isolation.

2.2.3   Isolation of HUVEC

HUVEC were prepared by digestion of umbilical veins with 0.1 g/L collagenase (Roche, Mannheim, Germany) as described in Jaffe et al. (Jaffe *et al.*, 1973). After digestion, cells were suspended in Earle's Medium 199 containing 10% [v/v] fetal calf serum gold and 1% [v/v] penicilline (100 U/ml)/streptomycine (100 µg/ml) and subsequently centrifuged (10 min, 200*xg*). The cells were resuspended in endothelial

cell growth-medium containing 10% [v/v] fetal calf serum gold, 1% [v/v] penicilline (100 U/ml)/streptomycine (100 µg/ml) and 1% [v/v] kanamycine and cultivated at 37°C and 5% CO_2 in a 25 cm^2 cell culture flask. On the following day the adherent cells were washed three times with PBS and cultured until confluence.

2.2.4 Cultivation of HUVEC

Experiments were performed with cells of passage three or four only. Upon reaching confluence cells were split 1:3 or 1:4 in 75 cm^2 cell culture flasks or seeded out in 6 well plates, 20 cm^2 dishes or on glass slides. For passaging, cells were washed three times with PBS before adding 2 ml trypsin to a 75 cm^2 cell culture flask. After incubation for 2 min at 37°C, the digestion was stopped with Earle's Medium 199 containing 10% [v/v] fetal calf serum gold and 1% [v/v] penicilline (100 U/ml)/streptomycine (100 µg/ml). The suspension was centrifuged (10 min, 200xg) and resuspended in endothelial cell growth-medium containing 10% [v/v] fetal calf serum gold, 1% [v/v] penicilline (100 U/ml)/streptomycine (100 µg/ml) and 1% [v/v] kanamycine. For siRNA transfection media without antibiotics were used.

2.2.5 Freezing and thawing of HUVEC

For freezing, confluent cells in passage one were used only. After washing three times with PBS, HUVEC were trypsinized and resuspended in Earle's Medium 199 containing 10% [v/v] fetal calf serum gold and 1% [v/v] penicilline (100 U/ml)/streptomycine (100 µg/ml). The suspension was centrifuged (10 min, 200xg), and cells obtained from one 75 cm^2 cell culture flask were resuspended in 1.5 ml ice cold freezing medium containing endothelial cell growth medium with 10% [v/v] fetal calf serum gold, 1% [v/v] penicilline (100 U/ml)/streptomycine (100 µg/ml) and 1% [v/v] kanamycine supplemented with 10% [v/v] DMSO. After transferring into cryovials, cells were gradually frozen for one day at -20°C, one week at -80°C, and afterwards transferred into liquid nitrogen at -196°C.

To minimize the cytotoxicity of DMSO, the cells were rapidly thawed for 2 or 3 min at 37°C and directly transferred into Earle's Medium 199 containing 10% [v/v] fetal calf serum gold and 1% [v/v] penicilline (100 U/ml)/streptomycine (100 µg/ml). The suspension was centrifuged (10 min, 200xg), and the pellet was resuspended in

endothelial cell growth medium containing 10% [v/v] fetal calf serum gold, 10% [v/v] penicilline (100 U/ml)/streptomycine (100 µg/ml) and 1% [v/v] kanamycine. Cells were cultivated as described in 2.2.4.

2.2.6 Characterisation of HUVEC

In order to characterize HUVEC and to exclude an isolation of other cells types such as smooth muscle cells or fibroblasts, immunostaining of von Willebrand factor followed by flow cytometric analysis was performed (Kiemer *et al.*, 2003). Von Willebrand factor is a multimeric protein, which plays a role in blood coagulation (Ruggeri & Ware, 1993). In contrast to endothelial cells, von Willebrand factor is not expressed in smooth muscle cells and fibroblasts.

von Willebrand factor staining was performed in HUVEC upon reaching confluence. After removing the culture medium, cells were washed three times with PBS and trypsinized as described above (see in 2.2.4). The cell suspension was centrifuged (5 min, 500xg) and washed two times with PBS. For fixation, cells were resuspended in 1 ml 0.25% [w/v] paraformaldehyde and incubated for 1 h at 4°C. A further centrifugation step was followed by permeabilisation with 1 ml 2% [v/v] Tween 20 for 15 min at 37°C. Subsequently, cells were centrifuged and washed twice with PBS. To avoid unspecific antibody binding, cells were incubated with 10 µl of 20% sheep serum for 30 min at room temperature, followed by incubation with 2 µl anti-von Willebrand factor antibody for 30 min at room temperature in darkness. Prior to measurement, cells were washed three times with PBS and resuspended in 300 µl PBS. To set up the measurement parameters of the flow cytometer, cells were treated as described above, but without antibody staining. Flow cytometric analysis was performed with a FACSCalibur and the software *CellQuestPro* (both from Becton Dickinson, Heidelberg, Germany). For quantification, the mean fluorescence of unstained HUVEC detected in the FL1 channel of the cytometer was subtracted from the mean fluorescence of von Willebrand factor stained HUVEC. By setting this value in proportion to unstained cells, the fraction for von Willebrand factor positive cells was given. As shown in Figure 5, isolated cells were identified >97% pure HUVEC.
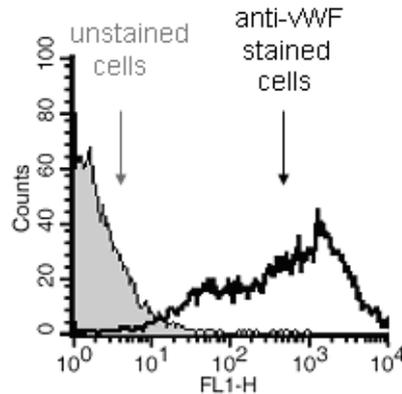
Figure 5: Flow cytometric detection of von Willebrand factor (vWF) protein in HUVEC. Cells were either left unstained (grey background) or stained with anti-vWF antibody (without background), and fluorescence intensities are shown as histogram. The figure shows one representative experiment out of three different cell isolations.

2.2.7 CHO-K1

CHO-K1 cells are epithelial cells from *Cricetulus griseus* (chinese hamster), derived from a subclone of a parental CHO-cell line. They were obtained by an ovarian biopsy of an adult animal (Puck, 1958). CHO-K1 cells were obtained from Prof. Dr. Markus Löbrich, University of Technology, Darmstadt, Germany.

CHO-K1 cells were cultured at 37°C and 5% CO_2 in Ham's 12 containing 10% [v/v] fetal calf serum gold, 1% [v/v] glutamine and 1% [v/v] penicilline (100 U/ml)/streptomycine (100 µg/ml) in a 75 cm^2 cell culture flask. Upon reaching confluence, cells were washed once with PBS, and 2 ml trypsin were added. After incubation for 5 min at 37°C, the digestion was stopped with culture medium and the cells were spit 1:5 into a new cell culture flask.

2.2.8 Detection of mycoplasms

To exclude contaminations with mycoplasms, HUVEC were tested using the Venor®GeM mycoplasm detection kit (Minerva Biolabs, Berlin) according to the manufacturer's instructions. The test is based on nucleic acid amplification by a polymerase chain reaction with a detection limit of 1 bis 5 fg mycoplasmic DNA.

2.3   Vessel specimens

Human normal aortae and intima cylinders of atherosclerotic coronary arteries as well as normal and atherosclerotic internal mammary arteries (IMA) were obtained from patients undergoing coronary bypass surgery and immediately transferred into RNAlater RNA stabilization reagent (Qiagen, Hildesheim, Germany). Until preparation, they were stored at 4°C or for long time storage at -20°C.

The vessels were obtained from PD Dr. Hanno Huwer, SHG Klinik Völklingen, Germany. All samples were obtained with the consent of patients and permission has been given by the local ethics committee.

2.4   Bacterial culture

2.4.1 Solutions

Ampicilline (amp) resistant bacteria were grown in Luria-Bertani (LB)-medium containing ampicilline. For selection of single clones LB$_{amp}$-agar plates were used.

LB$_{amp}$-medium pH7.5		LB$_{amp}$-agar	
tryptone	10% [w/v]	agar	30% [w/v]
yeast extract	5% [w/v]	in LB$_{amp}$-medium	
NaCl	171.1 mM		
in H$_2$O			
ampicilline	100 mg/ml		

2.4.2 Bacterial strains

As host organisms for plasmids the following bacterial strains were used:

Escherichia coli (*E.coli*) XL1-blue, genotype: *recA endA1 gyrA96 thi-1 hsdR17 supE44 relA1 lac* [F'*proAB lacI*^{q}*ZΔM15* Tn*10*(tet^r)];

Escherichia coli (*E.coli*) Top 10, genotype: F–*mcr*A Δ(*mrr-hsd*RMS-*mcr*BC) Φ80*lac*ZΔM15 Δ*lac*X74 *rec*A1 *ara*D139 Δ(*ara leu*) 7697 *gal*U *gal*K *rps*L (StrR) *end*A1

*nup*G (obtained from Prof. Dr. Jörn Walter, Saarland University, Saarbruecken, Germany).

2.4.3 Generation of competent bacteria

Generation of competent bacteria was performed by the $CaCl_2$ method. 100 ml LB-medium were inoculated with 5 ml bacteria of an overnight culture and grown at 37°C and 225 rpm up to an optical density of A_{650nm}=0.4. After incubation on ice for 30 min the suspension was centrifuged (5 min, 200*xg*, 4°C). The pellet was carefully resuspended in 2.5 ml ice cold $CaCl_2$ solution containing 75 mM $CaCl_2$ and 15% glycerine. Another 20 ml ice cold $CaCl_2$ were added, and after incubation for 30 min on ice the suspension was centrifuged again (5 min, 2,000*xg*, 4°C). The pellet was resuspended in 2.5 ml ice cold $CaCl_2$ solution and 100 µl aliquots were stored at -80°C.

2.4.4 Transformation

Transformation was performed by addition of 20 µl (50-150 ng) plasmid DNA to 100 µl competent bacteria. After 20 min incubation on ice, the suspension was heat shocked for 2 min at 42°C. 900 µl of 37°C prewarmed LB-medium were immediately added and shook for 45 min at 37°C and 225 rpm. 100 µl of the transformed bacteria were plated on LB_{amp}-agar plates and cultured overnight at 37°C and 5% CO_2.

2.4.5 Cultivation, freezing and thawing

In order to cultivate transformed bacteria, single clones were picked from the LB_{amp}-agar plate and LB_{amp}-medium was inoculated. After aerob cultivation for 16 h at 37°C and 225 rpm, 0.5 ml of the bacterial suspension were mixed with the same volume glycerol, transferred into cryovials and frozen at -80°C. Remaining bacterial suspension was used for plasmid isolation. For recultivation 10 µl of the glycerol stocks were plated on LB_{amp}-agar-plates and cultured as described above.

2.4.6 Plasmid isolation

Plasmids were isolated using the QIAprep Spin Miniprep kit and the QIAprep Spin Midiprep kit (both from Qiagen, Hildesheim, Germany) according to the manufacturer's instructions. The plasmids were solved in or eluated with TE buffer.

2.4.7 Photometric measurement of DNA concentration and purity

The determination of the DNA concentration was carried out by extinction measurement based on the Beer-Lambert law. Nucleic acids show a characteristic absorption maximum at 260 nm. An extinction of one equates to a DNA concentration of 50 µg/ml. The purity of DNA was measured at 280 nm, the characteristic absorption maximum of aromatic amino acids. The ratio between the absorption at 260 nm and the absorption at 280 nm should be 1.8. The measurements were done with a BioMate 3 UV-Vis spectrophotometer (ThermoElectron, Ulm, Germany).

2.5   Agarose gel electrophoresis

2.5.1 Solutions

TBE buffer		6x DNA loading buffer	
Tris base	89.1 mM	Ficoll Typ 400	18% [w/v]
boric acid	89.1 mM	EDTA, pH 8.0	0.5 M
EDTA	2.21 mM	10xTBE	60 ml
in H_2O		bromphenol blue	0.25% [w/v]
		xylencyanol	0.25% [w/v]
		H_2O	ad 100 ml

2.5.2 Experimental procedure

Agarose gel electrophoresis was applied for DNA detection. Depending on DNA size, 0.5-1.5% agarose gels were used and supplemented with 0.04% [v/v] ethidium bromide. After addition of a suitable volume of 6x DNA loading buffer, DNA was

loaded onto a gel and separated in TBE buffer at 100 V. To determine the size of the DNA, a 50 bp DNA ladder (Fermentas, St. Leon-Rot, Germany) or a 1 kb DNA ladder (Invitrogen, Karlsruhe, Germany) were used. The gel detection was carried out by an UV transilluminator (White Top Light Transilluminator) and the software *ArgusX1* (both from Biostep, Jahnsdorf, Germany).

2.6 Transfection of HUVEC

2.6.1 siRNA and plasmids

For knockdown experiments HUVEC were grown until approximately 80% confluence and transfected with 100 pmol/L siGILZ or siControl using Amaxa® Nucleofection® Technology according to the manufacturer's instructions (Lonza, Basel, Switzerland). Double-stranded (ds) mRNA is intracellularly cleaved by a dicer-enzyme-complex into fragments of 22 base pairs (bp). These fragments are bound by the RISC-complex, which separates the two complementary RNA strands. The single-strand bound to the RISC-complex binds to complementary mRNA resulting in cleavage and degradation of the mRNA (Carthew & Sontheimer, 2009). Experiments were performed 20 h after transfection.

For protein overexpression 2 µg pcR3.1-huGILZ-ORF or pcR3.1-empty as well as 2 µg pcDNA3-p38α-dn or pcDNA3-empty were transfected in the same way using nucleofection. Experiments were performed 16 h or 24 h later.

For luciferase assay the cells were co-transfected with 100 pmol/L siRNA and 1.5 µg pGL4.32[*luc*2P/NF-κB-RE/Hygro] using nucleofection. The luciferase plasmid contained five repetitive elements of the NF-κB consensus sequence GGGAATTTCC and the coding sequence of luciferase from the firefly *Photynus pyralis.* The luciferase catalyzes the oxidative decarboxylation of D-luciferin to oxyluciferin in presence of the co-factors adenosine triphosphat (ATP) and Mg^{2+}, which results in emission of light with a wavelength of 562 nm (Seliger & McElroy, 1964). Experiments were performed 20 h after transfection.

All plasmids were amplified and isolated using Midiprep (see in 2.4) and sterile filtration. The pmaxGFP™ plasmid (Lonza, Basel, Switzerland) encoding the green

fluorescent protein (GFP) of the crab *Pontellina pliumata* was used as transfection control. The transfection efficiency was determined *via* fluorescence microscope.

2.6.2 Decoy oligonucleotides

For decoy oligonucleotide transfection 0.05 µg/ml of the following decoy oligonucleotides were transfected using Superfect (Qiagen, Hildesheim, Germany) in a decoy to transfection reagent ratio of 1:20 (NF-κB) or 1:10 (AP-1): NF-κB decoy (5´-agttGAGGGGACTTTCCCagc-3´), NF-κB scrambled decoy (5´-ttcCGTACCTGACTTagcc-3´), AP-1 decoy (5´-cgctTGATGACTCAGCCggaa-3´) and AP-1 scrambled decoy (5´-cgctTGATGACTTGGCCggaa-3´), lower case letters show phosphorothionate backbones (Fürst *et al.*, 2005). Decoys are short double stranded oligonucleotides. They exhibit the consensus DNA sequence, to which the transcription factor normally binds after activation. Transfection of cells with decoy oligonucleotides leads to binding of the activated transcription factor to the oligonucleotides resulting in a diminished transcription factor/DNA-binding and therefore reduced gene expression (Tomita *et al.,* 2003). Experiments were performed 4 h after transfection.

2.7   Isolation of protein extracts

2.7.1 Solutions

PBS

see in 2.2.1

Lysis buffer for whole cell extracts

lysis buffer A		lysis buffer B	
Tris-HCl pH 6.8	50 mM	Tris base pH 7.5	20 mM
SDS	1% [v/v]	NaCl	120 mM
2-mercapthoethanol	2% [v/v]	glycerol	10% [v/v]
glycerol	10% [v/v]	EDTA, pH 8.0	2 mM
bromphenol blue	0.004% [v/v]	Triton X-100	1% [v/v]
freshly added before use:		freshly added before use:	
protease inhibitor	1x [v/v]	NaF	50 mM
		phosphatase inhibitor cocktail I	1% [v/v]
		phosphatase inhibitor cocktail II	1% [v/v]

Lysis buffer for nuclear and cytosolic proteins

hypotonic buffer A		hypertonic buffer B	
HEPES/KOH pH7.9	10 mM	HEPES/KOH pH 7.9	20 mM
EDTA	0.1 mM	NaCl	400 mM
KCl	10 mM	EDTA	1 mM
EGTA	0.1 mM	EGTA	1 mM
freshly added before use:		glycerol	25% [v/v]
DTT (in H_2O)	1 mM	freshly added before use:	
PMSF (in methanol)	0.5 mM	DTT (in H_2O)	1 mM
		PMSF (in methanol)	0.5 mM

2.7.2 Isolation of whole cell extracts

For Western blot analysis of GILZ, p65, IκBα and TLR6 cells were grown in 6-well plates or transfected as described in 2.6 and treated as indicated. After washing with PBS, cells were scraped and lysed in 100 µl of lysis buffer A. After 2 pulses of sonification followed by centrifugation (15 min, 20,000xg, 4°C) supernatant was

denatured for 5 min at 95°C and frozen at -80°C. Because this lysis buffer contained 2-mercapthoethanol, a determination of protein concentrations was not possible.

For detection of p38 and p-p38 MAPK cells were grown in 6-well plates and treated as indicated. They were washed with PBS, scraped and lysed in 100 µl lysis buffer B. After incubation for 30 min on ice followed by centrifugation (15 min, 20,000xg, 4°C), supernatants were denatured for 5 min at 90°C and frozen at -80°C. Protein concentrations were determined by Pierce BCA protein assay (Fisher Scientific, Nidderau, Germany) according to the manufacturer's instructions using a Sunrise[TM] absorbance reader and the software *Magellan* (both from Tecan, Grödig/Salzburg, Austria).

2.7.3 Isolation of nuclear and cytosolic extracts

HUVEC were cultured in 20 cm^2-dishes until confluence or transfected as described in 2.6 and treated as indicated. They were washed with PBS, scraped and centrifuged (5 min, 500xg, 4°C) followed by pellet resuspension in 200 µl hypotonic buffer A. After 15 min incubation on ice, 10% [v/v] Nonidet p-40 was added and immediately vortexed. After centrifugation (1 min, 14,000xg, 4°C), the supernatant with the cytosolic proteins was frozen at -80°C. The pellet with the nuclear fraction was resuspended in 20 µl hypertonic buffer B and incubated for 30 min at 4°C while vortexing. The extract was centrifuged (20 min, 12,000xg, 4°C), and the supernatant was frozen at -80°C. Protein concentrations were determined by Bradford assay (Bio-Rad, Munich, Germany) according to the manufacturer's instructions using the Sunrise[TM] absorbance reader and the software *Magellan* (both from Tecan, Grödig/Salzburg, Austria).

2.8   Electrophoretic mobility shift assay (EMSA)

2.8.1 Solutions

PBS   TBE

see in 2.2.1   see in 2.5.1

<u>7% non-denaturating polyacrylamide gel</u>

H$_2$O	23.5 ml
40% acrylamide/ 0.8% bisycrylamide solution	7.5 ml
Tris base (1 M, pH 7.5)	7.6 ml
glycine (1 M)	200 µl
EDTA (0.5 M)	160 µl
APS (10% [w/v])	200 µl
TEMED	30 µl

2.8.2 Experimental procedure

Equal amounts of nuclear protein were incubated for 20 min at room temperature in a 20 µl-reaction volume containing 10 mM Tris-HCL pH 7.5, 50 mM KCl, 1 mM DTT, 2.5 mM DTT/0.25% Tween 20, 2 ng poly(dIdC) and 25 nM IRdye labeled oligonucleotides. For supershift analysis, 1 µg of the suitable antibody was added to the EMSA reaction 10 min before addition of IRdye labeled oligonucleotides. The oligonucleotide sequences containing a consensus binding sequence for NF-κB (5´-AGTTGAGGGGACTTTCCCAGGC-3´) or AP-1 (5´-CGCTTGATGACTCAGCCG GAA-3´) were 5´end-labeled with IRdye700 or IRdye800. Formation of double-stranded oligonucleotides was performed by incubation for 5 min at 95°C and a slow cooling. Nucleoprotein-oligonucleotid-complexes were resolved by electrophoresis in a 7% non-denaturating polyacrylamide gel. The gels were cast and the electrophoresis was carried out with component parts of BioRad (Munich, Germany). Gel detection was performed by ODYSSEY® Infrared Imaging System (LI-COR®, LI-COR Biosiences, Bad Homburg, Germany). Specifity of the DNA-protein complexes was confirmed by competition with a twofold amount of unlabeled NF-κB and AP-1 oligonucleotides.

2.9 Western blot analysis of proteins

2.9.1 Solutions

SDS polyacrylamide gel

resolving gel	6% / 15%	stacking gel	
H_2O	10.6 ml / 4.6 ml	H_2O	6.8 ml
30% acrylamide / 0.8% bisacrylamide solution	4 ml / 10 ml	30% acrylamide / 0.8% bisacrylamide solution	1.7 ml
Tris base (1.5 M, pH 8.0)	5 ml	Tris base (1.0 M, pH 6.8)	1.25 ml
SDS (10% [w/v])	200 µl	SDS (10% [w/v])	100 µl
APS (10% [w/v])	200 µl	APS (10% [w/v])	100 µl
TEMED	20 µl	TEMED	10 µl

electrophoresis buffer		transfer buffer	
Tris base	24.8 mM	Tris base	24.8 mM
glycine	1.92 mM	glycine	1.92 mM
SDS	0.1% [w/v]	SDS (10%)	0.05% [w/v]
in H_2O		methanol	20% [v/v]
		in H_2O	

PBS	PBST	
see in 2.2.1	Tween 20	0.1% [v/v]
	in PBS	

gelatine buffer

gelatine A	0.75% [w/v]
in PBST	

2.9.2 Antibodies

Table 1: Antibodies and dilutions used for Western blot analysis

antibodies	used dilution
anti-human GILZ, *goat IgG*	1:200 in gelatine buffer
anti-human p65, *rabbit IgG*	1:2,000 in Rockland blocking buffer
anti-human p50, *rabbit IgG*	1:2,000 in Rockland blocking buffer
anti-human cRel, *rabbit IgG*	1:2,000 in PBST/5% [w/v] BSA
anti-human IκBα, *rabbit IgG*	1:400 in Rockland blocking buffer
anti-human TLR6, *goat IgG*	1:400 in Rockland blocking buffer
anti-human p38 MAPK, *mouse IgG$_1$*	1:200 in Rockland blocking buffer
anti-human p38 MAPK, *rabbit IgG*	1:1,000 in Rockland blocking buffer
anti-human phospho-p38 MAPK, *rabbit IgG*	1:1,000 in Rockland blocking buffer
IRDye® 800CW conjugated *goat anti-mouse IgG*	1:5,000 in Rockland blocking buffer
IRDye® 680 conjugated *goat anti-mouse IgG*	1:5,000 in Rockland blocking buffer
IRDye® 680 conjugated *goat anti-rabbit IgG*	1:5,000 in Rockland blocking buffer
IRDye® 680 conjugated donkey *anti-goat IgG*	1:5,000 in Rockland blocking buffer
IRDye® 680 conjugated goat *anti-rat IgG*	1:5,000 in Rockland blocking buffer

2.9.3 SDS-polyacrylamide gel electrophoresis

Protein separation was applied by denaturing SDS polyacrylamide gel electrophoresis (SDS-PAGE) according to Laemmli (Laemmli, 1970). The concentration of the acrylamide/bisacrylamide mixture in the resolving gel was chosen based on the molecular weight of the protein of interest. For TLR6 detection, 6% gels were used, while all other proteins were separated on 15% gels. Addition of strongly negatively charched sodium dodecyl sulfate (SDS) leads to masking of the protein charge to a constant ratio of mass to charge (1.4 g SDS per 1 g protein). Reducing agents (dithiothreitol (DTT), 2-mercaptoethanol) cleave and denaturate the disulfide bridges. To quantify the molecular weight a prestained protein marker (Fermentas, St. Leon-Rot, Germany) was used. Cell lysates were thawed on ice and after addition of sample buffer (5x loading dye, Roth, Karlsruhe, Germany; except for

stained lysis buffer) proteins were denaturated for 5 min at 95°C or for p-p38 detection 5 min at 90°C. Equal protein amounts were loaded onto the gel and separated in electrophoresis buffer. The gels were cast and the electrophoresis was carried out (80 V for 30 min followed by 120 V for 2 h) with component parts of BioRad (Munich, Germany).

2.9.4 Western blot

In order to transfer proteins onto a polyvinylidene fluoride (PVDF) membrane with a pore size of 0.45 µm (Immobilion-FL, Millipore), the tank blotting system was used after electrophoresis. The membrane was incubated for 30 sec in methanol followed by storage in transfer buffer before use. A sandwich containing two sponges, two blotting papers, the gel and the membrane was built avoiding air bubbles. All of these parts were equilibrated in transfer buffer before use. Blotting was carried out in transfer buffer (80 mA, overnight) with component parts of BioRad (Munich, Germany). Afterwards, the membranes were incubated for 30 min in Rockland blocking buffer (Rockland, Gilbertsville, USA) to block unspecific binding sites.

2.9.5 Immunodetection

The incubation with antibodies was carried out according to the antibody dilutions mentioned in 2.9.2. Primary antibodies were incubated under constant shaking for 3 h at room temperature or 37°C (anti-GILZ) or overnight at 4°C (all other antibodies). Following three washing steps with PBST/5% [w/v] milk, PBST/5% [w/v] BSA or gelatine buffer, the secondary antibodies were incubated for 2 h at room temperature. The membranes were washed two times with PBST and PBS accordingly. For detection, ODYSSEY® Infrared Imaging System and the software *Odyssey* (both from LI-COR®, LI-COR Biosiences, Bad Homburg, Germany) were used. Image editing was performed with *Adobe Photoshop 7.0* (Adobe Systems, Munich, Germany).

2.10 Detection of mRNA

Because of the rapid degradation of RNA by RNases only chlorophorm treated reaction tubes as well as protective gloves were used. Tips were decontaminated by UV light.

2.10.1 Solutions

PBS	DEPC-H$_2$O	
see in 2.2.1	DEPC	0.1% [v/v]
	in H$_2$O	

2.10.2 RNA isolation

HUVEC

Cells were grown in a 6-well plate until confluence and treated as indicated. For isolation of total RNA they were washed once with cold PBS and lysed in 1 ml Qiazol (Qiagen, Hildesheim, Germany). 250 µl chloroform were added followed by vortexing for 15 sec. After incubation for 3 min at room temperature, the suspension was centrifuged (15 min, 15,000xg, 4°C). 400 µl of the clear supernatant containing the RNA were mixed with the same volume of 100% isopropanol. The RNA was precipitated overnight at -20°C followed by centrifugation (10 min, 15,000xg, 4°C). The pellet was washed with 750 µl 75% ethanol ([v/v] in DEPC-H$_2$O) and after centrifugation (5 min, 20,000xg, 4 min), the RNA pellet was dried at 37°C. For RNA dissolving 20 µl DEPC-H$_2$O were added, and the samples were incubated for 10 min at 55°C.

Plasmid transfected cells (according to 2.6) were treated as indicated. RNA was isolated using RNeasy mini kit (Qiagen, Hildesheim, Germany) according to the manufacturer's instructions and eluted with 30 µl DEPC-H$_2$O.

Human arteries

Human arteries stored in RNAlater were cut into pieces of 0.3 mm edge length, transferred into Qiazol (Qiagen, Hildesheim, Germany), and dispersed for 2 min at

18,000 rpm using an Ultra-Turrax® (IKA, Staufen, Germany). Total RNA was isolated as described above.

2.10.3 DNase digestion

To eliminate any contaminations with genomic DNA, a DNAse digestion was performed using a DNA free kit (Ambion, Applied Biosystems, Darmstadt, Germany) according to the manufacturer's instructions.

2.10.4 Photometric measurement of RNA concentrations

The determination of the RNA concentration was carried out by extinction measurement based on the Beer-Lambert law. Because of the characteristic aromatic ring system of the bases, RNA shows an absorption maximum at 260 nm. An extinction of one equates to an RNA concentration of 40 µg/ml. The measurements were done in a BioMate 3 UV-Vis spectrophotometer (ThermoElectron, Ulm, Germany).

2.10.5 Determination of the RNA quality

The quality of the RNA was determined using a RNA 6000 Nano Lab Chip kit (Agilent, Böblingen, Germany) according to the manufacturer's instructions. The measurement was carried out in a Standard Agilent 2100 Bioanalyzer and the software *Agilent 2001 expert* (both from Agilent, Böblingen, Germany).

2.10.6 Polymerase chain reaction (PCR)

Polymerase chain reaction (PCR) means the amplification of nucleic acids by the use of Taq DNA polymerases and primers. Taq DNA polymerases are enzymes synthesizing double stranded (ds) DNA based on single stranded (ss) DNA. The prerequisite for this reaction is a small double stranded region, which functions as start point. These start points are generated by the addition of complementary primers for the coding (sense) and the non-coding (antisense) strand. In a first step of the PCR, the double stranded DNA is denatured by heat leading to primer binding to their target sequence on the single stranded DNA (annealing). Based from this

short double stranded region, in a next step the complementary strand is synthesized from the Taq DNA polymerase (elongation). A multiple repetition of these steps leads to DNA duplication per reaction cycle and thus to an exponential duplication of the DNA sequence flanked by the primers.

2.10.7 Alu-PCR

To investigate the success of the DNAse digestion an Alu-PCR was performed. Alu elements are repeats of 300 bp with similar, but not exactly identical sequence. In the human genome more than one million Alu repeats are located representing 15% of the whole genome.

Primer

For Alu-PCR the A1S primer with the sequence 5'-TCATGTCGACGCGAGACTCCATCTCAAA-3' was used.

Experimental procedure

The reaction mixture was assembled on ice by using a Taq polymerase from *Thermophilus aquatius* and a dNTP mix containing dATP, dCTP, dGTP, dTTP (both from GenScript, Piscataway, USA).

10x Taq buffer	2.5 µl
dNTPs (10 mM each)	0.5 µl
primer (50 µM)	0.5 µl
Taq polymerase (5U/µl)	0.5 µl
RNA	100 ng
H_2O	ad 25 ml

1 µg genomic DNA isolated from THP1 cells (provided from Nadège Ripoche, Saarland University, Saarbruecken, Germany) was used as positive control. The PCR was performed in a Thermocycler PX2 (ThermoElectron, Ulm, Germany).

Conditions

denaturation	5 min 94°C	1 cycle
denaturation	1 min 94°C	
annealing	1 min 56°C	30 cycles
elongation	2 min 72°C	
final elongation	10 min 72°C	1 cycle

When no amplification product was oberserved after resolving the samples on a 1.5% agarose gel (see in 2.5), the RNA was considered to be DNA-free and was subsequently used for reverse transcription.

2.10.8 Reverse transcription (RT)

Complementary DNA (cDNA) was obtained from mRNA using a High Capacity cDNA Reverse Transcription kit (Applied Biosystems, Darmstadt, Germany) according to manufacturer's instructions. The reverse transcriptase used exhibits three different enzymatic activities: an RNA-dependent DNA polymerase, an RNA:DNA-hybrid dependent exoribonuclease (RNase H) as well as a DNA-dependent DNA polymerase. The result of this reverse transcription was a ss cDNA, while complementary RNA was degraded.

Primer

For reverse transcription an oligo-dT primer with the sequence 5'-TTT TTT TTT TTT TTT TTT-3' was used.

Experimental procedure

The reaction mixture was assembled on ice using of an RNase inhibitor (Invitrogen, Karlsruhe, Germany). After incubation of 1 µg RNA for 5 min at 65°C to destroy DNases, the RNA was added to the mixture as template.

Reaction for one sample:

10x RT buffer	2 µl
25x dNTPs (25 mM each)	0.8 µl
primer (10 µM)	2.0 µl
reverse transcriptase (4 U/µl)	1 µl
RNaseOut (10 U/µl)	0.25 µg
RNA	1 µg
H_2O	ad 20 ml

Reverse transcription was performed for 10 min at 25°C followed by 2 h at 37°C. Afterwards, the enzymes were inactivated for 5 sec at 85°C and the cDNA was stored at -20°C. A reaction mixture without reverse transcriptase, but with RNA was prepared as a further control for successful DNase digestion as well as to exclude any DNA-contamination of the reaction mixture.

For use in real-time RT-PCR, cDNA was diluted 1:5 in H_2O.

2.10.9 Standard dilution series

Determination of the real-time RT-PCR efficiency and quantification of the cDNA concentration was performed using plasmids, which were applied in dilution series from 20 attomol/µl to $2*10^{-6}$ attomol/µl in TE. The required DNA sequence, the PCR product of the gene of interest, was cloned into the multiple cloning site of a pGEM®-T Easy vector (Promega, Heidelberg, Germany). Bacterial glycerol stocks with the required plasmids were provided by Prof. Dr. Alexandra K. Kiemer (Saarland University, Saarbruecken, Germany). Plasmid isolation was carried out by Miniprep (see in 2.4.6).

The applied amount of the plasmids was calculated as followed:

c (target DNA) [attomol/µl] = c (plasmid) [µg/ml] * 1000 * 1,515 / N (bp)

N (bp) = base pair number of insert and vector

2.10.10 Real-time RT-PCR

Real-time RT-PCR allows the detection of RNA and the quantification of the PCR during the amplification. First, the RNA has to be reverse transcribed into cDNA (see in 2.10.8), followed by amplification based on a conventional PCR (see in 2.10.6). Additionally, oligonucleotides were used, which bind to a sequence within the PCR product and function as probes. The 5'-ends of the oligonucleotides were marked with the reporter dye, 6-Carboxy-Fluorescein (FAM), the 3'-ends with the quencher dye, *Black Hole Quencher 1* (BHQ1). Because of the small distance to the quencher, the fluorescence is suppressed when the probe attached on the PCR product is excited by monochromatic light of 488 nm. This phenomen is termed *fluorescence resonance energy transfer* (FRET). With ongoing amplification, the probe is hydrolysed by the exonuclease activity of the Taq DNA polymerase resulting in a territorial separation of reporter and quencher dye. The fluorescence is not suppressed anymore and can be measured in real-time using specialized software. The fluorescence intensity is proportional to the amount of the PCR product.

Primers and Probes

All primer and probe sequences were obtained from Prof. Dr. Alexandra K. Kiemer (Saarland University, Saarbruecken, Germany).

Table 2: Primers used for real-time RT-PCR

mRNA	primer sense 5´→3´	primer antisense 3´→5´
β-actin	TGCGTGACATTAAGGAGAAG	GTCAGGCAGCTCGTAGCTCT
GILZ	TCCTGTCTGAGCCCTGAAGAG	AGCCACTTACACCGCAGAAC
TLR1	AGCAAAGAAATAGATTACACATCA	TTACCTACATCATACACTCACAAT
TLR2	GCAAGCTGCGGAAGATAATG	CGCAGCTCTCAGATTTACCC
TLR4	ATGAAATGAGTTGCAGCAGA	AGCCATCTGTGTCTCCCTAA
TLR6	TTTACTTGGATGATGGTGAATAGT	AGTTCCCCAGATGAAACATT
MCP-1	TTGATGTTTTAAGTTTATCTTTCATGG	CAGGGGTAGAACTGTGGTTCA

Table 3: Probes used for real-time RT-PCR

mRNA	probe
β-actin	5´FAM-CACGGCTGCTTCCAGCTCCTC-3´-BHQ1
GILZ	5´FAM-TCCCGAATCCCCACAAGTGCCCGA-3´-BHQ1
TLR1	5´FAM-ATTCCTCCTGTTGTATTGCTGCTTTTG-3´-BHQ1
TLR2	5´FAM-ATGGACGAGGCTCAGCGGGAAG-3´-BHQ1
TLR4	5´FAM-AAGTGATGTTTGATGGACCTCTGAATCT-3´-BHQ1
TLR6	5´FAM-GTCGTAAGTAACTGTSTGGAGGTGC-3´-BHQ1
MCP-1	5´FAM-AGATACAGAGACTTGGGGAAATTGCTTTTC-3´-BHQ1

Experimental procedure

All conditions were established and obtained from Prof. Dr. Alexandra K. Kiemer or Nadège Ripoche (Saarland University, Saarbruecken, Germany).

Taq polymerase from *Thermophilus Aquatius* and a dNTP mix containing dATP, dCTP, dGTP, dTTP (both from GenScript, Piscataway, USA) were used to prepare reaction mixtures. The reaction mixtures were assembled on ice and inserted into a 96 well plate and 5 µl cDNA were added. As negative controls, 5 µl of the RT-reaction mixture without reverse transcriptase (see in 2.10.8) or 5 µl H_2O were added to the real-time RT-PCR reaction mixture.

Reaction mixture for one sample:

10x Taq buffer	2.5 µl
dNTPs (10 mM each)	x µl
primer sense (50 µM)	0.25 µl
primer antisense (50 µM)	0.25 µl
$MgCl_2$ (50 mM)	x µl
Taq polymerase (5U/µl)	0.5 µl
probe (1 pmol/µl)	x µl
cDNA/template	5 µl
H_2O	ad 25 ml

Conditions:

Table 4: conditions for real-time PCR

mRNA	MgCl$_2$	dNTP	probe	annealing
β-Actin	5 mM	800 µM	2.5 pmole	58°C
GILZ	4 mM	200 µM	2.5 pmole	60°C
TLR1	9 mM	800 µM	1.5 pmole	57°C
TLR2	6 mM	800 µM	2.5 pmole	60°C
TLR4	5 mM	800 µM	2.5 pmole	58°C
TLR6	8 mM	800 µM	2.5 pmole	57°C
MCP-1	4 mM	200 µM	1.5 pmole	59°C

Real-time PCR was performed in an iQ5 Cycler using the software *iQ5* (both from BioRad, Munich, Germany). All samples and standards were analysed in triplicate on each plate.

Conditions

denaturation	8 min 95°C	1 cycle
denaturation	15 sec 95°C	
annealing	15 sec 57°-60°C	40 cycles
elongation	15 sec 72°C	
final elongation	30 sec 25°C	1 cycle

The curves of a real-time PCR show three different phases: an early phase with detection of the basal fluorescence, an exponential phase, in which the detected fluorescence signal is proportional to the amplified PCR product as well as a final plateau phase. The threshold, at which the fluorescence of the PCR product is stronger than the basal fluorescence, is determined by the software. The number of the cycles needed for the threshold excess is termed *threshold cycle* (Ct value). For reliable reproducibility of the experiments, the efficiency should be between 95 and 105%.

Quantification

The starting quantity mean (SQ mean) of each triplicate was determined For quantification, which was calculated by the software by comparison threshold cycles to the standard dilution series. All SQ means were normalised to the SQ means of the house-keeping gene β-actin, and the mean of the control values was calculated. The normalized values of all other samples were compared to this control mean, averaged, and shown as x-fold or percentaged expression.

2.11 Luciferase assay

After transfection as described in 2.6, the cells were grown in white 96-well plates with clear bottom (PerkinElmer, Rodgau-Juedesheim, Germany) and treated as indicated. Equal volumes of luciferase substrate buffer (Dual-Glo Luciferase Assay System, Promega, Heidelberg, Germany) were added, and after incubation for 35 min at room temperature whole luminescence was measured using a Wallac Victor2 multilabel counter and the software *Wallac 1420* (both from Wallac/PerkinElmer, Rodgau-Juedesheim, Germany). In previous experiments high fluctuations in the expression of the standardization gene renilla were observed resulting in incorrect normalization. Therefore, a co-transfection with a second plasmid for standardization was not performed in this work.

2.12 Immunofluorescence

2.12.1 Solutions

PBS   PBST

see in 2.2.1   see in 2.6.1

2.12.2 Antibodies

Table 5: Antibodies and dilutions used for immunofluorescence

antibody	used dilution	absorption/emission
anti-human p38 MAPK, *mouse IgG_1*	1:20	
anti-human phospho-p38 MAPK, *rabbit IgG*	1:25	
Alexa Fluor® 488 F(ab')$_2$ fragment, *goat anti-mouse IgG*	1:200	495 nm/519 nm
Alexa Fluor® 594 F(ab')$_2$ fragment, *goat anti-rabbit IgG*	1:300	590 nm/617 nm

2.12.3 Experimental proceduce

HUVEC were grown until 80% confluence on coverslips with a diameter of 12 mm coated with 0.1% gelatine A ([w/v] in PBS) for 45 min. The cells were treated as indicated, washed with PBS and fixed with ice cold methanol for 20 min at -20°C. Before permeabilisation with 0.2% Triton X-100 ([v/v] in PBS/1% [v/v] FCS), cells were washed three times with PBS. After washing two times with PBS/1% FCS, unspecific binding sites were saturated for 1 h at 4°C with PBS/1% FCS.

2.12.4 Immunodetection

Immunofluorescence staining was performed in a wet chamber. 40 µl of the primary antibody dilution in PBST/1% [v/v] FCS (see in 2.12.2) were added on the coverslips and incubated overnight at 4°C. After washing three times with PBST/1% FCS, 70 µl of the secondary antibody dilution (see in 2.12.2) were added and incubated for 1 h at room temperature. Afterwards, the coverslips were washed twice with PBST and once with PBS. For nuclear staining 4',6-diamidino-2-phenylindoldihydrochloride (DAPI, Sigma, Taufkirchen, Germany) was used. This dye binds strongly to AT cluster in the DNA and is excited by UV light (absorption at 350 nm, emission at 460 nm). The coverslips were incubated 5 min at room temperature with 100 µl 0.1 µg/ml DAPI in PBS followed by three washing steps with PBS. 3 µl FluorSave (Calbiochem, Merck, Darmstadt, Germany) were added on a glass slide, the coverslipes were applied with the cell side down and dried for 24 h at 4°C. Cells stained without

primary antibody were used as control for unspecific bindings of the secondary antibody. Photographs were taken with a laser scanning microscope LSM 710 and the software *LSM Image Browser Release 4.2.* (both from Zeiss, Jena Germany). Image editing was performed with *Adobe Photoshop 7.0* (Adobe Systems, Munich, Germany).

2.13 Flow cytometric analysis

2.13.1 Solutions

PBS

see in 2.2.1

TEN buffer

Tris-HCl, pH 7.5	40 mM
EDTA	1 mM
NaCl	150 mM
in H_2O	

FACS buffer

BSA	0.5% [w/v]
azide	0.01% [v/v]
in PBS	

saponin buffer

BSA	0.5% [w/v]
azide	0.01% [v/v]
saponin	0.5% [w/v]
in PBS	

2.13.2 Antibodies

Table 6: Antibodies and dilutions used for flow cytometric analysis

antibodies	used dilution	concentration per 5*10^5 cells
anti-human TLR1, *mouse IgG$_{1, \kappa}$*	1:100	0.05 mg/ml
mouse IgG$_{1, \kappa}$, isotype control	1:100	0.05 mg/ml
anti-human TLR2, *mouse IgG$_{2a}$*	1:10	0.4 mg/ml
mouse IgG$_{2a,}$ isotype control	1:2.5	0.4 mg/ml
anti-human TLR4, *mouse IgG$_{2a, \kappa}$*	1:200	0.025 mg/ml
mouse IgG$_{2a, \kappa}$, isotype control	1:200	0.025 mg/ml
biotin-SP-conjugated F(ab')$_2$ fragment, *goat anti-mouse*	1:10	0.1 mg/ml
R-PE-conjugated anti-biotin streptavidin	1:10	0.1 mg/ml
R-PE-conjugated *goat anti-mouse IgG*	TLRs 1, 2: 1:10 TLR4: 1:20	TLRs 1, 2: 1 mg/ml TLR4: 0.5 mg/ml

2.13.3 Analysis of the anti-TLR2 antibody specifity

Plasmid

To determine the specifity of the used anti-TLR2 antibody CHO-K1 cells were transfected with pcDNA3-huTLR2-YFP (Latz *et al.*, 2002). The insert contained a human TLR2 cDNA sequence cloned into a vector containg the sequence of the yellow fluorescent protein (YFP). The result was the expression of the fusion protein TLR2 with YFP at the C-terminus. The plasmid was amplified and isolated using Midiprep (see in 2.4).

Experimental procedure

CHO-K1 cells were grown in 6-well plates until 50% confluence. Before transfection, the cell culture medium was substituted by fresh medium without antibiotics. 100 μl medium without any supplements were mixed with 2 μg pcDNA3-huTLR2-YFP followed by addition of 8 μl FuGENE$^{®}$ HD transfection reagent (Roche, Basel, Switzerland; equals an 8:2 ratio of FuGENE HD transfection reagent to DNA). After

vortexing for 2 sec and incubation for 5 min at room temperature, the mixture was added to the cells. The plates were carefully shaken for 30 sec and cultivated for 46 h.

For TLR2 antibody staining the cells were trypsinized as described above (see in 2.2.7). Removal of the medium was followed by centrifugation (5 min, 500xg) and two washing steps with PBS. After fixation with 4% [v/v] formaldehyde for 15 min at room temperature, cells were washed once with PBS and once with saponin buffer. 2 µl human IgG (Jackson ImmunoResearch, Camebridgeshire, UK) were added for blocking of unspecific binding sites, and cells were incubated for 15 min at room temperature. 20 µl of the anti-TLR2 antibody or isotype control dilution in saponin buffer were added (see in 2.13.2), and the mixture was incubated 1 h at room temperature. The cells were washed three times with saponin buffer and after addition of 20 µl of the biotin-conjugated F(ab')$_2$ fragment dilution (see in 2.13.2) incubated for 30 min on ice. After three washing steps with saponin buffer, 20 µl of the R-PE-conjugated streptavidin dilution (see in 2.13.2) were added, and cells were incubated for 30 min at room temperature. Afterwards, cells were washed three times with saponin buffer and resuspended in 300 µl 0.2% [v/v] formaldehyde.

Measurement

Flow cytometric analysis was carried out by a FACSCalibur and the software *CellQuestPro* (both from Becton Dickinson, Heidelberg, Germany). The settings for compensation were done using only fixed cells, transfected cells, as well as transfected and stained cells.

2.13.4 TLR-staining

Experimental procedure

HUVEC were grown in 6-well plates until confluence and treated as indicated. The culture medium was removed, and the cells were washed with ice cold PBS. 500 µl ice cold TEN buffer were added to the cells followed by incubation for 20 min on ice and scraping. After centrifugation (5 min, 500xg) cells were washed twice with ice cold PBS. After a further centrifugation step, the supernatant was completely decanted, and the cells were fixed drop wise with 1 ml ice cold 70% [v/v] ethanol

under constant vortexing. Until immunostaining the suspensions were frozen at -20°C.

The following steps were done on ice. For removal of the ethanol, the cells were centrifuged (5 min, 500*xg*) and washed two times with PBS, once with FACS buffer and once with saponin buffer. 2 µl human IgG (Jackson ImmunoResearch, Camebridgeshire, UK) were added for blocking of unspecific binding sites, and cells were incubated for 15 min at room temperature. 20 µl antibody dilution (see in 2.13.2) were added, and the mixture was incubated for 30 min at room temperature. Cells were washed three times with saponin buffer and 20 µl of the secondary antibody dilution (see in 2.13.2) were added. After 30 min incubation on ice, the cells were washed once with saponin buffer and two times with FACS buffer. For cytometric measurement cells were resuspended in 300 µl FACS buffer. Cells stained with the respective isotype control were used as control for unspecific bindings. To set up the measurement parameters of the flow cytometer, completely unstained cells were used.

Measurement and quantification

For flow cytometric analysis a FACSCalibur and the software *CellQuestPro* were used (both from Becton Dickinson, Heidelberg, Germany). An intact cell population was gated and the fluorescence signals of 10,000 cells were detected in the FL2 channel. The geometric mean (*median*) was regarded for quantification describing the middle signal intensity of all measured fluorescence signals.

The raw data of the TLR cytometric measurements were quantified by forming the ratio of stained cells and isotype control and normalizing the treated cells to the corresponding control.

2.14 Statistical analysis

For independent experiments, HUVEC preparations of different donors were used. Data are shown using the software *OriginPro 8.1G* (OriginLab Corporation, Northampton, USA) and are expressed as mean ±SEM. Statistical significance was determined by student's t-test (one sample) using the software *Excel* (Microsoft, Redmond, USA) and/or *OriginPro 8.1G* (OriginLab Corporation, Northampton, USA).

3. Results

3.1   GILZ expression in endothelial cells

3.1.1 GILZ protein expression at baseline and after dexamethasone

Since the presence of GILZ in untreated endothelial cells has as yet been unknown, GILZ expression at baseline and after dexamethasone treatment was examined by Western blot analysis. As shown in Figure 6, GILZ protein was constitutively expressed in HUVEC and as described for other cell types (Eddleston *et al.*, 2007; D'Adamio *et al.*, 1997) increased after treatment with dexamethasone.
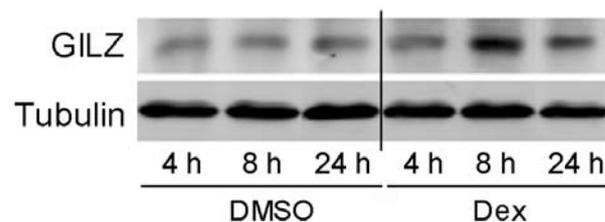
Figure 6: GILZ expression in HUVEC at baseline and after dexamethasone (Dex). Cells were treated with 1 μM Dex or an equal volume of DMSO as solvent control for the indicated times. Equal amounts of protein were assessed by Western blot analysis using tubulin as loading control. Data are shown as one representative out of three independent experiments.

When comparing GILZ mRNA expression in HUVEC to alveolar macrophages after normalisation on the house-keeping gene β-actin, similar GILZ levels were found (HUVEC: 0.007 attomol/μl, SEM±0.001, n=18; alveolar macrophages: 0.003 attomol/μl, SEM±0.0006, n=12; Jessica Hoppstädter, unpublished data).

3.1.2 GILZ expression after TNF-α

In contrast to the dexamethasone-mediated downregulation, Western blot analysis showed that treatment of HUVEC with TNF-α led to a decreased protein GILZ expression by about 50% (Figure 7).
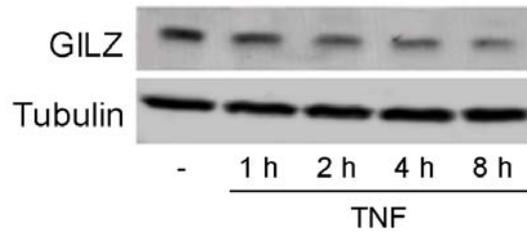
Figure 7: GILZ protein expression after TNF-α. HUVEC were either left untreated (-) or treated with 10 ng/ml TNF-α for the indicated times. Equal amounts of protein were assessed by Western blot analysis using tubulin as loading control. Data are shown as one representative out of four independent experiments.

To verify if GILZ downregulation after TNF-α treatment occurred not only on protein, but also on mRNA level, the GILZ mRNA levels after TNF-α treatment were measured using real-time RT-PCR. As shown in Figure 8, GILZ expression was also significantly decreased on mRNA level.
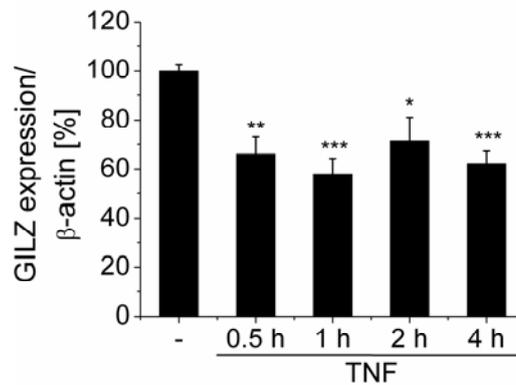
Figure 8: GILZ mRNA expression after TNF-α. HUVEC were either left untreated (-) or treated with 10 ng/ml TNF-α for the indicated times. mRNA expression was measured by real-time RT-PCR using β-actin for normalisation. Data for untreated cells were set as one hundred percent and expression is shown as mean ±SEM of three independent experiments performed in duplicates. *p<0.05, **p<0.01, ***p<0.001 compared to untreated cells.

3.2   TLR mRNA expression after TNF-α

3.2.1 TLR2 mRNA expression after TNF-α

TNF-α has been shown to induce the expression of TLR2 as well as the expression of the inflammation marker MCP-1 (Satta *et al.*, 2008; Weber *et al.*, 2003). In order to confirm these data from the literature, mRNA levels were measured after TNF-α treatment. Using real-time RT-PCR both TLR2 and MCP-1 mRNA expression was significantly increased (Figure 9).
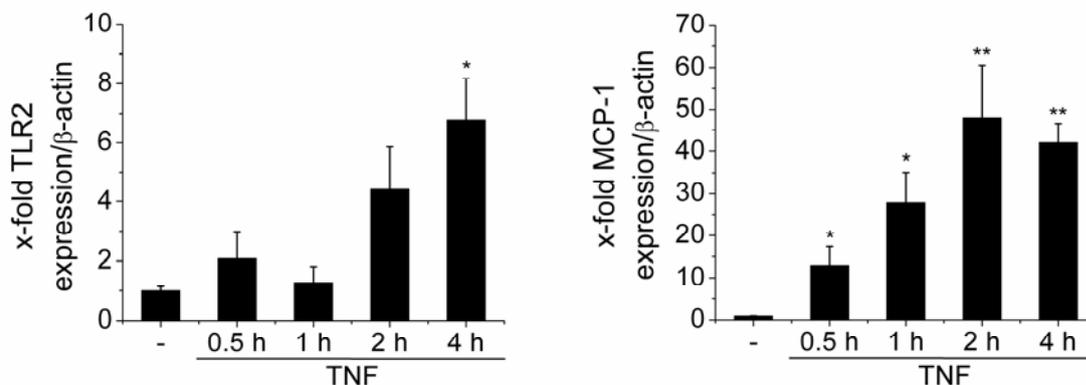

Figure 9: TLR2 and MCP-1 mRNA expression after TNF-α. HUVEC were either left untreated (-) or treated with 10 ng/ml TNF-α for the indicated times. mRNA expression was measured by real-time RT-PCR using β-actin for normalisation. Data for untreated cells were set as one and x-fold expression is shown as mean ±SEM of three independent experiments performed in duplicates. *p<0.05, **p<0.01 compared to untreated cells.

3.2.2 TLRs 1, 4 and 6 mRNA expression after TNF-α

Because of the TNF-α-induced expression of TLR2, we aimed to determine the effect of TNF-α on the expression of the TLR2 co-receptors TLR1 and TLR6 as well as on TLR4 expression. Concordantly to TLR2, TLR1 mRNA was upregulated by TNF-α, whereas TLR4 mRNA expression was diminished (Nadège Ripoche, unpublished data). In contrast to the TLR2 co-receptor TLR1, TLR6 mRNA expression was diminished when TLR2 mRNA was maximally expressed (Figure 10). At earlier timepoints, however, a increased expression of TLR6 mRNA could be observed.
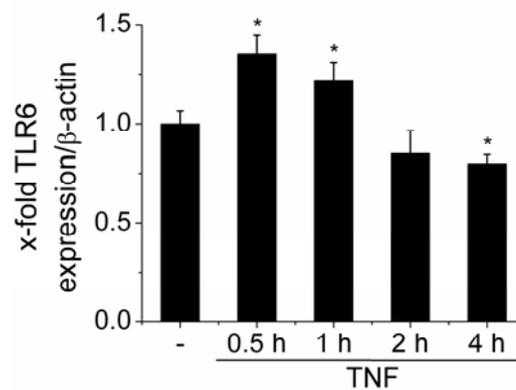
Figure 10: TLR6 mRNA expression after TNF-α. HUVEC were either left untreated (-) or treated with 10 ng/ml TNF-α for the indicated times. mRNA expression was measured by real-time RT-PCR using β-actin for normalisation. Data for untreated cells were set as one and x-fold expression is shown as mean ±SEM of three independent experiments performed in duplicates. *p<0.05 compared to untreated cells.

3.3   Effect of GILZ on TLR mRNA expression

3.3.1 TLR mRNA expression after GILZ knockdown

The TNF-α-mediated diminished expression of GILZ, while TLR2 and MCP-1 were significantly upregulated, led to the suggestion that GILZ downregulation might have functional implications in inflammatory activation of endothelial cells. Therefore, we decided to knock down GILZ by siRNA. Functionality of siRNA transfection was confirmed by Western blot analysis and real-time RT-PCR (Figure 11). To determine the effect of GILZ knockdown on TLR2 mRNA expression, we aimed to investigate the earliest time point when GILZ protein levels were reduced. GILZ protein was firstly knocked down 20 h after siRNA transfection, and 24 h after siRNA transfection the knockdown of GILZ protein was still evident (Figure 11 and data not shown).

A

B
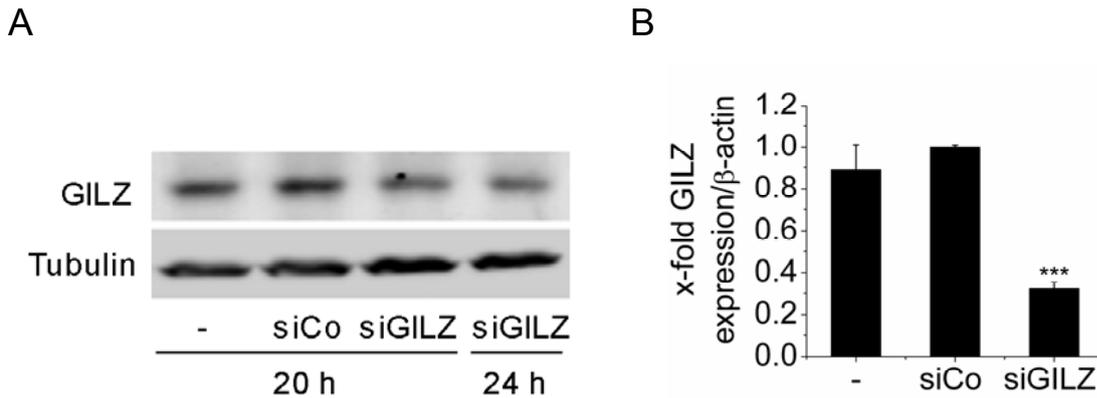
**Figure 11: GILZ knockdown after siRNA transfection. HUVEC were either nucleofected in the absence of siRNA (-) or transfected with siControl (siCo) or siGILZ for 20 h (A, B) and 24 h (A). A: Equal amounts of protein were assessed by Western blot analysis using tubulin as loading control. Data are shown as one representative out of four independent experiments. B: mRNA expression was measured by real-time RT-PCR using β-actin for normalisation. Data for siCo transfected cells were set as one and x-fold expression is shown as mean ±SEM of three independent experiments performed in duplicates. ***p<0.001 compared to siCo transfected cells.**

After determination of the earliest time point, when GILZ protein was knocked down, the effect of GILZ knockdown on TLR2 mRNA expression was examined. As shown in Figure 12, TLR2 mRNA was significantly increased after siGILZ knockdown.
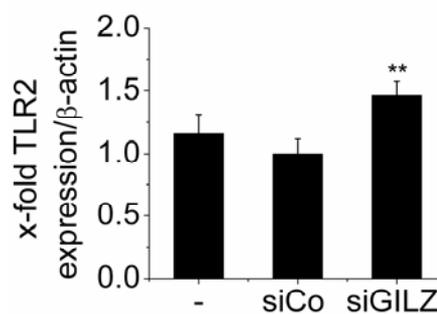
Figure 12: Effect of GILZ knockdown on TLR2 mRNA expression. HUVEC were either nucleofected in the absence of siRNA (-) or transfected with siControl (siCo) or siGILZ for 20 h. mRNA expression was measured by real-time RT-PCR using β-actin for normalisation. Data for siCo transfected cells were set as one and x-fold expression is shown as mean ±SEM of three independent experiments performed in duplicates. **p<0.01 compared to siCo transfected cells.

Because of the influence of GILZ on TLR2 expression, we also measured the expression levels of the TLR2 co-receptors TLR1 and TLR6 as well as TLR4 after GILZ knockdown. Using real-time RT-PCR a significantly increased TLR6 mRNA expression was found after GILZ knockdown, while TLR1 and TLR4 mRNA expression levels were not affected (Figure 13).
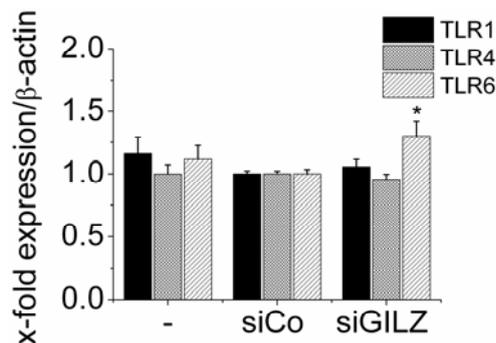

Figure 13: Effect of GILZ knockdown on TLRs 1, 4 and 6 mRNA expression. HUVEC were either nucleofected in the absence of siRNA (-) or transfected with siControl (siCo) or siGILZ for 20 h. mRNA expression was measured by real-time RT-PCR using β-actin for normalisation. Data for siCo transfected cells were set as one and x-fold expression is shown as mean ±SEM of three independent experiments performed in duplicates. *p<0.05 compared to siCo transfected cells.

3.3.2 TLR mRNA expression after GILZ overexpression

In order to clarify the inverse correlation of GILZ and TLR2 and TLR6 expression, we aimed to overexpress GILZ. Transfection of HUVEC with a plasmid containing a cDNA of human GILZ-ORF (*open reading frame*) as insert led to a GILZ overexpression on mRNA level, which was investigated by real-time PCR (Figure 14). However, an overexpression of GILZ protein was never possible (data not shown).
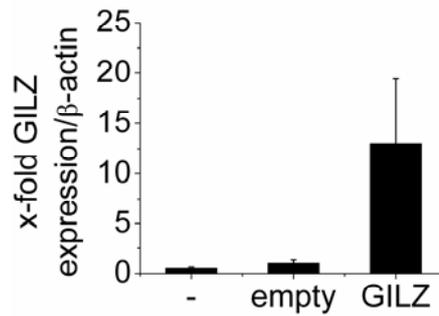
Figure 14: GILZ mRNA levels after GILZ overexpression. HUVEC were either left untreated (-) or transfected with empty control vector (empty) or GILZ plasmid for 16 h. mRNA expression was measured by real-time RT-PCR using β-actin for normalisation. Data for empty vector transfected cells were set as one and x-fold expression is shown as mean ±SEM of one experiment performed in duplicates.

Because GILZ overexpression after plasmid transfection was only possible on mRNA level, the cells were alternatively treated cells with dexamethasone for 8 h in order to induce GILZ protein (Figure 6). A significantly decreased mRNA expression for TLR2, both of its co-receptors TLR6 and TLR1, as well as for the inflammation marker MCP-1 was oberserved by real-time RT-PCR (Figure 15).
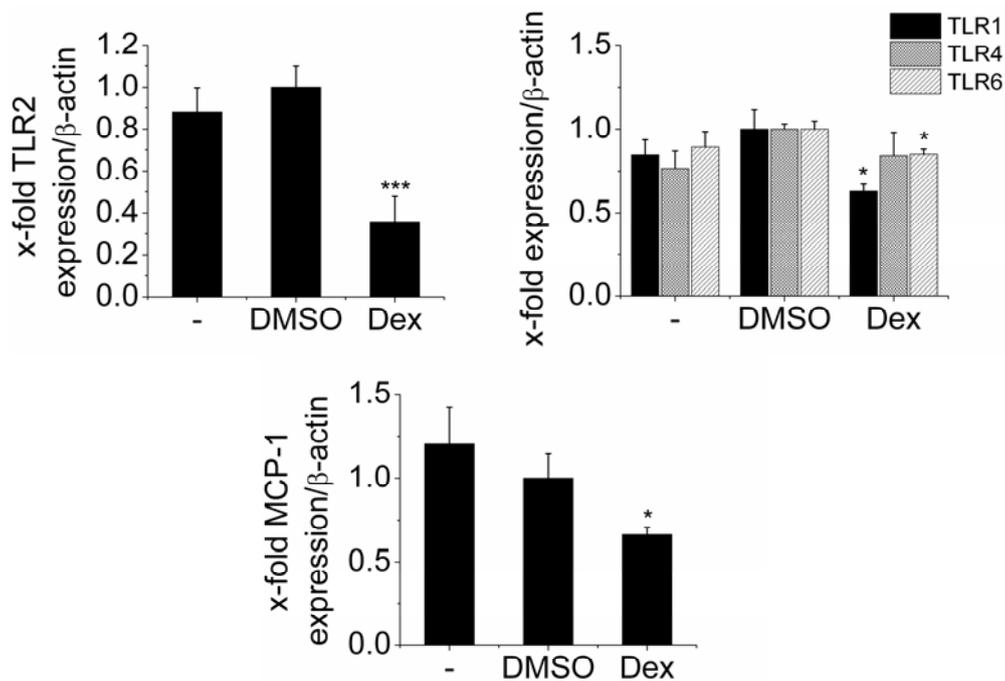

Figure 15: Effect of GILZ induction by dexamethasone (Dex) on TLRs 1, 2, 4, 6 and MCP-1 mRNA expression. HUVEC were either left untreated (-) or treated with Dex or an equal volume

of DMSO as solvent control for 8 h. mRNA expression was measured by real-time RT-PCR using β-actin for normalisation. Data for DMSO treated cells were set as one and x-fold expression is shown as mean ±SEM of three independent experiments preformed in duplicates. *p<0.05, ***p<0.001 compared to DMSO treated cells.

Taken together, knockdown and induction studies indicated that GILZ is involved in regulation of TLR2 and TLR6 expression.

3.4 GILZ mRNA expression in atherosclerotic arteries

In order to establish the inverse expression of TLR2 and GILZ also in atherosclerotic lesions, samples from human atherosclerosis patients were analyzed. This preliminary set of experiments was performed in atherosclerotic intima cylinders of coronary arteries compared to healthy aortae using real-time RT-PCR. Because coronary arteries are originated from the ascending aorta, it was possible to compare both with each other. As shown in Figure 16, GILZ mRNA expression levels in atherosclerotic coronary arteries were diminished, while TLR2 mRNA was increased when comparing geometric as well as arithmetic means.
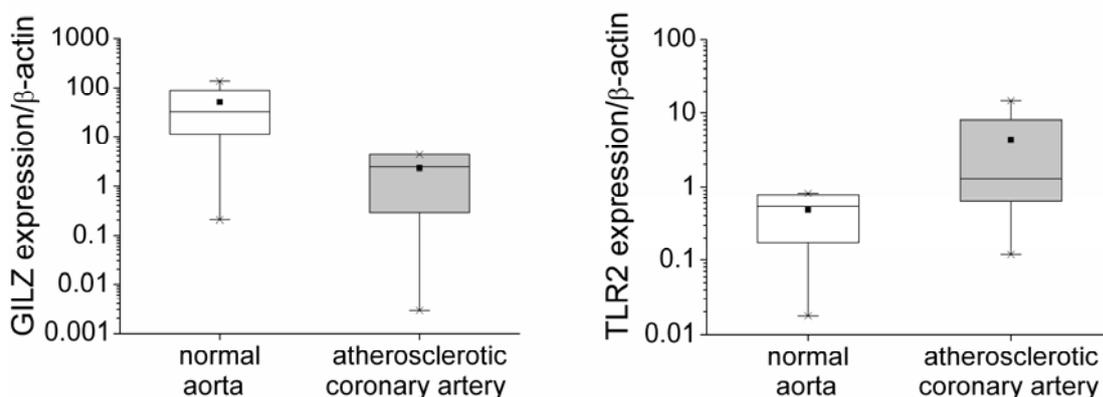

Figure 16: GILZ and TLR2 mRNA expression in atherosclerotic coronary arteries. mRNA expression in normal aortae (n=4) and atherosclerotic intima cylinders of coronary arteries (n=4) was measured by real-time RT-PCR using β-actin for normalisation. Data are presented as boxes with arithmetic medians (square), 25th and 75th percentiles as boxes within geometric medians (line), and 10th and 90th percentiles as whiskers.

To confirm these findings GILZ and TLR mRNA expression levels were also investigated in atherosclerotic and normal internal mammary arteries (IMA) using real-time RT-PCR. As shown in Figure 17, GILZ expression was also downregulated in atherosclerotic compared to normal IMA, while for TLR2 an increased expression was observed.
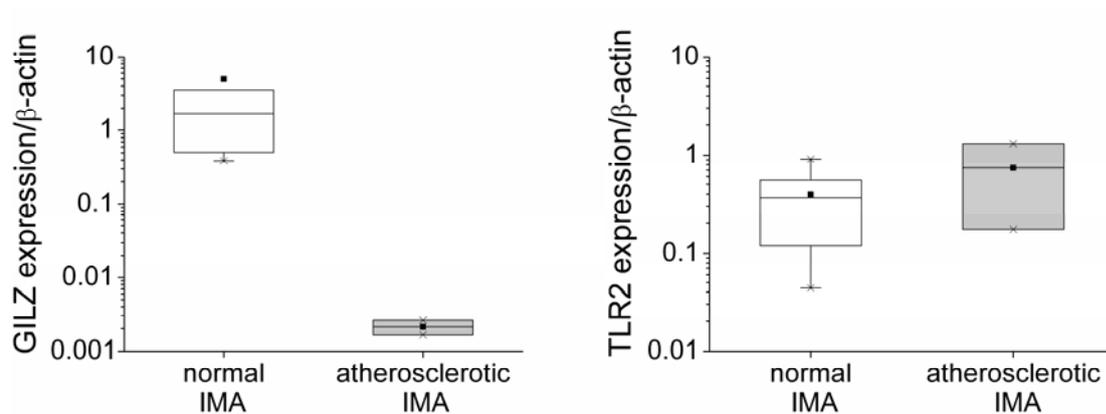

Figure 17: GILZ and TLR2 mRNA expression in atherosclerotic internal mammary arteries (IMA). mRNA expression in normal IMA (n=5) and atherosclerotic IMA (n=2) was measured by real-time RT-PCR using β-actin for normalisation. Data are presented as boxes with arithmetic medians (square), 25th and 75th percentiles as boxes within geometric medians (line), and 10th and 90th percentiles as whiskers.

3.5 Role of NF-κB and AP-1 in TLR expression

The results in atherosclerotic arteries verified the observations made in HUVEC that GILZ downregulation is connected to TLR2 upregulation.

In order to clarify the mechanisms of GILZ-dependent TLR expression the role of transcription factors probably involved had to be determined. GILZ has been described to inhibit both NF-κB and AP-1 (Ayroldi & Riccardi, 2009). We therefore aimed to investigate the role of these transcription factors in TLR expression and to analyze this aspect in TNF-α-activated cells using decoy oligonucleotide transfection. Functionality of NF-κB and AP-1 oligonucleotide decoy transfection was confirmed by EMSA (Figure 18).

A

B
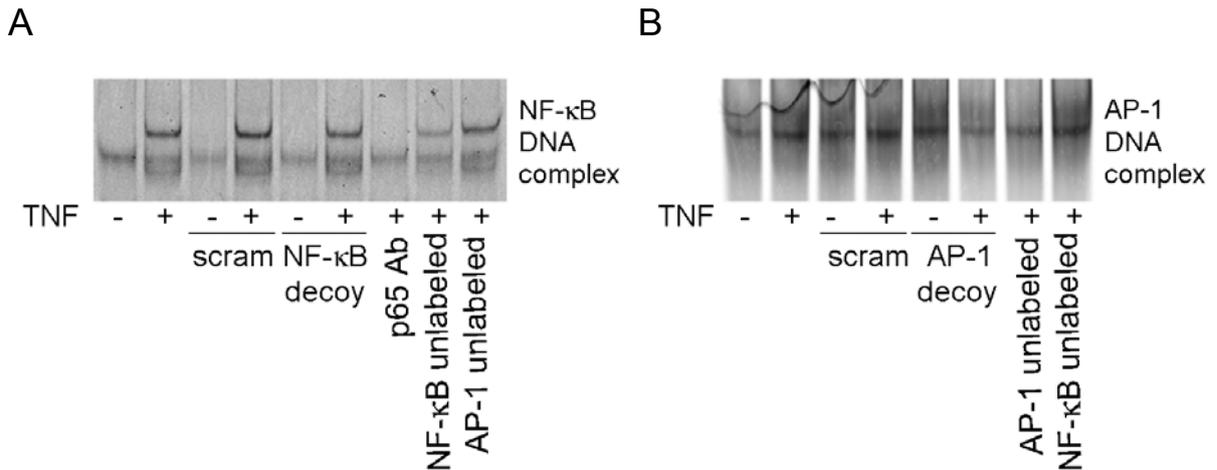
Figure 18: Inhibition of NF-κB and AP-1 activation after decoy oligonucleotide transfection. HUVEC were either left untransfected or transfected with scrambled (scram), NF-κB (A) or AP-1 (B) decoy oligonucleotides. 4 h after transfection they were either left untreated (-) or additionally treated with 10 ng/ml TNF-α (+), 20 min for NF-κB activation (A) or 1 h for AP-1 activation (B) and EMSA was performed. Functionality of the EMSA was confirmed using unlabeled NF-κB and AP-1 decoy oligonucleotides for control (A, B) or using anti-p65 antibody for NF-κB supershift (A). Data are shown as one representative out of five independent experiments.

Successful NF-κB decoy oligonucleotide transfection was not only confirmed by EMSA for each experiment (data not shown), but also by MCP-1 mRNA measurement (Figure 19). MCP-1 has been known to be regulated *via* NF-κB in endothelial cells (Ishizuka *et al.*, 2000). To determine the expression of TLRs 1, 2, 4, and 6 expression after NF-κB oligonucleotide decoy transfection real-time RT-PCR was performed. As shown in Figure 19, NF-κB was significantly involed in the TNF-α-induced expression of TLR2, but neither in the expression of its co-receptors TLR1 and TLR6 nor in TLR4 expression.
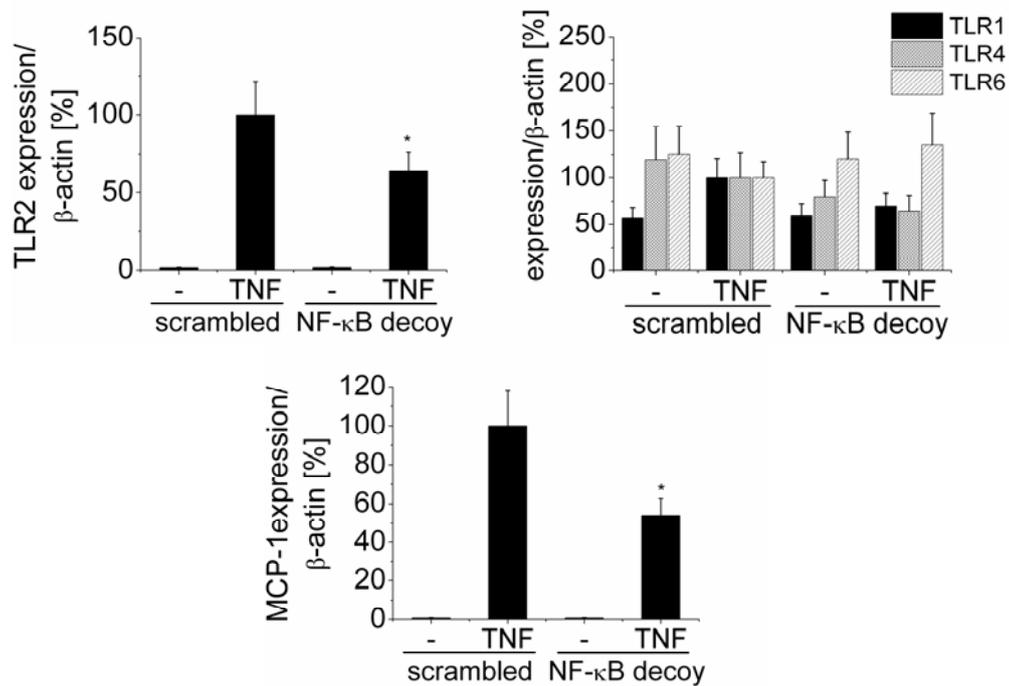
Figure 19: Involvement of NF-κB in TLRs 1, 2, 4, 6 and MCP-1 mRNA expression. HUVEC were either transfected with scrambled or NF-κB decoy oligonucleotides for 4 h, and were either left untreated (-) or treated with 10 ng/ml TNF-α for another 4 h. mRNA expression was measured by real-time RT-PCR using β-actin for normalisation. Data for scrambled transfected and TNF-α treated cells were set as one hundred percent and expression is shown as mean ±SEM of three independent experiments performed in duplicates. *p<0.05 compared to scrambled transfected and TNF-α treated cells.

To investigate the role of AP-1 in GILZ-dependent TLR expression, AP-1 oligonucleotide decoy transfection was confirmed for each experiment by EMSA (data not shown). In contrast to NF-κB, data did not indicate an involvement of AP-1 in TNF-α-induced TLR expression (Figure 20). TNF-α-induced MCP-1 expression, known to be regulated in endothelial cells *via* AP-1 (Ishizuka *et al.*, 2000), was significantly reduced in AP-1 decoy transfected cells.
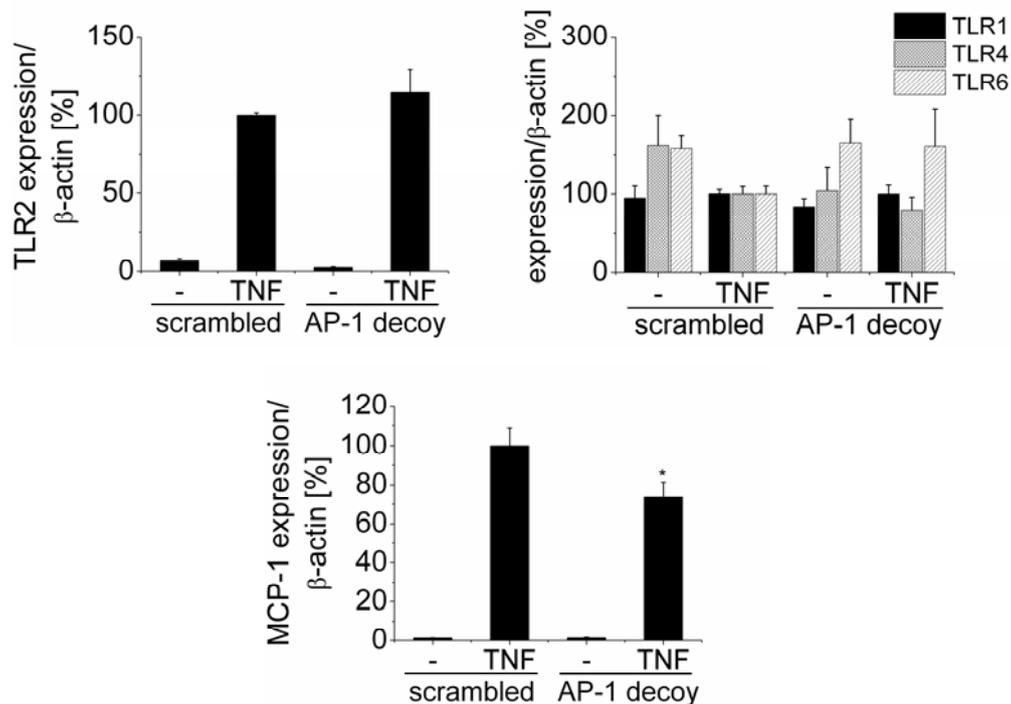
Figure 20: Involvement of AP-1 in TLRs 1, 2, 4, 6 and MCP-1 mRNA expression. HUVEC were either transfected with scrambled or AP-1 decoy oligonucleotides for 4 h, and were either left untreated (-) or treated with 10 ng/ml TNF-α for another 4 h. mRNA expression was measured by real-time RT-PCR using β-actin for normalisation. Data for scrambled transfected and TNF-α treated cells were set as one hundred percent and percentaged expression is shown as mean ±SEM of four independent experiments preformed in duplicates. *p<0.05 compared to scrambled transfected and TNF-α treated cells.

3.6 NF-κB activation after GILZ knockdown

3.6.1 Nuclear translocation of NF-κB after GILZ knockdown

Since NF-κB was critical in the induction of TLR2 expression and since GILZ knockdown induced TLR2 expression, we hypothesized that absence of GILZ might release NF-κB and induce nuclear translocation. GILZ was therefore knocked down by siRNA transfection and nuclear translocation of the NF-κB subunits p65 and p50 was investigated. In fact, as shown in Figure 21, a nuclear translocation of p65 and p50 was observed by Western blot analysis after GILZ knockdown.
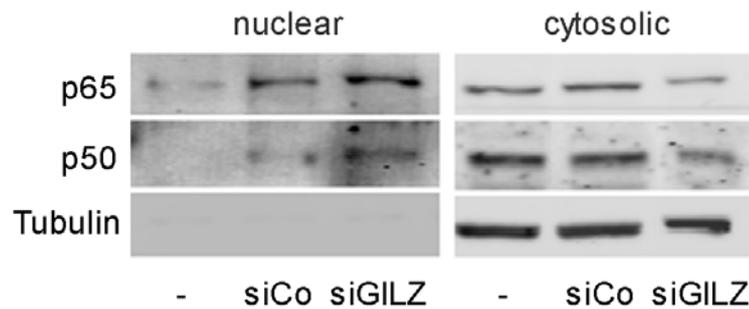
Figure 21: Nuclear translocation of NF-κB after GILZ knockdown. Cells were either left untransfected (-) or transfected with siControl (siCo) or siGILZ for 20 h. Equal amounts of protein of nuclear and cytosolic fractions were assessed by Western blot analysis using tubulin as loading control. Data are shown as one representative out of three independent experiments.

3.6.2 NF-κB activation after GILZ knockdown

In order to test whether siGILZ-induced nuclear translocated NF-κB was in fact transcriptionally active, a luciferase reporter gene under an NF-κB promoter was used for promoter gene assay. Successful GILZ knockdown after additional transfection with the luciferase plasmid was confirmed using Western blot analysis (Figure 22).
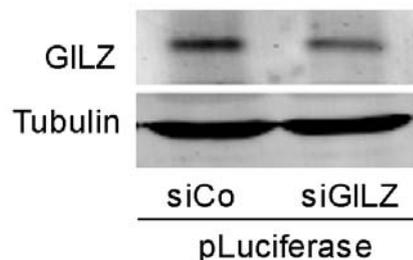

Figure 22: GILZ knockdown after additional luciferase plasmid (pLuciferase) transfection. HUVEC were transfected with either siControl (siCo) or siGILZ and pLuciferase for 20 h. Equal amounts of protein were assessed by Western blot analysis using tubulin as loading control. Data are shown as one representative out of five independent experiments.

GILZ knockdown after additional luciferase plasmid transfection was performed for each experiment (data not shown). As shown in Figure 23, GILZ knockdown led to a significantly increased NF-κB activity compared to control transfected cells.
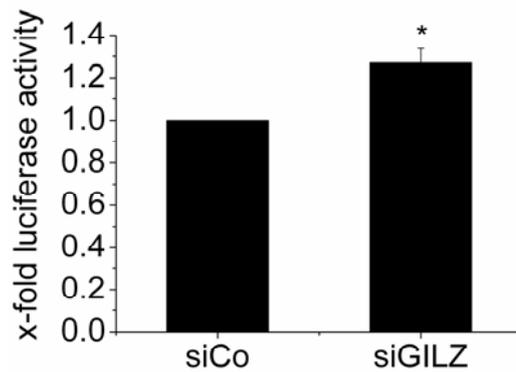
Figure 23: NF-κB activation after GILZ knockdown. HUVEC were transfected with either siControl (siCo) or siGILZ and a luciferase plasmid for 20 h. NF-κB activity was measured by luciferase assay. Data for siCo transfected cells were set as one and are shown as mean ±SEM of three independent experiments performed in quinticates. *p<0.05 compared to siCo transfected cells.

Since NF-κB is known to be activated by TNF-α, functionality of the luciferase assay was confirmed measuring TNF-α-induced NF-κB activity (Figure 24).
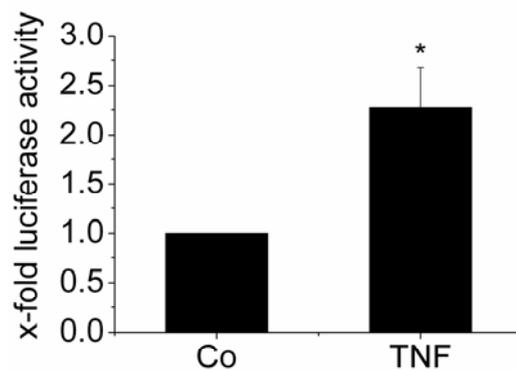

Figure 24: NF-κB activation after TNF-α. HUVEC were transfected with a luciferase plasmid for 20 h, and were either left untreated (Co) or treated with 10 ng/ml TNF-α for another 5 h. NF-κB activity was measured by luciferase assay. Data for Co transfected cells were set as one and x-fold luciferase activity is shown as mean ±SEM of three independent experiments performed in quinticates. *p<0.05 compared to Co.

3.6.3 IκB protein level after GILZ knockdown

IκB degradation is essential for NF-κB activation (Kiemer e*t al*., 2002c). Therefore, IκBα protein levels were examined after GILZ knockdown by Western blot analysis. In

parallel to GILZ decay and NF-κB activation, diminished IκBα protein levels were detected (Figure 25).
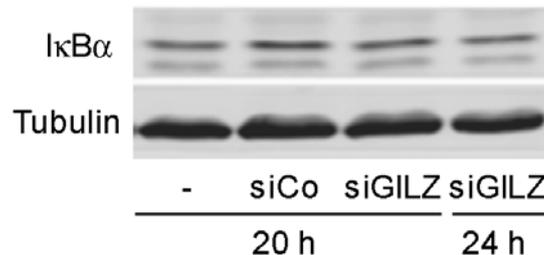
**Figure 25: IκBα protein level after GILZ knockdown. HUVEC were either left untransfected (-) or transfected with siControl (siCo) or siGILZ for the indicated times. Equal amounts of protein were assessed by Western blot analysis using tubulin as loading control. Data are shown as one representative out of three independent experiments.**

3.6.4 NF-κB translocation after GILZ knockdown and TNF-α

For endothelial cells a desensitization after cell activation has been described (Wada *et al.*, 2005), i.e. activation of NF-κB after a prior activation is suppressed. This led to the hypothesis that NF-κB activation of HUVEC by GILZ knockdown results in a reduced activation after TNF-α treatment. In cells transfected with GILZ siRNA for 20 h, subsequent treatment with TNF-α in fact led to a diminished nuclear translocation of the NF-κB subunits p65, p50 and c-Rel as investigated by Western blot analysis (Figure 26).
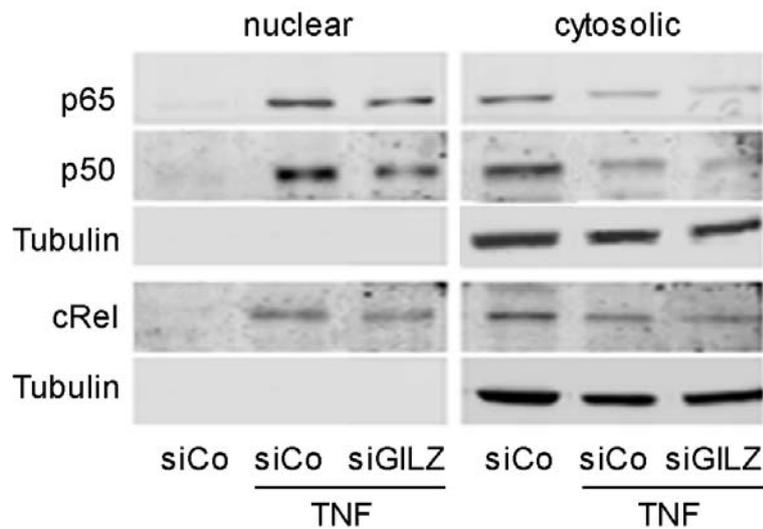
Figure 26: Nuclear translocation of p65, p50 and cRel after GILZ knockdown und additional TNF-α treatment. Cells were either transfected with siControl (siCo) or siGILZ for 20 h, and were either left untreated or treated with 10 ng/ml TNF-α for another 20 min. Equal amounts of protein of nuclear and cytosolic fractions were assessed by Western blot analysis using tubulin as loading control. Data are shown as one representative out of three independent experiments.

Interestingly, not only the nuclear translocation of the NF-κB subunits was diminished, but also the cytosolic protein levels in general seemed to be reduced after GILZ knockdown (Figure 26). In order to test whether the NF-κB protein levels indeed were diminished after GILZ knockdown, whole cell extracts were examined by Western blot analysis. As shown in Figure 27, p65 protein levels were in fact diminished after GILZ knockdown.
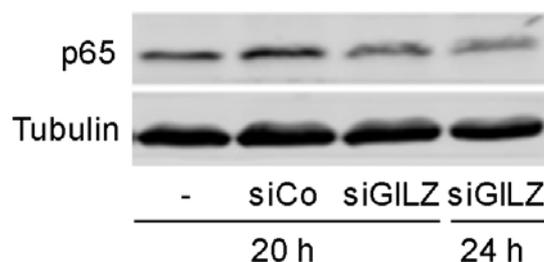

Figure 27: p65 protein level after GILZ knockdown. HUVEC were either left untransfected (-) or transfected with siControl (siCo) or siGILZ for the indicated times. Equal amounts of protein were assessed by Western blot analysis using tubulin as loading control. Data are shown as one representative out of three independent experiments.

3.6.5 NF-ĸB activation after GILZ knockdown and TNF-α

In order to investigate whether reduced NF-ĸB translocation was correlated with reduced transcriptional activity, NF-ĸB activation after GILZ knockdown and additional treatment with TNF-α was investigated using luciferase assay. As shown in Figure 28, a significantly reduced NF-ĸB activity compared to siControl (siCo) transfected and TNF-α treated cells was observed.
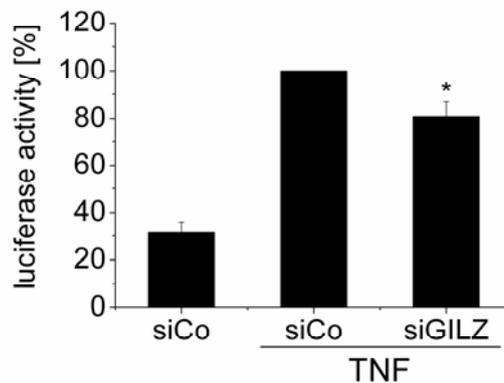

Figure 28: NF-ĸB activation in TNF-α treated cells after prior GILZ knockdown. HUVEC were either transfected with siControl (siCo) or siGILZ and additionally with a luciferase plasmid. 20 h after transfection cells were either left untreated or treated with 10 ng/ml TNF- α for another 5 h. NF-ĸB activity was measured by luciferase assay. Data for siCo transfected and TNF-α treated cells were set as one hundred percent and luciferase activity is shown as mean ±SEM of three independent experiments performed in quinticates. *p<0.05 compared to siCo transfected and TNF-α treated cells.

These findings showed that disappearance of GILZ can liberate NF-ĸB and induce its nuclear translocation and activation of endothelial cells.

3.7 Role of p38 MAPK in TNF-α-mediated TLR mRNA expression

Chemical inhibitors of p38 MAPK have been shown to inhibit endothelial TLR2 expression. However, neither effects of p38 MAPK on other TLRs nor the responsible p38 MAPK isoform has been described. We therefore aimed to study these aspects and to determine a potential role of GILZ in p38 MAPK-induced actions. Inhibition of p38 MAPK was accomplished by either SB203580 (4-[5-(4-fluorophenyl)-2-(4-

methylsulfinylphenyl)-3Himidazol-4-yl]pyridine) or atrial natriuretic peptide (ANP) in TNF-α treated cells.

3.7.1 Inhibition of p38 MAPK by SB203580

p38 MAPK activation by TNF-α and its inhibition by SB203580 were confirmed by Western blot analysis (Figure 29).
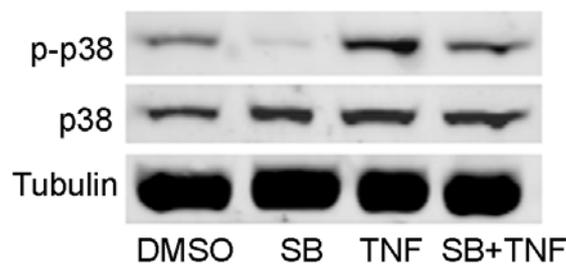

Figure 29: Inhibition of p38 MAPK activation by SB203580 (SB). HUVEC were either pretreated with 10 ng/ml SB or an equal volume of DMSO as solvent control for 30 min and treated with 10 ng/ml TNF-α for 20 min. Cells treated with TNF-α were also pretreated with DMSO. Equal amounts of protein were assessed by Western blot analysis using tubulin as loading control. Data are shown as one representative out of three independent experiments.

To confirm these findings for p38 MAPK activation and inhibition and to investigate the cellular translocation of p38 MAPK in this context, immunofluorescence staining was performed. As shown in Figure 30, p38 MAPK was phosphorylated after TNF-α treatment, which led to p38 MAPK translocation into the nucleus, whereas SB203580 inhibited both this activation and nuclear translocation. Interestingly, phosphorylated p38 MAPK was not only localized in the nucleus, but also in the cytoplasm.
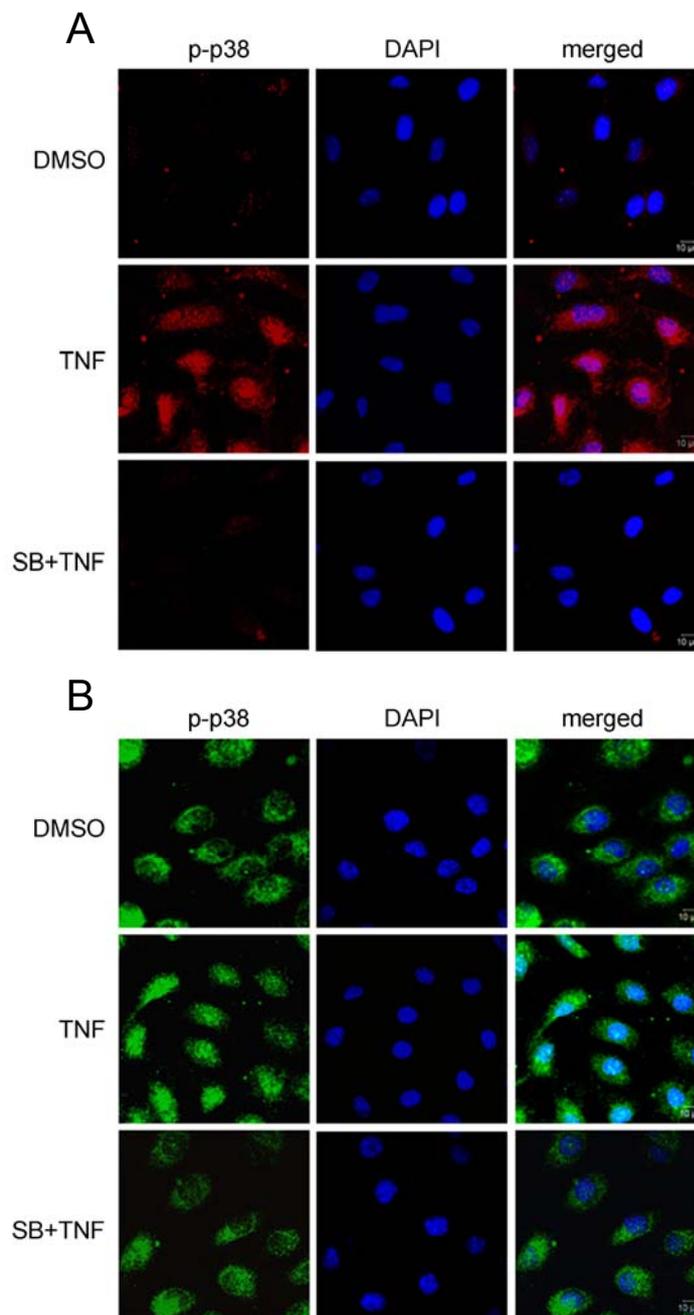
Figure 30: Inhibition of phosphorylation and nuclear translocation of p38 MAPK by SB203580 (SB). Cells were either pretreated with 10 ng/ml SB or an equal volume of DMSO as solvent control for 30 min and treated with 10 ng/ml TNF-α for 20 min. Cells treated with TNF-α were also pretreated with DMSO. p-p38 (A) and p38 (B) were stained using immunofluorescence and nuclear staining was performed using DAPI. Photographs were taken with 400-fold magnification. Data are shown as one representative out of three independent experiments.

Examinations of p38 MAPK-dependent TLR expression were assessed by real-time RT-PCR. The inflammatory marker MCP-1 mRNA was also measured, as it is known to be regulated *via* p38 MAPK (Weber *et al.*, 2003).

As shown in Figure 31, an abrogation of TNF-α-induced actions on both TLR2 and MCP-1 expression by SB203580 was observed. TLR4 and TLR6 were significantly downregulated upon TNF-α treatment, whereas TLR1 was induced. TLR6 downregulation was significantly abrogated by p38 MAPK inhibition, whereas neither TLR1 nor TLR4 expression was influenced.
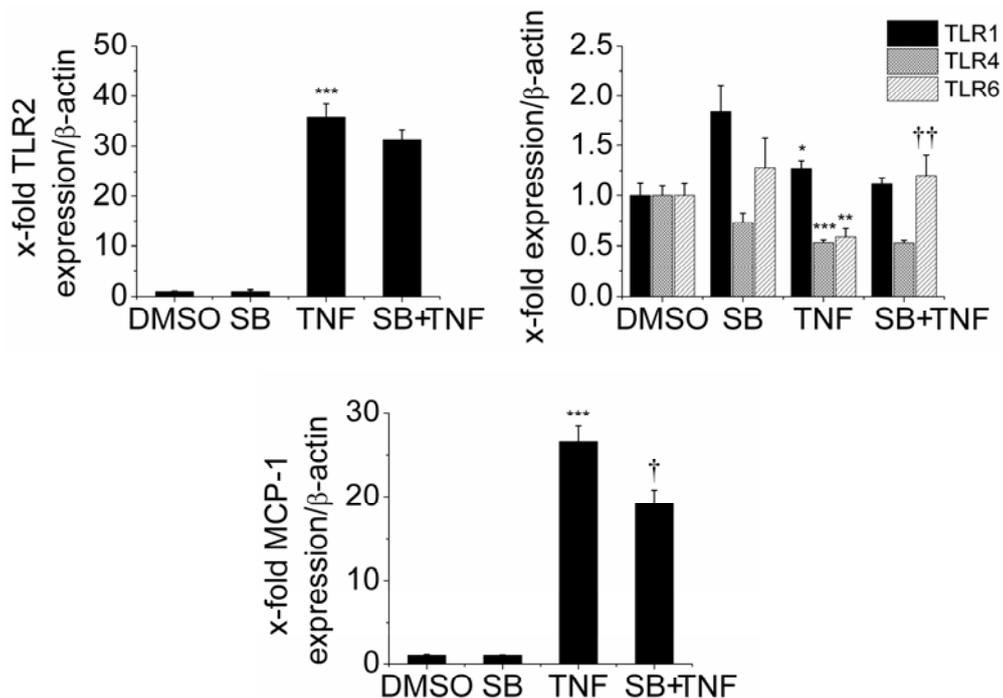
Figure 31: Involvement of p38 MAPK in TLRs 1, 2, 4, 6 and MCP-1 mRNA expression by SB203580 (SB). HUVEC were either pretreated with 10 ng/ml SB or an equal volume of DMSO as solvent control for 30 min and treated with 10 ng/ml TNF-α for 4 h. Cells treated with TNF-α were also pretreated with DMSO. mRNA expression was measured by real-time RT-PCR using β-actin for normalisation. Data for DMSO treated cells were set as one and x-fold expression is shown as mean ±SEM of five independent experiments performed in triplicates. *p<0.05, **p<0.01, ***p<0.001 compared to DMSO treated cells; †p<0.05, ††p<0.01 compared to TNF-α treated cells.

3.7.2 Inhibition of p38 MAPK by ANP

ANP was applied as a second pharmacological inhibitor of p38 MAPK, which has been described to inhibit p38 MAPK phosphorylation (Weber *et al.*, 2003). The inhibition of p38 MAPK activation was confirmed by Western blot analysis (Figure 32).
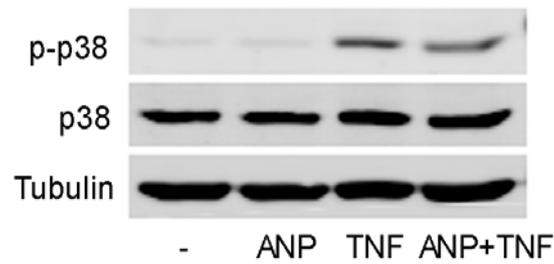
Figure 32: Inhibition of p38 MAPK activation by ANP. HUVEC were either left untreated (-) or pretreated with 10 ng/ml ANP for 30 min and treated with 10 ng/ml TNF-α for 20 min. Equal amounts of protein were assessed by Western blot analysis using tubulin as loading control. Data are shown as one representative out of three independent experiments.

The p38 MAPK-dependent TLR expression using ANP for p38 MAPK inhibition was examined by real-time RT-PCR. As shown in Figure 33, the previous observations were confirmed. TLR2 and MCP-1 were significantly and TLR1 slightly upregulated by TNF-α treatment, while TLR4 and TLR6 were downregulated. TNF-α-induced expression of TLR2 and TLR6 was partially abrogated by p38 MAPK inhibition, whereas TLR1 and TLR4 expression was not influenced.
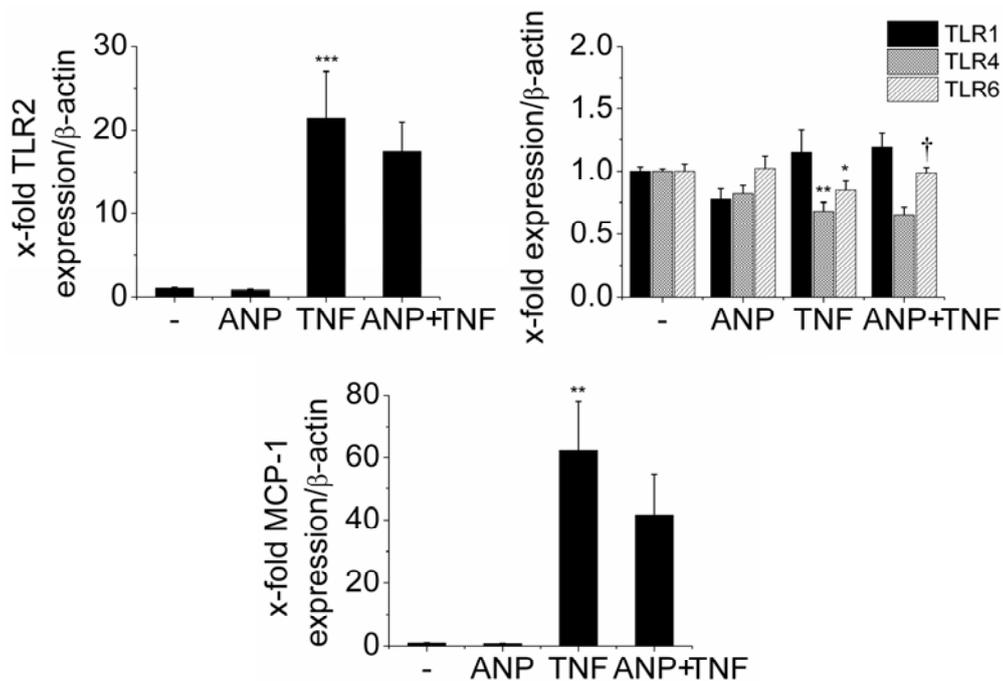
**Figure 33: Involvement of p38 MAPK in TLRs 1, 2, 4, 6 and MCP-1 mRNA expression by ANP. HUVEC were either left untreated (-) or pretreated with 10 ng/ml ANP for 30 min and treated with 10 ng/ml TNF-α for 4 h. mRNA expression was measured by real-time RT-PCR using β-actin for normalisation. Data for untreated cells were set as one and x-fold expression is shown**

as mean ±SEM of three independent experiments preformed in duplicates. *p<0.05, **p<0.01, ***p<0.001 compared to untreated cells; †p<0.05 compared to TNF-α treated cells.

3.7.3 p38 MAPK isoform dependent regulation of TLR expression

In order to determine the p38 MAPK isoform responsible for TNF-α-induced TLR expression, dominant negative (dn) mutants of p38α and p38β2, the major splice variant of p38β (Hale *et al.*, 1999), were overexpressed using plasmid transfection. Western blot analysis showed that only p38α was expressed in HUVEC (Figure 34).
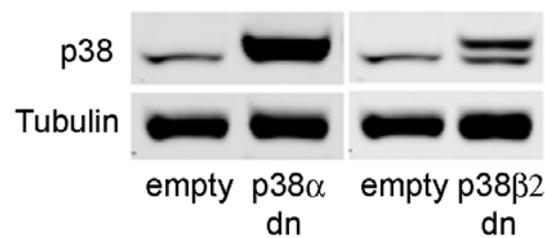
Figure 34: Expression of p38α and p38β2 MAPK in HUVEC. Cells were transfected with either empty control vector (empty) or dominant negative (dn) p38α or dn p38β2 or for 24 h. Equal amounts of protein were assessed by Western blot analysis using tubulin as loading control. Data are shown as one representative out of three independent experiments.

Therefore, the effect of p38α in TNF-α-induced TLR expression was examined by overexpression of dn p38α MAPK. The subsequent inhibition of phosphorylation was confirmed by Western blot analysis (Figure 35).
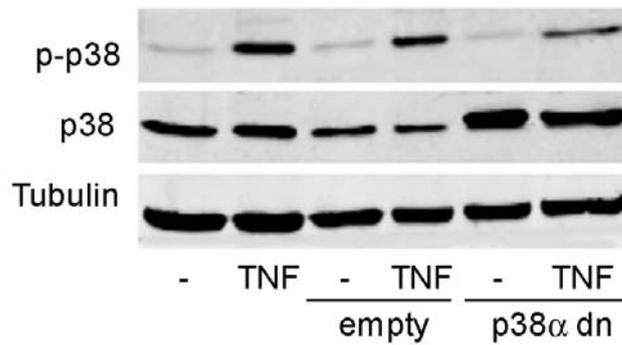
Figure 35: p38 MAPK phosphorylation after dominant negative (dn) p38α MAPK overexpression. HUVEC were either left untransfected or transfected with empty control vector (empty) or dn p38α for 24 h, and were either left untreated or treated with 10 ng/ml TNF-α for another 20 min. Equal amounts of protein were assessed by Western blot analysis using tubulin as loading control. Data are shown as one representative out of three independent experiments.

Examinantion regarding p38α MAPK-dependent TLR expression was performed by real-time RT-PCR. As shown in Figure 36, a significantly diminished TNF-α-induced mRNA expression for TLR2 and MCP-1 was observed after dn p38α overexpression. Again, TLR4 and TLR6 expression was downregulated by TNF-α, whereas TLR1 was slightly induced. The dn p38α MAPK mutant abrogated the TNF-α-induced tendency of TLR6 downregulation, while TLR1 and TLR4 expression was not affected.
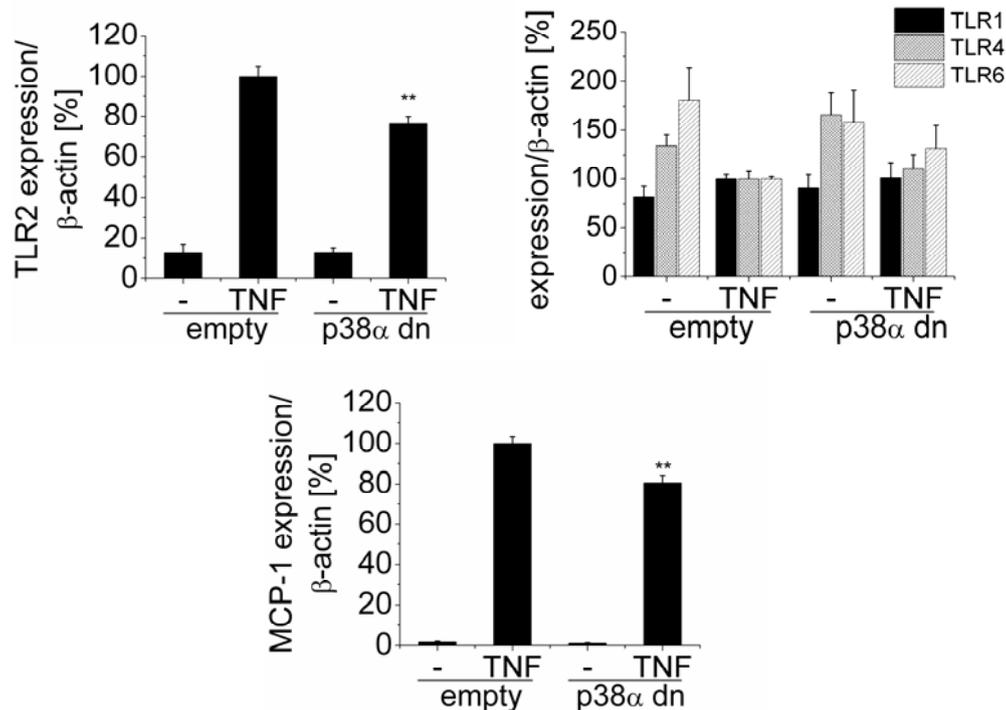
Figure 36: TLRs 1, 2, 4, 6 and MCP-1 mRNA expression after dominant negative (dn) p38α MAPK overexpression. HUVEC were either transfected with empty control vector (empty) or dn p38α for 24 h, and were either left untreated or treated with 10 ng/ml TNF-α for another 4 h. mRNA expression was measured by real-time RT-PCR using β-actin for normalisation. Data for empty vector transfected and TNF-α treated cells were set as one hundred percent and expression is shown as mean ±SEM of four independent experiments preformed in duplicates. **p<0.01, compared to empty vector transfected and TNF-α treated cells.

These findings demonstrated that p38α MAPK abrogates the TNF-α-mediated TLR2 and TLR6 expression, whereas TLR1 and TLR4 expression was not affected.

3.8   Role of p38 MAPK in TNF-α-mediated TLR protein expression

In order to confirm our findings for p38 MAPK-dependent TLR expression on mRNA level, the protein levels were investigated by flow cytometric analysis.

3.8.1   Specifity of the anti-TLR2 antibody

To confirm the specific binding of the anti-TLR2 antibody used for flow cytometric analysis, CHO-K1 cells were used, as these cells have been described to express no functional TLR2 transcript (Heine *et al.*, 1999). Human TLR2 tagged with yellow

fluorescent protein (YFP) was transfected into CHO-K1 and overexpressed. TLR2-YFP protein expression was confirmed by flow cytometric analysis *via* YFP signal detection in the FL1 channel of the cytometer. As shown in Figure 37, TLR2-YFP was expressed in transfected CHO-K1 cells.
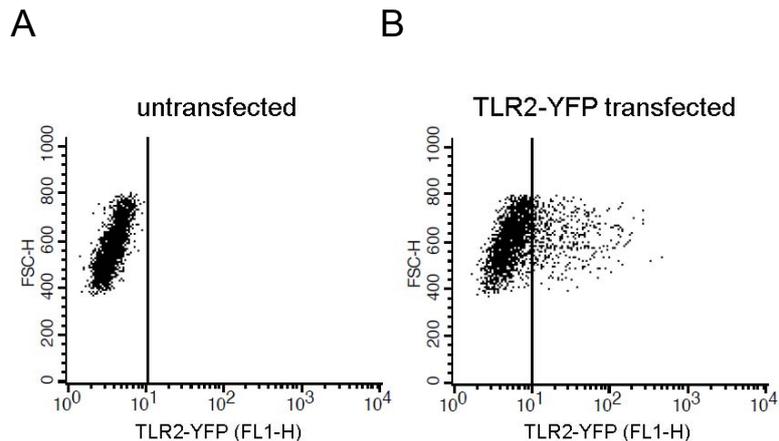
Figure 37: TLR2-YFP expression after plasmid transfection. CHO-K1 cells were either left untransfected (A) or transfected with plasmid containing human TLR2-YFP as insert (B). Flow cytometric investigations were performed 46 h after transfection by measurement of an intact population consisting of 10,000 cells as shown as dot plots (A, B). Data are shown as one representative out of two independent experiments.

In order to examine the binding of anti-TLR2 antibody, TLR2-YFP-negative and -positive cells were stained with anti-TLR2 antibody or a corresponding isotype control. Fluorescence signals were amplified using biotine and streptavidine. Streptavidine was labeled with R-phycoerythrin (R-PE) and therefore detected in the FL2 channel of the cytometer. As shown in Figure 38 A, a small shift was detected in non-transfected antibody-stained cells when compared to isotype control cells. This shift may be explained by antibody binding to endogenous TLR2. Despite CHO-K1 cells exhibit no functional TLR2 protein, they express a TLR2 protein consisting only of the extracellular domain (Heine *et al.*, 1999). When only TLR2-YFP expressing cells were examined, a much clearer shift in the histogram compared to untransfected cells as well as a shift of the cell population shown as dot plots could be demonstrated (Figure 38 B, C and D).
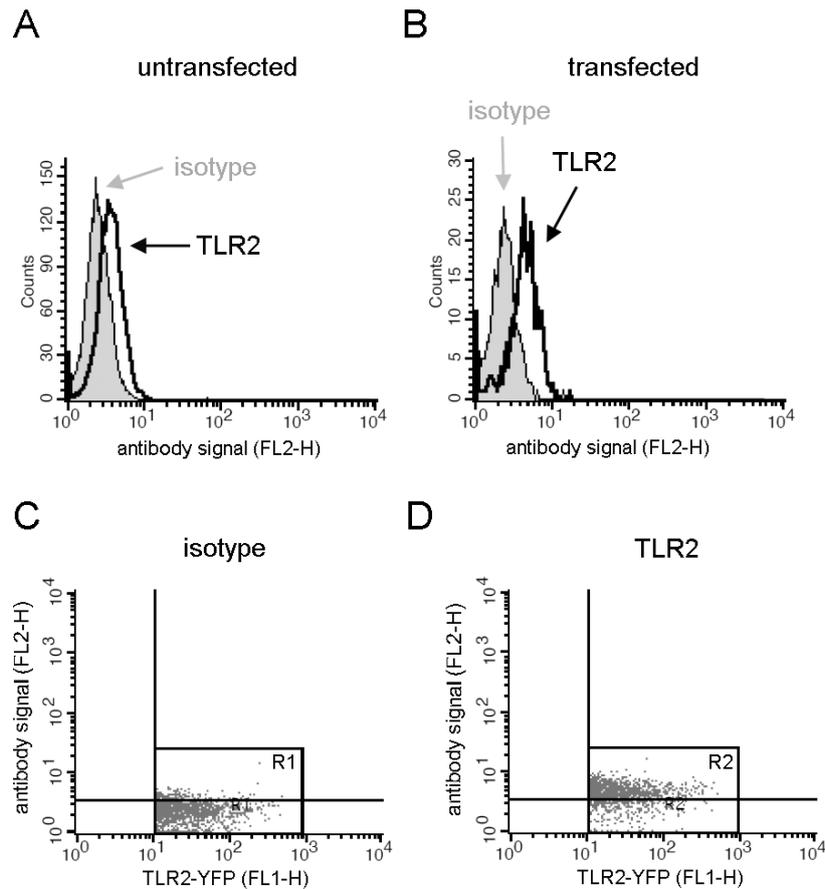
Figure 38: Binding of the anti-TLR2 antibody measured by flow cytometry. Untransfected (A) or TLR2-YFP transfected CHO-K1 cells (B, C, D) were stained with either isotype control (A, B, C) or anti-TLR2 antibody (A, B, D), and cell populations consisting of 10,000 cells were measured. The histograms show the fluorescence intensities of anti-TLR2 antibody staining (without background) compared to isotype control staining (grey background) (A, B). Dot plots (C, D) show TLR2-YFP expressing cells and gates (C: R1, D: R2) were examined regarding their fluorescence intensities (B). Data are shown as one representative out of two independent experiments.

These data demonstrated that the anti-TLR2 antibody binds specific to TLR2 antigens.

3.8.2 p38 MAPK-dependent TLR2 protein expression

After demonstrating that p38 MAPK abrogates TNF-α-induced TLR2 mRNA expression, we aimed to confirm the p38-MAPK dependency in TNF-α-induced TLR2 upregulation on protein level by flow cytometric analysis. As shown in Figure 39, TNF-α induced a significant upregulation of TLR2 protein expression, whereas

inhibition of p38 MAPK by SB203580 led to a diminished TNF-α induced TLR2 expression.
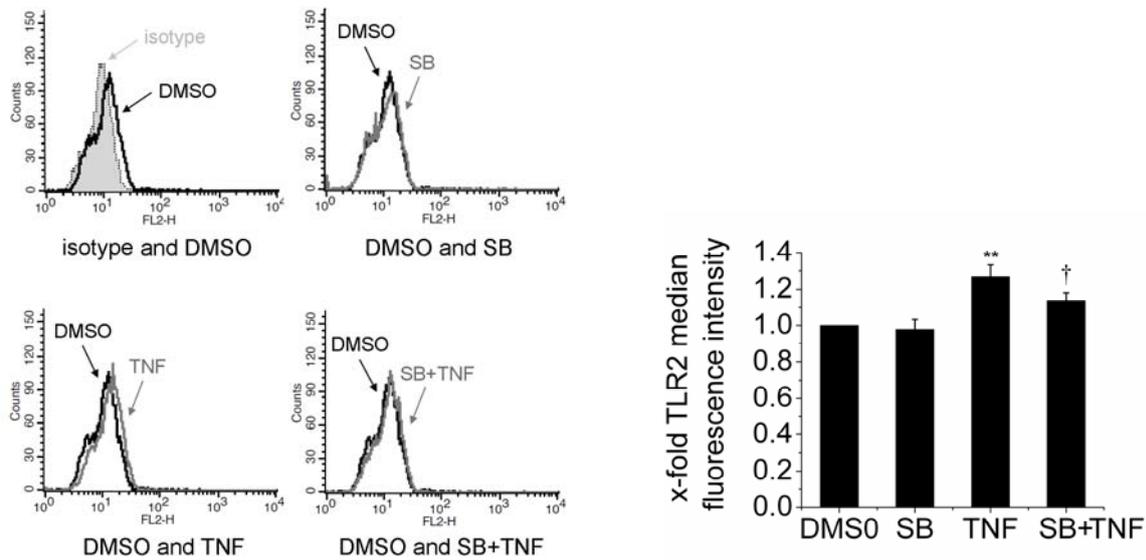
Figure 39: Involvement of p38 MAPK in TLR2 protein expression. HUVEC were either pretreated with 10 ng/ml SB203580 (SB) or an equal volume of DMSO as solvent control for 30 min and treated with 10 ng/ml TNF-α for 8 h. Cells treated with TNF-α were also pretreated with DMSO. Protein expression was measured by flow cytometric analysis. Left panel: representative histograms out of three independent experiments with isotype control (grey background), DMSO treated control (black line) and SB pretreated and/or TNF-α treated cells (grey line). Right panel: after normalisation on isotype control values, DMSO treated control cells were set as one and x-fold expression is shown as mean ±SEM of three independent experiments. **p<0.01 compared to DMSO treated cells; †p<0.05 compared to TNF-α treated cells.

3.8.3 p38 MAPK-dependent TLR1 protein expression

In order to investigate the p38-MAPK dependency in TNF-α-induced TLR1 upregulation, TLR1 protein levels were measured by flow cytometric analysis.

As shown in Figure 40 and confirming the previous results on mRNA level, TLR1 protein expression was slightly increased after TNF-α treatment, while pretreatment with SB203580 does not show an abrogation of this induction.
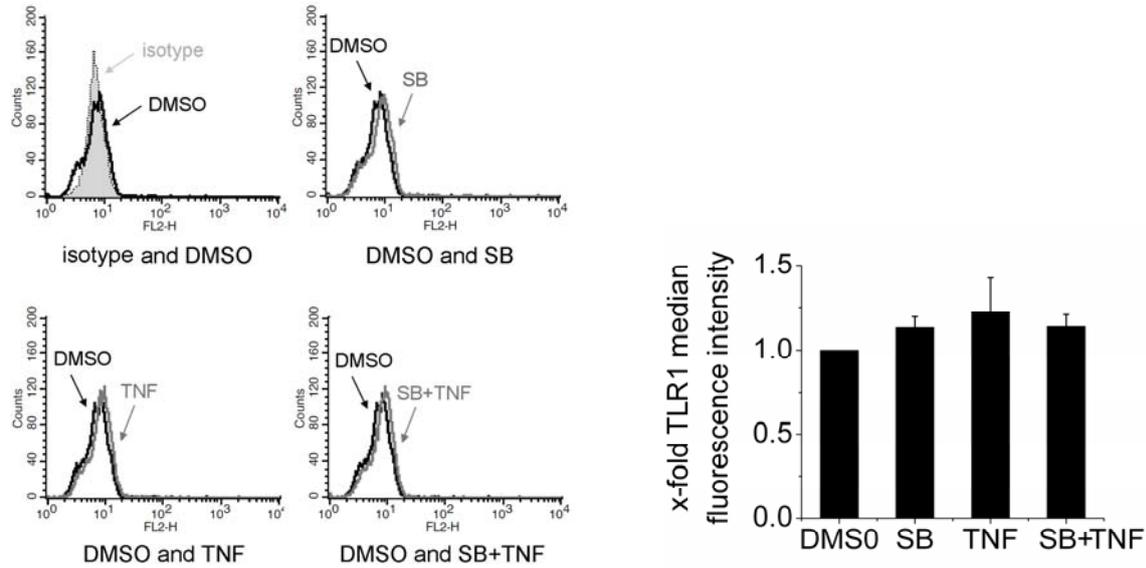
Figure 40: Involvement of p38 MAPK in TLR1 protein expression. HUVEC were either pretreated with 10 ng/ml SB203580 (SB) or an equal volume of DMSO as solvent control for 30 min and treated with 10 ng/ml TNF-α for 8 h. Cells treated with TNF-α were also pretreated with DMSO. Protein expression was measured by flow cytometric analysis. Left panel: representative histograms out of three independent experiments with isotype control (grey background), DMSO treated control (black line) and SB pretreated and/or TNF-α treated cells (grey line). Right panel: after normalisation on isotype control values, data for DMSO treated control cells were set as one and x-fold expression is shown as mean ±SEM of three independent experiments.

3.8.4 p38 MAPK-dependent TLR4 protein expression

In order to examine the p38-MAPK dependency in TNF-α-mediated TLR4 downregulation, TLR4 protein levels were measured by flow cytometric analysis. As shown in Figure 41, the TLR4 protein expression was neither altered by TNF-α treatment for 8 h nor after pretreatment with SB203580.
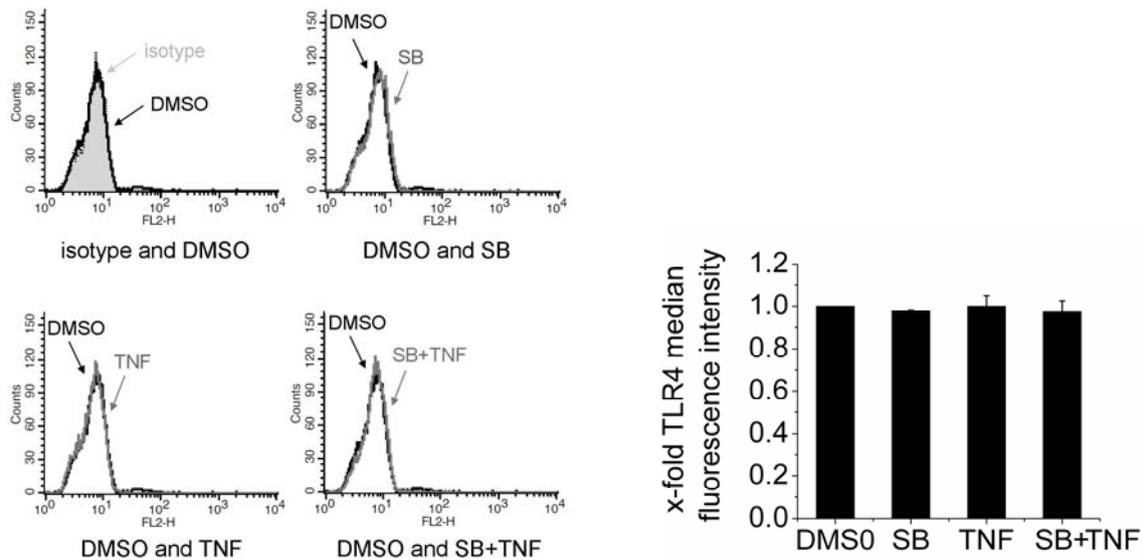
Figure 41: Involvement of p38 MAPK in TLR4 protein expression. HUVEC were either pretreated with 10 ng/ml SB203580 (SB) or an equal volume of DMSO as solvent control for 30 min and treated with 10 ng/ml TNF-α for 8 h. Cells treated with TNF-α were also pretreated with DMSO. Protein expression was measured by flow cytometric analysis. Left panel: representative histograms out of three independent experiments with isotype control (grey background), DMSO treated control (black line) and SB and/or TNF-α treated cells (grey line). Right panel: after normalisation on isotype control values, data for DMSO treated control cells were set as one and x-fold expression is shown as mean ±SEM of three independent experiments.

3.8.5 p38 MAPK-dependent TLR6 protein expression

In contrast to the other TLRs examined, TLR6 protein expression was determined by Western blot analysis. This was caused by high unspecific bindings of the anti-TLR6 antibody in flow cytometric investigations. As shown in Figure 42 and confirming the results on mRNA level, TLR6 protein expression was significantly diminished after TNF-α treatment, whereas an abrogation of this downregulation was observed after pretreatment with SB203580.
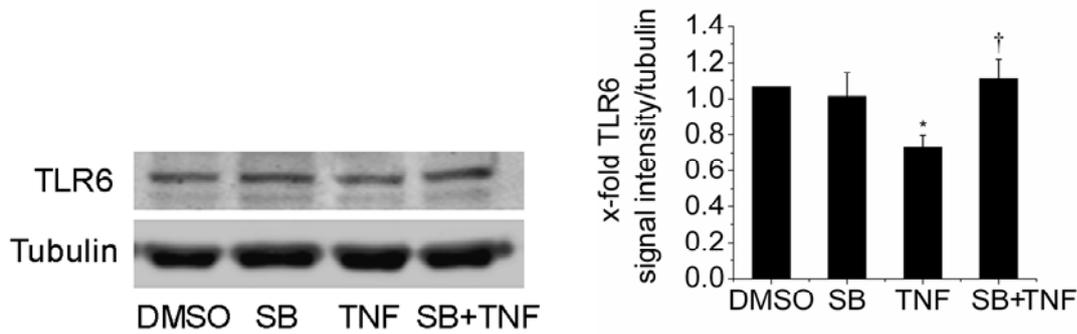
Figure 42: Involvement of p38 MAPK in TLR6 protein expression. HUVEC were either pretreated with 10 ng/ml SB203580 (SB) or an equal volume of DMSO as solvent control for 30 min and treated with 10 ng/ml TNF-α for 8 h. Cells treated with TNF-α were also pretreated with DMSO. Equal amounts of protein were assessed by Western blot analysis using tubulin as loading control. Left panel: one representative out of three independent experiments. Right panel: data for DMSO treated control cells were set as one and x-fold expression is shown as mean ±SEM of four independent experiments. *p<0.05 compared to DMSO treated cells; †p<0.05 compared to TNF-α treated cells.

3.9   Interaction between GILZ and p38 MAPK

Because TLR2 expression was dependent on both GILZ and p38 MAPK, we aimed to clarify whether GILZ is involved in the regulation of p38 MAPK, i.e. whether GILZ knockdown reduces p38 MAPK activation. Levels of p38 and p-p38 MAPK were monitored after GILZ knockdown by Western blot analysis. However, as shown in Figure 43, decreased GILZ levels did not activate p38 MAPK. In contrast, after 24 h even a slightly decreased phosphorylation of p38 MAPK was observed. These findings suggested no direct interaction between GILZ and p38 MAPK.
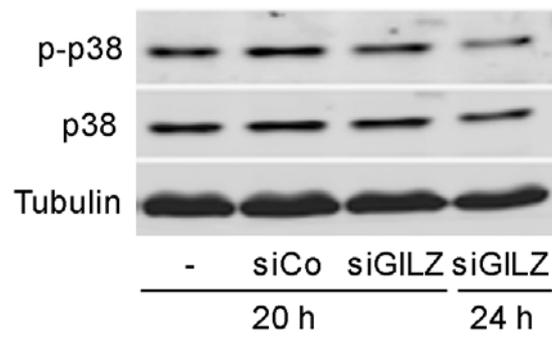
Figure 43: p38 MAPK after GILZ knockdown. HUVEC were either left untransfectd (-) or transfected with siControl (siCo) or siGILZ for the indicated times. Equal amounts of protein were assessed by Western blot analysis using tubulin as loading control. Data are shown as one representative out of three independent experiments.

4. Discussion

4.1   GILZ expression in endothelial cells

The anti-inflammatory action of GILZ is based on the inhibition of the transcription factors NF-κB and AP-1, and GILZ expression has been described for many human cells (Ayroldi & Riccardi, 2009). For endothelial cells, however, GILZ mRNA expression has only been reported after IL-10 stimulation (Gleissner *et al.*, 2007), but no constitutive expression has ever been shown. The present work shows for the first time that HUVEC express GILZ at baseline and upregulate its expression after dexamethasone treatment. This GILZ upregulation by glucocorticoids is in line with previous studies performed in murine thymocytes and lymphocytes (D'Adamio *et al.*, 1997). Also in human cells, such as airway epithelial cells (Eddleston *et al.*, 2007), monocytes (Berrebi *et al.*, 2003), lens epithelial cells (Gupta *et al.*, 2007), mast cells (Godot *et al.*, 2006), and dendritic cells (Cohen *et al.*, 2006), a glucocorticoid-induced GILZ upregulation was observed. Glucocorticoids act *via* binding to glucocorticoid response elements (GREs) in the promoter region of the GILZ gene. Three of four GRE sequences in the distal 5' region of the GILZ gene are functionally active, and may require additional regulatory regions and proteins (Ayroldi & Riccardi, 2009).

In contrast to the dexamethasone-induced upregulation, treatment of HUVEC with TNF-α led to a downregulation of GILZ on mRNA and protein level. These data of a cytokine-dependent GILZ reduction correspond to previous results in human airway epithelial cells after treatment with TNF-α, IL-1β, IFN-γ, or with a mix containing all of them (Eddleston *et al.*, 2007). The findings of a substantial constitutive expression of GILZ and its distinct downregulation under inflammatory conditions suggested that this anti-inflammatory mediator plays an important role in endothelial cells.

4.2   TLR expression after TNF-α

Recently, TLR2 expression has been shown to be upregulated in HUVEC after treatment with TNF-α, LPS or IFN-γ (Satta *et al.*, 2008). Also in earlier publications has been described that TLR2 is highly upregulated after TNF-α or LPS treatment in human microvascular endothelial cells (HMEC) as well as after LPS in HUVEC (Faure *et al.*, 2001). Additionally, a TLR2 upregulation has been observed in murine

macrophages after TNF-α or LPS treatment (Matsuguchi *et al.*, 2000). In this work increased TLR2 expression after TNF-α treatment was confirmed. For the TLR2 co-receptor TLR1 a slightly increased expression was found, whereas the expression of the other TLR2 co-receptor TLR6 as well as TLR4 expression was downregulated. These findings for TLRs 1, 4 and 6 are in accordance with Satta *et al*. (Satta *et al.*, 2008), who also observed these effects at early time points after TNF-α-treatment. Equally, in human monocytes a downregulation of TLR4 after TNF-α has been described (Tamandl *et al.*, 2003).

4.3   Regulation of inflammatory TLR2 expression by GILZ

TLR-dependent activation of endothelial cells plays an important role in the development of atherosclerosis (Erridge, 2008). However, little is known how the expression of these receptors is regulated. One aim of this work was therefore to decipher the role of GILZ in TLR expression and to clarify the involved mechanisms.

4.3.1   Effect of GILZ in TLR2 expression

It has been shown that GILZ overexpression inhibits the LPS-induced TLR2 expression in monocytes (Berrebi *et al.*, 2003). Our findings that TLR2 is upregulated while GILZ is decreased, suggested that GILZ decay itself might induce TLR2 expression. Concordantly, knockdown of GILZ led to an increased TLR2 mRNA expression in HUVEC. In order to confirm this finding, we aimed to overexpress GILZ. However, GILZ overexpression was only successful on mRNA, but not on protein level. The underlying mechanisms were not studied within this work, but an involvement of microRNAs (miRNA) might be suggested. microRNAs represent a cellular strategy for the control of gene expression. miRNAs have been characterized as non–coding RNAs, which are able to induce either posttranscriptional degradation or translational repression of their target mRNA by respective binding to the 3'-untranslated region (3'-UTR) (Zhang, 2008; Dixon *et al.*, 2000). In the 3'-UTR sequence of GILZ mRNA 142 target sites for miRNAs have been identified (www.microrna.org). Thus, the expression of GILZ seems highly regulated by microRNAs. For GILZ overexpression, however, a plasmid construct containing the

reverse transcribed cDNA from the open reading frame (ORF) was used. Therefore, a microRNA-dependent regulation *via* the 3'-UTR can be excluded. However, microRNA binding sites have recently also been discovered in the translated region (Qin *et al.*, 2010; Ko *et al.*, 2009). Indeed, in the GILZ ORF two putative microRNA target sites have been found: hsa-miR-129-5p and hsa-miR-1224-3p (www.mirbase.org). These findings suggest that GILZ expression was either posttranscriptionally or translationally regulated by microRNAs resulting in mRNA but not in protein overexpression.

Nevertheless, to confirm the inverse correlation of TLR2 and GILZ, GILZ protein was overexpressed using dexamethasone, a synthetic glucocorticoid. Glucocorticoids affect many signalling pathways and act anti-inflammatory *via* binding to the glucocorticoid receptor, a ligand-dependent transcription factor (Chinenov & Rogatsky, 2007), and are well described inhibitors of NF-κB (Chinenov & Rogatsky, 2007; De Bosscher *et al.*, 2003; De Bosscher *et al.*, 1997). Accordingly, our investigations showed a dexamethasone-mediated downregulation of inflammatory innate immune receptor TLR2. Interestingly, investigations in other cell types than HUVEC showed a glucocorticoid-mediated induction of TLR2 expression. Respective experiments were done in dendritic cells, human respiratory epithelial cells, and human cervix epithelial cells (HeLa cells) (Rozkova *et al.*, 2006; Homma *et al.*, 2004; Shuto *et al.*, 2002) suggesting cell-specific regulatory actions of glucocorticoids. In addition, glucocorticoids can act on diverse levels of transcriptional regulation, which might be independent of GILZ (Chinenov & Rogatsky, 2007).

4.3.2 GILZ mRNA expression in atherosclerotic arteries

Our findings of an inverse correlation between GILZ and TLR2 exression were confirmed for human healthy *vs.* atherosclerotic vessels. An overexpression of TLR2 in human atherosclerotic plaques has been reported a couple of years ago (Edfeldt *et al.*, 2002). Additionally, in several mouse models it has been shown that TLR2 is involved in the development of atherosclerosis (Madan & Amar, 2008; Tobias & Curtiss, 2008; Liu *et al.*, 2008; Mullick *et al.*, 2005). In the literature, there are no data regarding GILZ expression in atherosclerosis. Thus, this work for the first time links

TLR2 overexpression to GILZ downregulation, although the data do not reach statistical significance because of a rather small number of donors.

The vessels prepared for our investigations contained not only endothelial cells, but e.g. also macrophages. In addition to TNF-α-induced GILZ downregulation in endothelial cells, GILZ downregulation on mRNA and protein level has also been found in macrophages (Jessica Hoppstädter, unpublished data). Concordantly, TLR2 overexpression in human atherosclerotic lesions of carotid arteries was observed in both endothelial cells and macrophages (Edfeldt *et al.*, 2002). In the literature, a GILZ downregulation or even absence in inflammatory diseases, such as chronic rhinosinusitis, Crohn disease or tuberculosis has been reported (Zhang *et al.*, 2009; Berrebi *et al.*, 2003). Additionally, low GILZ expression in Kupffer cells is suggested to contribute to inflammation in alcoholic hepatitis, (Hamdi *et al.*, 2007). These findings confirm our results in endothelial cells and suggest an importance of GILZ downregulation in inflammatory cell activation.

4.3.3   Transcription factors involved in GILZ-dependent TLR2 expression

Since a correlation between GILZ downregulation and TLR2 overexpression in endothelial cells as well as in atherosclerosis was shown, the underlying mechanisms were examined. In murine macrophages and in HeLa cells TLR2 is upregulated in an NF-κB dependent fashion (Musikacharoen *et al.*, 2001; Sakai *et al.*, 2004; Shuto *et al.*, 2002). Studies in HMEC also showed an NF-κB dependent TLR2 induction after LPS treatment, which was investigated by chemical inhibitors of NF-κB as well as transfection with sense and anti-sense p65 oligonucleotides (Faure *et al.*, 2001). In HUVEC an NF-κB regulated TLR2 upregulation was only shown using the chemical NF-κB inhibitor BAY11-7082 (Satta *et al.*, 2008). Since pharmacological compounds can have unspecific effects, we aimed to confirm a contribution of NF-κB to TLR expression in HUVEC by a more specific approach using NF-κB decoy oligonucleotides. Our finding of NF-κB involvement are in accordance with the literature and also with the TLR2 downregulation observed after dexamethasone treatment, which is a well described inhibitor for NF-κB (Chinenov & Rogatsky, 2007; De Bosscher *et al.*, 2003; De Bosscher *et al.*, 1997).

Since GILZ can inhibit AP-1-mediated transcription (Mittelstadt & Ashwell, 2001) and putative AP-1 binding sites have been suggested for the human trl1 gene (Izadi *et al.*, 2007), the role of AP-1 in TLR expression was also investigated using decoy oligonucleotides. The transcription factor AP-1 is composed of members of the five families Jun, Fos, activating transcription factor (ATF) or Maf, which act either as homo- or heterodimers. Earliest activated proteins in inflammatory response are members of the Jun and Fos families, which in contrast to other families are directly activated without transcription and translation (De Bosscher *et al.*, 2003). GILZ can bind to both c-Jun and c-Fos *via* its N-terminal GILZ domain (Mittelstadt & Ashwell, 2001). A role of c-Jun in endothelial TLR2 induction has already been suggested by employing the chemical inhibitor SP600125 (Satta *et al.*, 2008). In contrast, our findings using decoy oligonucleotides showed no involvement for AP-1 in the regulation of TLR2 expression. This approach, however, is more specific than chemichal agents. In addition, the promoter analysis of tlr2 gene showed no binding sites for AP-1 (www.genomatix.de).

4.3.4 NF-κB activation after GILZ knockdown

The mammalian NF-κB family consists of the five members p65 (RelA), RelB, c-Rel, p50 (with the precursor p105, NF-κB1), and p52 (with the precursor p100, NF-κB2), and they all contain a C-terminal nuclear localisation sequence (NLS). In order to induce gene expression, they form homo- or heterodimers. The predominant heterodimer in all species is the p65:p50 complex (Hoffmann *et al.*, 2002). In unstimulated cells the homo- or heterodimers are bound to IκB family proteins (Ghosh *et al.*, 1998). An activation of the homo- or heterodimers is induced by degradation of IκB, which subsequently liberates the NLS and induces NF-κB translocation into the nucleus. Herein, NF-κB binds to promoter and enhancer regions, which contain κB sites with the highly conserved consensus sequence GGGAATTTCC (Hayden & Ghosh, 2004). Genes, which are regulated by NF-κB, are e.g. involved in apoptosis, cell adhesion, proliferation, innate and adaptive immune responses, as well as in inflammation (Perkins, 2007). GILZ binding to p65 has been shown to be critical for the inhibition of NF-κB-induced gene transcription (Di Marco *et al.*, 2007; Berrebi *et al.*, 2003; Ayroldi *et al.*, 2001; Riccardi *et al.*, 2001). Herein, this interaction is facilitated by the C-terminal PER domain of homodimered GILZ (Di

Marco *et al.*, 2007). While aa 98-127 of the proline-rich region are important for functional repression of NF-κB, aa 121-123 are necessary for binding to NF-κB. The GILZ binding site of NF-κB, however, is still unknown. GILZ binding to NF-κB is independent of IκB, which was investigated in human neuronal cells (Ntera-2) lacking IκB expression as well as in a cell free system (Ayroldi *et al.*, 2001; Riccardi *et al.*, 2001). Inversely, binding of IκB to NF-κB *in vitro* is also independent of GILZ (Ayroldi *et al.*, 2001) suggesting that GILZ does not mask the NLS sequence like IκBs, but stabilizes the NF-κB:IκB complex to inhibit nuclear translocation.

Interestingly, we observed in the absence of any external stimulus a nuclear translocation of the subunits p65 and p50 and an increased NF-κB activity after GILZ knockdown. Vice versa, in human airway epithelial cells, THP-1 monocytes, human kidney epithelial carcinoma cell line 293 (HEK-293), and murine T-cells NF-κB activation is diminished after GILZ overexpression (Eddleston *et al.*, 2007; Di Marco *et al.*, 2007; Cannarile *et al.*, 2006; Berrebi *et al.*, 2003; Ayroldi *et al.*, 2001). Moreover, GILZ knockdown has been shown to activate airway epithelial cells by increased cytokine expression, whereby the underlying mechanisms have not been investigated (Eddleston *et al.*, 2007). In contrast, lung epithelial cells with stable GILZ knockdown did not show increased cytokine induction compared to GILZ-expressing cells (Gomez *et al.*, 2010). It has to be noted, however, that the early cellular response after knockdown can not be examined in stably transfected cells. Since NF-κB activation results in a functional feedback loop, e.g. by induction of IκB, a knockdown-induced NF-κB activation is expected only to be transient.

Three different IκBs are known, IκBα, IκBβ, and IκBε, whereby IκBα has been described as the primary regulator of p65:p50. In general, IκBs function by masking the conserved NLS of the p65 NF-κB subunit, while the NLS of p50 remains accessible. Stimulus-dependent phosphorylation of IKKs leads to IκB protein ubiquitination and degradation *via* the 26S proteasome (Pajonk & McBride, 2001) resulting in NF-κB-dependent gene expression. Our investigations after GILZ knockdown showed diminished IκBα levels, which most likely are responsible for NF-κB activation. In contrast, it has been reported that GILZ does not interfere with IκB in T-cells (Ayroldi *et al.*, 2001). However, the study only focussed on GILZ overexpression and not on GILZ knockdown.

4.3.5 NF-κB expression after GILZ knockdown

Interestingly, GILZ knockdown and additional TNF-α treatment led to a diminished nuclear translocation of p65, p50 and cRel and decreased NF-κB activation. Macrophage desensitization is known for many years (Remold-O'Donnell, 1974), and this phenomenon has also been described for endothelial cells. Stimulation of endothelial cells with TNF-α or LPS leads to a desensitization regarding NF-κB activation (Wada *et al.*, 2005). Subsequent stimulation with thrombin, which also leads to NF-κB activation, does neither activate NF-κB nor induce its translocation into the nucleus. Also phosphorylation as well as degradation of IκBα are not induced. Concordantly, mouse macrophages pretreated with LPS show a highly reduced NF-κB activation upon further LPS treatment as well as a diminished degradation of IκBα (Medvedev *et al.*, 2000). These findings of desensitization confirm our data that GILZ decay leads to an activation of NF-κB.

In addition to attenuated NF-κB activation, also the protein expression of NF-κB subunits in whole cell lysates was diminished after GILZ knockdown. In the literature, there are no data on NF-κB degradation after its activation. Therefore, we hypothesize that GILZ decay alters NF-κB expression levels. Few data exist in the literature regarding transcriptional regulation of NF-κB subunits. Although p50 and cRel promoters contain binding sites for NF-κB (Ueberla *et al.*, 1993) and NF-κB activity was increased by GILZ decay, p50 and cRel protein levels were decreased. A self-regulation of p65 by transcriptional repression can be excluded because its promoter misses an adequate binding site (Ueberla *et al.*, 1993). The p65 promoter, however, contains three GC-rich elements (GC boxes) (Ueberla *et al.*, 1993), which are potential binding sites for Sp-1 (Dynan & Tjian, 1983). Concordantly, Sp1-mediated p65 expression has been described (Gu *et al.*, 2002). Because of the GILZ knockdown in our experiment, a regulation *via* Ras described to be inhibited by GILZ (Ayroldi *et al.*, 2007) and to activate SP-1 (Zheng *et al.*, 2001) can be excluded. However, it has been shown that c-Jun is able to repress transcriptional activity through Sp1 binding sites (Wang *et al.*, 2000). Since c-Jun is inhibited by GILZ (Mittelstadt & Ashwell, 2001), GILZ decay might lead to c-Jun release and repression of Sp1-mediated NF-κB transcription. Contrary to diminished NF-κB protein levels we observed after GILZ decay, GILZ overexpression did not affect p65 protein levels in T-cells (Ayroldi *et al.*, 2001). In THP-1 monocytes and peripheral leukocytes from

trauma patients, increased GILZ levels are correlated with decreased p65 proteins (Bai *et al.*, 2007). However, in livers of p62 transgenic mice increased GILZ levels were paralleled by elevated NF-κB levels (Sonja Kessler, Elisabeth Tybl, unpublished data). Thus, the regulation of NF-κB by GILZ seems different in various cell types and organs.

4.4   Regulation of inflammatory TLR2 expression by p38 MAPK

Employment of a chemical inhibitor of p38 MAPK has been described to attenuate TLR2 expression in endothelial cells (Satta *et al.*, 2008). In contrast, in human airway epithelial cells, in HeLa cells and in murine dendritic cells a negative effect of p38 MAPK on TLR2 expression has been postulated (Regueiro *et al.*, 2009; Mikami *et al.*, 2006; An *et al.*, 2002). Because of these conflicting data on the role of p38 MAPK in TLR2 expression, we aimed to clarify its contribution to TLR2 expression using pharmacological inhibitors and isoform-specific overexpression. For investigations of TLR mRNA and protein levels, the exposure time for TNF-α treatment was chosen according to maximal TLR2 mRNA or protein expression levels (Nadège Ripoche, unpublished data).

4.4.1   Abrogation of TNF-induced p38 MAPK activation by SB203580

As described in the literature, a TNF-α-induced phosphorylation of p38 MAPK was observed (Kiemer *et al.*, 2002b; Raingeaud *et al.*, 1995; Lee *et al.*, 1994) and the results for abrogated TNF-α-induced actions by SB203580 were consistent with the literature (Weber *et al.*, 2003; Kiemer *et al.*, 2002b). The pyridinyl inhibitor SB203580 is a competitive inhibitor acting at the ATP binding site of p38 MAPK α and β (Kumar *et al.*, 1997; Young *et al.*, 1997). After activation, we observed a nuclear as well as cytoplasmatic localisation of p38 MAPK, while non-activated p38 MAPK was mainly in the cytoplasm. The cellular localisation of p38 has been discussed in the literature (Roux & Blenis, 2004): in p38 MAPK overexpressing monkey kidney cells (COS-1) a cytoplasmatic as well as a nuclear localisation for non-activated p38 MAPK has been observed (Raingeaud *et al.*, 1995). In HEK-293 the arsenite-induced activation of p38 MAPK led to a nuclear export (Ben-Levy *et al.*, 1998). In synovial fibroblasts p-p38

MAPK is also present in the nucleus (Schett *et al.*, 2000). Cellular distribution of p38 and p-p38 MAPK therefore seems to be dependent on the cell type and maybe also on the examined isoform.

In concordance with Satta *et al.* (Satta *et al.*, 2008), TNF-α-induced TLR2 expression was partially abrogated by SB203580 indicating a positive involvement of p38 MAPK in endothelial TLR2 mRNA upregulation. The small effect herein may be explained by either a minor role for p38 MAPK in TLR2 expression or by unrequested actions through inhibition of other MAP kinases.

4.4.2 Abrogation of TNF-induced p38 MAPK activation by ANP

As a second pharmacological inhibitor ANP was used, which has been described to inhibit p38 MAPK activation in endothelial cells *via* MKP-1 induction (Kiemer *et al.*, 2002b). A suppression of p38-mediated activities by ANP was also published in macrophages (Tsukagoshi *et al.*, 2001). ANP was first isolated by de Bold *et al.* (de Bold *et al.*, 1981), and it has been characterized as a potent diuretic and natriuretic hormone expressed and secreted by atrial myocytes after local wall stretch (Venugopal, 2001). Furthermore, ANP was also found in lower concentrations in e.g. lung, brain, kidney, and thymus, and it plays an important role in the regulation of blood pressure. It has been shown , moreover, that ANP acts as an anti-inflammatory mediator, which reduces inflammatory actions *in vitro* (Kiemer *et al.*, 2002a; Kiemer *et al.*, 2002b) and *in vivo* (Ladetzki-Baehs *et al.*, 2007). Confirming our previous results using the p38 MAPK inhibitor SB203580, a positive involvement of p38 MAPK in TLR2 mRNA upregulation was observed, which seems in contrast to cell types other than endothelial cells (Regueiro *et al.*, 2009; Mikami *et al.*, 2006; An *et al.*, 2002).

4.4.3 Abrogation of TNF-induced p38 MAPK activation by dn p38 MAPK overexpression

Since pharmacological inhibitors have often been discussed to exert unrequested actions (Lee *et al.*, 1999), we aimed to confirm the previous results by overexpression of dn p38 MAPK. Therefore, the isoform-dependency of p38 MAPK

should be clarified. In mammalian cells the four different p38 MAPK isoforms, p38α, p38β, p38γ, p38δ (Hale *et al.*, 1999) seem to play different physiological roles (Zhou *et al.*, 2008; Pramanik *et al.*, 2003). While HUVEC have been described to express mainly p38α and p38β (Hale *et al.*, 1999), we only detected p38α MAPK. The overexpressed isoform p38β2 is the major splice variant of p38β (Hale *et al.*, 1999) and differs from p38β by depletion of 24 nucleotides equating eight amino acids (Kumar *et al.*, 1997). The expression of only p38α in our cells may be explained by the use of a different culture medium containing a different composition of growth factors and supplements. In any case, the isoform p38α seems to play a major role in immune responses (Kim *et al.*, 2008; Hale *et al.*, 1999).

The p38 coding sequence of our plasmid used for overexpression contained two mutations in the phosphorylation site of p38α (threonine188→alanine, tyrosine190→phenylalanin) (Pramanik *et al.*, 2003). Concordantly, our western blot anlalysis showed reduced TNF-α-induced phosphorylation of p38α MAPK after dn p38α overexpression. Confirming our results obtained by the use of pharmacological inhibitors, overexpression of dn p38α MAPK showed a significant abrogation of TNF-α-induced TLR2 expression investigated by Real-time RT-PCR. Taken together, our data indicate that TLR2 mRNA expression is enhanced by p38α MAPK in endothelial cells. These findings lead to the conclusion that the role of p38 MAPK in TLR expression is not only different between mice and humans (Haehnel *et al.*, 2002), but is also dependent on the cell type investigated.

4.4.4 p38 MAPK-dependent TLR2 protein expression

In the literature there are no data regarding endothelial TLR2 protein levels after p38 MAPK abrogation. Our preliminary investigations have shown that the anti-TLR2 antibody, which is recommended by the manufacturer for flow cytometric analysis, recognices TLR2 antigens.

The cellular localisation of TLR2 seems different in different species. It has been described that in unstimulated HUVEC, TLR2, its co-receptors TLRs 1 and 6 as well as TLR4 are intracellularly located, and only after stimulation by pro-inflammatory cytokines, such as IFN-γ or IL-1, translocated into the outer cell membrane (Shuang

et al., 2007). This was confirmed by Satta *et al.* (Satta *et al.*, 2008), who postulated that a large pool of TLR2 is located intracellularly. An intracellular localisation of TLRs 1, 2 and 6 as well as an intracellular heterotypic assembly of TLR2/TLR6 with CD36 has also been observed in TLR-transfected HEK-293 cells (Triantafilou *et al.*, 2006). After activation by its ligands the TLR2/TLR6 dimer can be found as clusters in the membrane (Triantafilou *et al.*, 2006). However, these findings are in contrast to the observation in unstimulated murine endothelial cells, in which the mentioned TLRs also are located in the outer membrane (Shuang *et al.*, 2007). In order to detect all cellular TLRs, either already located in the outer membrane or intracellularly in the Golgi, immunostaining was performed after cell permeabilisation. Confirming our observation on mRNA level, TNF-α-induced TLR2 protein expression was abrogated by p38 MAPK inhibition. We therefore conclude that p38 MAPK is an important positive mediator in the upregulation of TLR2 expression under inflammatory conditions in endothelial cells.

4.5 Interaction between GILZ and p38 MAPK

Because we observed that expression of TLR2 is regulated by GILZ as well as by p38 MAPK, we sought to clarify whether GILZ is linked to the p38 MAPK pathway. It has been published that glucocorticoids inhibit p38 MAPK activation *via* induction of MAPK phosphatase 1 (MKP-1) (King *et al.*, 2009; Fürst *et al.*, 2007). Since we observed a dimished phosphorylation of p38 MAPK after GILZ decay and since glucocorticoids induce GILZ expression, a direct GILZ-induced regulation of p38 MAPK could be excluded. In fact, a negative interaction of NF-κB and p38 MAPK after TNF-α treatment has been reported earlier (Weber *et al.*, 2003; Beyaert *et al.*, 1996). This seems to be in contrast to other publications, in which an LPS-induced and NF-κB-dependent TLR2 induction *via* positive p38 MAPK was observed, i.e. chemical inhibition of either MAPK or NF-κB abrogates LPS-induced TLR2 upregulation (An *et al.*, 2002). However, An *et al.* showed no causal coherency. Since p38 MAPK abrogates TNF-α-induced TLR2 expression paralleld by TLR2 upregulation *via* GILZ decay and NF-κB activation, our investigations show for the first time that p38 MAPK and NF-κB act independently in the regulation of TLR2 expression. These findings suggest that other transcription factors are involved in

p38 MAPK-dependent regulation of TLR expression. It has already been reported that SP-1 and STAT5 seem to play a role in TLR2 expression (Dunzendorfer *et al.*, 2004; Wang *et al.*, 2001; Musikacharoen *et al.*, 2001), and that SP-1 activation is dependent on p38 MAPK (Chanteux *et al.*, 2007; Ma *et al.*, 2001).

4.6   Regulation of TNF-α-induced expression of TLRs 1, 4 and 6

This work is the first report about a distinct regulation of TLR2 co-receptors TLR1 and TLR6 as well as for TLR4 expression. Besides an induction of TLR2 mRNA, GILZ knockdown also increases TLR6 mRNA expression, whereas TLR1 and TLR4 are not affected. Investigations of the underlying mechanism showed that in contrast to TLR2 neither the expression of the co-receptors TLR1 and TLR6 nor of TLR4 is induced *via* NF-κB after TNF-α treatment. In addition, a TNF-α-mediated expression *via* AP-1 was excluded.

In contrast to TLR1 and TLR4, the mechanisms regulating TLR6 expression on mRNA as well as on protein level involved p38 MAPK. Since p38 MAPK is a major determinant for 3'-UTR mediated mRNA stability (Khabar, 2005), an active destabilisation of TLR6 mRNA might be the mechanism involved. p38 MAPK phosphorylates *trans*-acting factors, which can either act as mRNA stabilisators or destabilisators (Frevel *et al.*, 2003). The 3'-UTR of TLR6 mRNA conatins no typical destabilizing adenine and uridine-rich elements (AREs) consisting of 50-150 bp A and U repeats (www.ensembl.org) (Shaw & Kamen, 1986). However, the typical pentamer AUUUA is found twice, which could confirm our hypothesis on TLR6 mRNA destabilisation. Both GILZ as well as p38 MAPK seem to suppress TLR6 expression. Since TNF-α treatment suppresses GILZ expression, but induces p38 MAPK activation, the small extent of TLR6 expression changes can be explained.

TLR4 mRNA has been described to be a target for numerous microRNAs (http://www.microrna.org, 97 identified miRNA target sites), which might function in TNF-α-mediated downregulation. The lacking effect on TLR4 protein level both after TNF-α treatment and after pretreatment with SB203580 might be explained by the choice of the wrong time point. Interestingly, the TNF-α-mediated TLR4

downregulation, which was observed in endothelial cells by ourselves and in human monocytes by Tamandl *et al.* (Tamandl *et al.*, 2003), is in contrast to TLR4 upregulation in atherosclerotic plaques (Edfeldt *et al.*, 2002). For TLR6 an upregulation in atherosclerotic lesions has also been described (Edfeldt *et al.*, 2002). These findings lead to the suggestion that the action of a different mediator than TNF-α determines TLR4 and TLR6 induction in atherosclerosis.

4.7   The inflammatory marker MCP-1

MCP-1 has been described as a general marker for inflammatory activation of endothelial cells (Szmitko *et al.*, 2003; Ikeda *et al.*, 2002) and to be inducible by TNF-α treatment (Weber *et al.*, 2003; Rollins *et al.*, 1990). Interestingly, our findings showed that MCP-1 regulation was largely parallel to TLR2: we observed an NF-κB and p38 MAPK dependent upregulation, which was antagonized by GILZ. A role for NF-κB in endothelial MCP-1 expression has been described earlier (Ishizuka *et al.*, 2000), and also the involvement of p38 MAPK has been shown (Lu *et al.*, 2009; Weber *et al.*, 2003; Goebeler *et al.*, 1999). Similar to TLR2 expression, a causal link between p38 MAPK and NF-κB is missing, which confirms our hypothesis that p38 MAPK and NF-κB function independently in TLR2 and MCP-1 expression regulation. Interestingly, MCP-1 expression seems positively regulated by AP-1, which was confirmed by the literature (Sutcliffe *et al.*, 2009; Ishizuka *et al.*, 2000). Therefore, it might be speculated that MCP-1 expression by GILZ suppression involves actions on AP-1.

5. Summary and Conclusion

Endothelial cells represent the inner cell layer in blood vessels and are involved in inflammatory actions. Herein, the activation of the pattern recognition receptors plays an important role. TLRs have been described to be involved in the development of atherosclerosis, a chronic inflammatory disease characterized by endothelial dysfunction. Mainly TLR2 and TLR4 have been described to be overexpressed in atherosclerotic lesions. However, the regulation of their expression as well as the regulation of TLR1 and TLR6 expression, which function as co-receptors of TLR2, has been completely unknown. GILZ has been described as an anti-inflammatory mediator, but its basal expression in endothelial cells as well as its role in endothelial inflammation has as yet been unknown. p38 MAPK has also been described to function in inflammatory actions. Aim of this work was therefore to decipher the roles of GILZ and p38 MAPK in endothelial TLR expression.
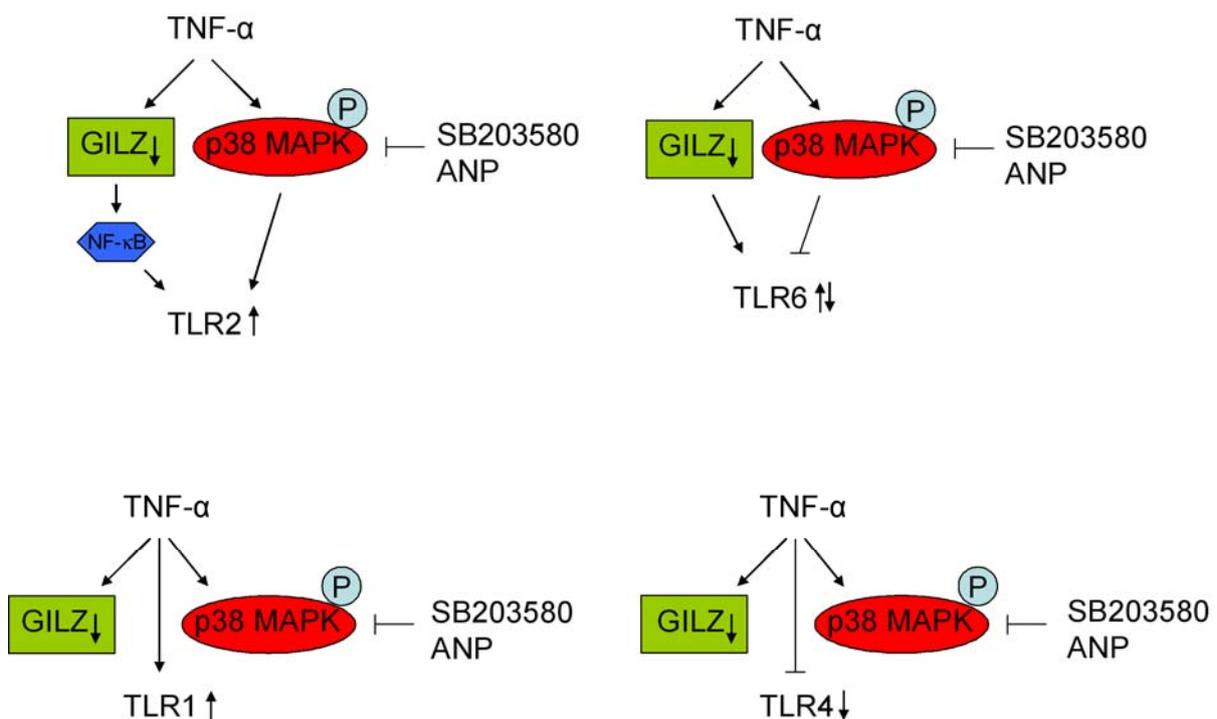

Figure 44: Schematic overview about the regulation of TLR expression by GILZ and p38 MAPK in human endothelial cells. Abbreviations: ANP=Atrial natriuretic peptide, GILZ=glucocorticoid-induced leucine zipper, MAPK=mitogen activated protein kinase, NF-κB=nuclear factor kappa B, P=phosphorylation, TLR=toll-like receptor.

A pronounced constitutive expression of GILZ has been found in HUVEC, which was downregulated under inflammatory conditions. Mechanistic investigations showed that reduction of GILZ protein levels in human endothelial cells led to an induction of NF-κB activity (Figure 44). In detail, GILZ decay induced IκBα degradation, NF-κB nuclear translocation, and transcriptional activity. This NF-κB activation induced the expression of TLR2, as it could be observed in atherosclerotic vessels, paralleled by GILZ downregulation. In addition, TLR6 expression was also increased by GILZ decay, an effect independent of NF-κB activities. These findings suggest an upregulation of GILZ as a potential target for the treatment of the inflamed endothelium.

TLR2 as well as TLR6 TNF-α-mediated expression was dependent on p38α MAPK, whose inhibition led to an abrogation of TNF-α-mediated actions. p38 MAPK is therefore a further potential target for therapeutic treatment. In contrast, TLR1 and TLR4 expression were neither regulated by GILZ nor by p38 MAPK. Despite of our findings that both TLR2 and TLR6 expression were regulated by GILZ as well as by p38 MAPK, the p38 MAPK mediated action was independent of GILZ.

Taken together, this work provides evidence for functional implications of GILZ and p38 MAPK in the regulation of endothelial TLR2 and TLR6 expression in human endothelial cells and contributes to a better understanding of inflammatory actions in atherosclerosis.

6. References

Aggarwal BB. **2003.** Signalling pathways of the TNF superfamily: a double-edged sword. *Nat Rev Immunol* **3:** 745-756.

Aird WC. **2007.** Phenotypic heterogeneity of the endothelium: I. Structure, function, and mechanisms. *Circ Res* **100:** 158-173.

Alber T. **1992.** Structure of the leucine zipper. *Curr Opin Genet Dev* **2:** 205-210.

An H, Yu Y, Zhang M, Xu H, Qi R, Yan X, Liu S, Wang W, Guo Z, Guo J, Qin Z, Cao X. **2002.** Involvement of ERK, p38 and NF-kappaB signal transduction in regulation of TLR2, TLR4 and TLR9 gene expression induced by lipopolysaccharide in mouse dendritic cells. *Immunology* **106:** 38-45.

Anderson KV, Nüsslein-Volhard C. **1984.** Information for the dorsal--ventral pattern of the Drosophila embryo is stored as maternal mRNA. *Nature* **311:** 223-227.

Ayroldi E, Migliorati G, Bruscoli S, Marchetti C, Zollo O, Cannarile L, D'Adamio F, Riccardi C. **2001.** Modulation of T-cell activation by the glucocorticoid-induced leucine zipper factor via inhibition of nuclear factor kappaB. *Blood* **98:** 743-753.

Ayroldi E, Riccardi C. **2009.** Glucocorticoid-induced leucine zipper (GILZ): a new important mediator of glucocorticoid action. *FASEB J* **23:** 3649-3658.

Ayroldi E, Zollo O, Bastianelli A, Marchetti C, Agostini M, Di Virgilio R, Riccardi C. **2007.** GILZ mediates the antiproliferative activity of glucocorticoids by negative regulation of Ras signaling. *J Clin Invest* **117:** 1605-1615.

Bai XJ, Li B, Wang HP, Yang ZH, Li SQ. **2007.** Primary investigation of the relationship between glucocorticoid induced leucine zipper and inflammatory reaction. *Chin Crit Care Med* **19:** 7-10.

Barnes PJ, Karin M. **1997.** Nuclear factor-kappaB: a pivotal transcription factor in chronic inflammatory diseases. *N Engl J Med* **336:** 1066-1071.

Baud V, Karin M. **2001.** Signal transduction by tumor necrosis factor and its relatives. *Trends Cell Biol* **11:** 372-377.

Ben-Levy R, Hooper S, Wilson R, Paterson HF, Marshall CJ. **1998.** Nuclear export of the stress-activated protein kinase p38 mediated by its substrate MAPKAP kinase-2. *Curr Biol* **8:** 1049-1057.

Berrebi D, Bruscoli S, Cohen N, Foussat A, Migliorati G, Bouchet-Delbos L, Maillot MC, Portier A, Couderc J, Galanaud P, Peuchmaur M, Riccardi C, Emilie D. **2003.** Synthesis of glucocorticoid-induced leucine zipper (GILZ) by macrophages: An anti-inflammatory and immunosuppressive mechanism shared by glucocorticoids and IL-10. *Blood* **101:** 729-738.

Beutler B. **2004.** Inferences, questions and possibilities in Toll-like receptor signalling. *Nature* **430:** 257-263.

Bevilacqua MP. **1993.** Endothelial-leukocyte adhesion molecules. *Annu Rev Immunol* **11:** 767-804.

Beyaert R, Cuenda A, Vanden BW, Plaisance S, Lee JC, Haegeman G, Cohen P, Fiers W. **1996.** The p38/RK mitogen-activated protein kinase pathway regulates interleukin-6 synthesis response to tumor necrosis factor. *EMBO J* **15:** 1914-1923.

Björkbacka H. **2006.** Multiple roles of Toll-like receptor signaling in atherosclerosis. *Curr Opin Lipidol* **17:** 527-533.

Björkbacka H, Kunjathoor VV, Moore KJ, Koehn S, Ordija CM, Lee MA, Means T, Halmen K, Luster AD, Golenbock DT, Freeman MW. **2004.** Reduced atherosclerosis in MyD88-null mice links elevated serum cholesterol levels to activation of innate immunity signaling pathways. *Nat Med* **10:** 416-421.

Bruscoli S, Donato V, Velardi E, Di Sante M, Migliorati G, Donato R, Riccardi C. **2010.** Glucocorticoid-induced leucine zipper (GILZ) and long GILZ inhibit myogenic differentiation and mediate anti-myogenic effects of glucocorticoids. *J Biol Chem* **285:** 10385-10396.

Busch SJ, Sassone-Corsi P. **1990.** Dimers, leucine zippers and DNA-binding domains. *Trends Genet* **6:** 36-40.

Cannarile L, Fallarino F, Agostini M, Cuzzocrea S, Mazzon E, Vacca C, Genovese T, Migliorati G, Ayroldi E, Riccardi C. **2006.** Increased GILZ expression in transgenic mice up-regulates Th-2 lymphokines. *Blood* **107:** 1039-1047.

Cannarile L, Zollo O, D'Adamio F, Ayroldi E, Marchetti C, Tabilio A, Bruscoli S, Riccardi C. **2001.** Cloning, chromosomal assignment and tissue distribution of human GILZ, a glucocorticoid hormone-induced gene. *Cell Death Differ* **8:** 201-203.

Carthew RW, Sontheimer EJ. **2009.** Origins and Mechanisms of miRNAs and siRNAs. *Cell* **136:** 642-655.

Chanteux H, Guisset AC, Pilette C, Sibille Y. **2007.** LPS induces IL-10 production by human alveolar macrophages via MAPKinases- and Sp1-dependent mechanisms. *Respir Res* **8:** 71.

Chen Z, Gibson TB, Robinson F, Silvestro L, Pearson G, Xu B, Wright A, Vanderbilt C, Cobb MH. **2001.** MAP kinases. *Chem Rev* **101:** 2449-2476.

Chinenov Y, Rogatsky I. **2007.** Glucocorticoids and the innate immune system: crosstalk with the toll-like receptor signaling network. *Mol Cell Endocrinol* **275:** 30-42.

Cohen N, Mouly E, Hamdi H, Maillot MC, Pallardy M, Godot V, Capel F, Balian A, Naveau S, Galanaud P, Lemoine FM, Emilie D. **2006.** GILZ expression in human dendritic cells redirects their maturation and prevents antigen-specific T lymphocyte response. *Blood* **107:** 2037-2044.

D'Adamio F, Zollo O, Moraca R, Ayroldi E, Bruscoli S, Bartoli A, Cannarile L, Migliorati G, Riccardi C. **1997.** A new dexamethasone-induced gene of the leucine zipper family protects T lymphocytes from TCR/CD3-activated cell death. *Immunity* **7:** 803-812.

de Bold AJ, Borenstein HB, Veress AT, Sonnenberg H. **1981.** A rapid and potent natriuretic response to intravenous injection of atrial myocardial extract in rats. *Life Sci* **28:** 89-94.

De Bosscher K, Schmitz ML, Vanden Berghe W, Plaisance S, Fiers W, Haegeman G. **1997.** Glucocorticoid-mediated repression of nuclear factor-kappaB-

dependent transcription involves direct interference with transactivation. *Proc Natl Acad Sci U S A* **94:** 13504-13509.

De Bosscher K, Vanden Berghe W, Haegeman G. **2003.** The interplay between the glucocorticoid receptor and nuclear factor-kappaB or activator protein-1: molecular mechanisms for gene repression. *Endocr Rev* **24:** 488-522.

dela Paz NG, D'Amore PA. **2009.** Arterial versus venous endothelial cells. *Cell Tissue Res* **335:** 5-16.

den Dekker WK, Cheng C, Pasterkamp G, Duckers HJ. **2010.** Toll like receptor 4 in atherosclerosis and plaque destabilization. *Atherosclerosis* **209:** 314-320.

Deshmane SL, Kremlev S, Amini S, Sawaya BE. **2009.** Monocyte chemoattractant protein-1 (MCP-1): an overview. *J Interferon Cytokine Res* **29:** 313-326.

Di Marco B, Massetti M, Bruscoli S, Macchiarulo A, Di Virgilio R, Velardi E, Donato V, Migliorati G, Riccardi C. **2007.** Glucocorticoid-induced leucine zipper (GILZ)/NF-kappaB interaction: role of GILZ homo-dimerization and C-terminal domain. *Nucleic Acids Res* **35:** 517-528.

Dixon DA, Kaplan CD, McIntyre TM, Zimmerman GA, Prescott SM. **2000.** Post-transcriptional control of cyclooxygenase-2 gene expression. The role of the 3'-untranslated region. *J Biol Chem* **275:** 11750-11757.

Dunzendorfer S, Lee HK, Tobias PS. **2004.** Flow-dependent regulation of endothelial toll-like receptor 2 expression through inhibition of SP1 activity. *Circ Res* **95:** 684-691.

Dynan WS, Tjian R. **1983.** The promoter-specific transcription factor Sp1 binds to upstream sequences in the SV40 early promoter. *Cell* **35:** 79-87.

Eddleston J, Herschbach J, Wagelie-Steffen AL, Christiansen SC, Zuraw BL. **2007.** The anti-inflammatory effect of glucocorticoids is mediated by glucocorticoid-induced leucine zipper in epithelial cells. *J Allergy Clin Immunol* **119:** 115-122.

Edfeldt K, Swedenborg J, Hansson GK, Yan ZQ. **2002.** Expression of toll-like receptors in human atherosclerotic lesions: a possible pathway for plaque activation. *Circulation* **105:** 1158-1161.

Erridge C. **2008.** The roles of pathogen-associated molecular patterns in atherosclerosis. *Trends Cardiovasc Med* **18:** 52-56.

Erridge C. **2009.** The Roles of Toll-Like Receptors in Atherosclerosis. *J Innate Immun* **1:** 340-349. http://content.karger.com/ProdukteDB/produkte.asp?Aktion =ShowPDF&ArtikelNr=191413&Ausgabe=248737&ProduktNr=234234&filename=19 1413.pdf. Accessed January 8, 2009.

Farhat K, Riekenberg S, Heine H, Debarry J, Lang R, Mages J, Buwitt-Beckmann U, Roschmann K, Jung G, Wiesmuller KH, Ulmer AJ. **2007.** Heterodimerization of TLR2 with TLR1 or TLR6 expands the ligand spectrum but does not lead to differential signaling. *J Leukoc Biol* **83:**692-701.

Faure E, Thomas L, Xu H, Medvedev A, Equils O, Arditi M. **2001.** Bacterial lipopolysaccharide and IFN-gamma induce Toll-like receptor 2 and Toll-like receptor 4 expression in human endothelial cells: role of NF-kappa B activation. *J Immunol* **166:** 2018-2024.

Frevel MA, Bakheet T, Silva AM, Hissong JG, Khabar KS, Williams BR. **2003.** p38 Mitogen-activated protein kinase-dependent and -independent signaling of mRNA stability of AU-rich element-containing transcripts. *Mol Cell Biol* **23:** 425-436.

Fürst R, Brueckl C, Kuebler WM, Zahler S, Krötz F, Görlach A, Vollmar AM, Kiemer AK. **2005.** Atrial natriuretic peptide induces mitogen-activated protein kinase phosphatase-1 in human endothelial cells via Rac1 and NAD(P)H oxidase/Nox2-activation. *Circ Res* **96:** 43-53.

Fürst R, Schroeder T, Eilken HM, Bubik MF, Kiemer AK, Zahler S, Vollmar AM. **2007.** MAPK phosphatase-1 represents a novel anti-inflammatory target of glucocorticoids in the human endothelium. *FASEB J* **21:** 74-80.

Ghosh S, May MJ, Kopp EB. **1998.** NF-kappa B and Rel proteins: evolutionarily conserved mediators of immune responses. *Annu Rev Immunol* **16:** 225-260.

Gleissner CA, Zastrow A, Klingenberg R, Kluger MS, Konstandin M, Celik S, Haemmerling S, Shankar V, Giese T, Katus HA, Dengler TJ. **2007.** IL-10 inhibits endothelium-dependent T cell costimulation by up-regulation of ILT3/4 in human vascular endothelial cells. *Eur J Immunol* **37:** 177-192.

Godot V, Garcia G, Capel F, Arock M, Durand-Gasselin I, Asselin-Labat ML, Emilie D, Humbert M. **2006.** Dexamethasone and IL-10 stimulate glucocorticoid-induced leucine zipper synthesis by human mast cells. *Allergy* **61:** 886-890.

Goebeler M, Kilian K, Gillitzer R, Kunz M, Yoshimura T, Bröcker EB, Rapp UR, Ludwig S. **1999.** The MKK6/p38 stress kinase cascade is critical for tumor necrosis factor-alpha-induced expression of monocyte-chemoattractant protein-1 in endothelial cells. *Blood* **93:** 857-865.

Gomez M, Raju SV, Viswanathan A, Painter RG, Bonvillain R, Byrne P, Nguyen DH, Bagby GJ, Kolls JK, Nelson S, Wang G. **2010.** Ethanol Upregulates Glucocorticoid-Induced Leucine Zipper Expression and Modulates Cellular Inflammatory Responses in Lung Epithelial Cells. *J Immunol* **184:** 5715-5722.

Gu L, Findley HW, Zhou M. **2002.** MDM2 induces NF-kappaB/p65 expression transcriptionally through Sp1-binding sites: a novel, p53-independent role of MDM2 in doxorubicin resistance in acute lymphoblastic leukemia. *Blood* **99:** 3367-3375.

Gupta SK, Lysko PG, Pillarisetti K, Ohlstein E, Stadel JM. **1998.** Chemokine receptors in human endothelial cells. Functional expression of CXCR4 and its transcriptional regulation by inflammatory cytokines. *J Biol Chem* **273:** 4282-4287.

Gupta V, Awasthi N, Wagner BJ. **2007.** Specific activation of the glucocorticoid receptor and modulation of signal transduction pathways in human lens epithelial cells. *Invest Ophthalmol Vis Sci* **48:** 1724-1734.

Haehnel V, Schwarzfischer L, Fenton MJ, Rehli M. **2002.** Transcriptional regulation of the human toll-like receptor 2 gene in monocytes and macrophages. *J Immunol* **168:** 5629-5637.

Hale KK, Trollinger D, Rihanek M, Manthey CL. **1999.** Differential expression and activation of p38 mitogen-activated protein kinase alpha, beta, gamma, and delta in inflammatory cell lineages. *J Immunol* **162:** 4246-4252.

Hamdi H, Bigorgne A, Naveau S, Balian A, Bouchet-Delbos L, Cassard-Doulcier AM, Maillot MC, Durand-Gasselin I, Prévot S, Delaveaucoupet J, Emilie D, Perlemuter G. **2007.** Glucocorticoid-induced leucine zipper: A key protein in the sensitization of monocytes to lipopolysaccharide in alcoholic hepatitis. *Hepatology* **46:** 1986-1992.

Hansson GK. **2005.** Inflammation, atherosclerosis, and coronary artery disease. *N Engl J Med* **352:** 1685-1695.

Hansson GK. **2009.** Inflammatory mechanisms in atherosclerosis. *J Thromb Haemost* **7:** 328-331.

Hashimoto S, Gon Y, Matsumoto K, Takeshita I, Horie T. **2001.** N-acetylcysteine attenuates TNF-alpha-induced p38 MAP kinase activation and p38 MAP kinase-mediated IL-8 production by human pulmonary vascular endothelial cells. *Br J Pharmacol* **132:** 270-276.

Hayden MS, Ghosh S. **2004.** Signaling to NF-kappaB. *Genes Dev* **18:** 2195-2224.

Heine H, Kirschning CJ, Lien E, Monks BG, Rothe M, Golenbock DT. **1999.** Cutting edge: cells that carry A null allele for toll-like receptor 2 are capable of responding to endotoxin. *J Immunol* **162:** 6971-6975.

Heller RA, Kronke M. **1994.** Tumor necrosis factor receptor-mediated signaling pathways. *J Cell Biol* **126:** 5-9.

Herlaar E, Brown Z. **1999.** p38 MAPK signalling cascades in inflammatory disease. *Mol Med Today* **5:** 439-447.

Hoffmann A, Levchenko A, Scott ML, Baltimore D. **2002.** The IkappaB-NF-kappaB signaling module: temporal control and selective gene activation. *Science* **298:** 1241-1245.

Homma T, Kato A, Hashimoto N, Batchelor J, Yoshikawa M, Imai S, Wakiguchi H, Saito H, Matsumoto K. **2004.** Corticosteroid and cytokines synergistically enhance toll-like receptor 2 expression in respiratory epithelial cells. *Am J Respir Cell Mol Biol* **31:** 463-469.

Hong-Geller E, Chaudhary A, Lauer S. **2008.** Targeting toll-like receptor signaling pathways for design of novel immune therapeutics. *Curr Drug Discov Technol* **5:** 29-38.

Ikeda U, Matsui K, Murakami Y, Shimada K. **2002.** Monocyte chemoattractant protein-1 and coronary artery disease. *Clin Cardiol* **25:** 143-147.

Ishizuka T, Sawada S, Sugama K, Kurita A. **2000.** Thromboxane A2 (TXA2) receptor blockade suppresses monocyte chemoattractant protein-1 (MCP-1) expression by stimulated vascular endothelial cells. *Clin Exp Immunol* **120:** 71-78.

Izadi H, Motameni AT, Bates TC, Olivera ER, Villar-Suarez V, Joshi I, Garg R, Osborne BA, Davis RJ, Rincon M, Anguita J. **2007.** c-Jun N-terminal kinase 1 is required for Toll-like receptor 1 gene expression in macrophages. *Infect Immun* **75:** 5027-5034.

Jaffe EA, Nachman RL, Becker CG, Minick CR. **1973.** Culture of human endothelial cells derived from umbilical veins. Identification by morphologic and immunologic criteria. *J Clin Invest* **52:** 2745-2756.

Jenkins KA, Mansell A. **2010.** TIR-containing adaptors in Toll-like receptor signalling. *Cytokine* **49:** 237-244.

Jiang Y, Chen C, Li Z, Guo W, Gegner JA, Lin S, Han J. **1996.** Characterization of the structure and function of a new mitogen-activated protein kinase (p38beta). *J Biol Chem* **271:** 17920-17926.

Jiang Y, Gram H, Zhao M, New L, Gu J, Feng L, Di PF, Ulevitch RJ, Han J. **1997.** Characterization of the structure and function of the fourth member of p38 group mitogen-activated protein kinases, p38delta. *J Biol Chem* **272:** 30122-30128.

Karin M, Liu Z, Zandi E. **1997.** AP-1 function and regulation. *Curr Opin Cell Biol* **9:** 240-246.

Kawai T, Akira S. **2006.** TLR signaling. *Cell Death Differ* **13:** 816-825.

Khabar KSA. **2005.** The AU-rich transcriptome: More than interferons and cytokines, and its role in disease. *J Interferon Cytokine Res* **25:** 1-10.

Kiemer AK, Bildner N, Weber NC, Vollmar AM. **2003.** Characterization of heme oxygenase 1 (heat shock protein 32) induction by atrial natriuretic peptide in human endothelial cells. *Endocrinology* **144:** 802-812.

Kiemer AK, Lehner MD, Hartung T, Vollmar AM. **2002a.** Inhibition of cyclooxygenase-2 by natriuretic peptides. *Endocrinology* **143:** 846-852.

Kiemer AK, Weber NC, Fürst R, Bildner N, Kulhanek-Heinze S, Vollmar AM. **2002b.** Inhibition of p38 MAPK activation via induction of MKP-1: atrial natriuretic peptide reduces TNF-alpha-induced actin polymerization and endothelial permeability. *Circ Res* **90:** 874-881.

Kiemer AK, Weber NC, Vollmar, AM. 2002c. Induction of IkappaB: atrial natriuretic peptide as a regulator of the NF-kappaB pathway. *Biochem Biophys Res Commun* **295:** 1068-1076.

Kim C, Sano Y, Todorova K, Carlson BA, Arpa L, Celada A, Lawrence T, Otsu K, Brissette JL, Arthur JS, Park JM. **2008.** The kinase p38 alpha serves cell type-specific inflammatory functions in skin injury and coordinates pro- and anti-inflammatory gene expression. *Nat Immunol* **9:** 1019-1027.

King EM, Holden NS, Gong W, Rider CF, Newton R. **2009.** Inhibition of NF-kappaB-dependent transcription by MKP-1: transcriptional repression by glucocorticoids occurring via p38 MAPK. *J Biol Chem* **284:** 26803-26815.

Klingenberg R, Hansson GK. **2009.** Treating inflammation in atherosclerotic cardiovascular disease: emerging therapies. *Eur Heart J* **30:** 2838-2844.

Ko HY, Lee DS, Kim S. **2009.** Noninvasive imaging of microRNA124a-mediated repression of the chromosome 14 ORF 24 gene during neurogenesis. *FEBS J* **276:** 4854-4865.

Kracht M, Saklatvala J. **2002.** Transcriptional and post-transcriptional control of gene expression in inflammation. *Cytokine* **20:** 91-106.

Kumar S, Boehm J, Lee JC. **2003.** p38 MAP kinases: key signalling molecules as therapeutic targets for inflammatory diseases. *Nat Rev Drug Discov* **2:** 717-726.

Kumar S, McDonnell PC, Gum RJ, Hand AT, Lee JC, Young PR. **1997.** Novel homologues of CSBP/p38 MAP kinase: activation, substrate specificity and sensitivity to inhibition by pyridinyl imidazoles. *Biochem Biophys Res Commun* **235:** 533-538.

Ladetzki-Baehs K, Keller M, Kiemer AK, Koch E, Zahler S, Wendel A, Vollmar AM. **2007.** Atrial natriuretic peptide, a regulator of nuclear factor-kappaB activation in vivo. *Endocrinology* **148:** 332-336.

Laemmli UK. **1970.** Cleavage of structural proteins during the assembly of the head of bacteriophage T4. *Nature* **227:** 680-685.

Landschulz WH, Johnson PF, McKnight SL. **1988.** The leucine zipper: a hypothetical structure common to a new class of DNA binding proteins. *Science* **240:** 1759-1764.

Latz E, Visintin A, Lien E, Fitzgerald KA, Monks BG, Kurt-Jones EA, Golenbock DT, Espevik T. **2002.** Lipopolysaccharide rapidly traffics to and from the Golgi apparatus with the toll-like receptor 4-MD-2-CD14 complex in a process that is distinct from the initiation of signal transduction. *J Biol Chem* **277:** 47834-47843.

Lee JC, Kassis S, Kumar S, Badger A, Adams JL. **1999.** p38 mitogen-activated protein kinase inhibitors--mechanisms and therapeutic potentials. *Pharmacol Ther* **82:** 389-397.

Lee JC, Laydon JT, McDonnell PC, Gallagher TF, Kumar S, Green D, McNulty D, Blumenthal MJ, Heys JR, Landvatter SW, **. **1994. A protein kinase involved in the regulation of inflammatory cytokine biosynthesis. *Nature* **372:** 739-746.

Lemaitre B, Nicolas E, Michaut L, Reichhart JM, Hoffmann JA. **1996.** The dorsoventral regulatory gene cassette spatzle/Toll/cactus controls the potent antifungal response in Drosophila adults. *Cell* **86:** 973-983.

Li Z, Jiang Y, Ulevitch RJ, Han J. **1996.** The primary structure of p38 gamma: a new member of p38 group of MAP kinases. *Biochem Biophys Res Commun* **228:** 334-340.

Liu X, Ukai T, Yumoto H, Davey M, Goswami S, Gibson FC 3rd, Genco CA. **2008.** Toll-like receptor 2 plays a critical role in the progression of atherosclerosis that is independent of dietary lipids. *Atherosclerosis* **196:** 146-154.

Lu ZY, Jensen LE, Huang Y, Kealey C, Blair IA, Whitehead AS. **2009.** The up-regulation of monocyte chemoattractant protein-1 (MCP-1) in Ea.hy 926 endothelial cells under long-term low folate stress is mediated by the p38 MAPK pathway. *Atherosclerosis* **205:** 48-54.

Lundberg AM, Hansson GK. **2010.** Innate immune signals in atherosclerosis. *Clin Immunol* **134:** 5-24.

Lusis AJ. **2000.** Atherosclerosis. *Nature* **407:** 233-241.

Ma W, Lim W, Gee K, Aucoin S, Nandan D, Kozlowski M, Diaz-Mitoma F, Kumar A. **2001.** The p38 mitogen-activated kinase pathway regulates the human interleukin-10 promoter via the activation of Sp1 transcription factor in lipopolysaccharide-stimulated human macrophages. *J Biol Chem* **276:** 13664-13674.

Madan M, Amar S. **2008.** Toll-like receptor-2 mediates diet and/or pathogen associated atherosclerosis: Proteomic Findings. *PLoS ONE* **3:** e3204. http://www.plosone.org/article/info%3Adoi%2F10.1371%2Fjournal.pone.0003204. Accessed September 12, 2008.

Matsuguchi T, Musikacharoen T, Ogawa T, Yoshikai Y. **2000.** Gene expressions of Toll-like receptor 2, but not Toll-like receptor 4, is induced by LPS and inflammatory cytokines in mouse macrophages. *J Immunol* **165:** 5767-5772.

Medvedev AE, Kopydlowski KM, Vogel SN. **2000.** Inhibition of lipopolysaccharide-induced signal transduction in endotoxin-tolerized mouse macrophages: dysregulation of cytokine, chemokine, and toll-like receptor 2 and 4 gene expression. *J Immunol* **164:** 5564-5574.

Medzhitov R, Preston-Hurlburt P, Janeway CA, Jr. 1997. A human homologue of the Drosophila Toll protein signals activation of adaptive immunity. *Nature* **388:** 394-397.

Michelsen KS, Arditi M. **2006.** Toll-like receptor signaling and atherosclerosis. *Curr Opin Hematol* **13:** 163-168.

Michelsen KS, Wong MH, Shah PK, Zhang W, Yano J, Doherty TM, Akira S, Rajavashisth TB, Arditi M. **2004.** Lack of Toll-like receptor 4 or myeloid differentiation factor 88 reduces atherosclerosis and alters plaque phenotype in mice deficient in apolipoprotein E. *Proc Natl Acad Sci U S A* **101:** 10679-10684.

Mikami F, Lim JH, Ishinaga H, Ha UH, Gu H, Koga T, Jono H, Kai H, Li JD. **2006.** The transforming growth factor-beta-Smad3/4 signaling pathway acts as a positive regulator for TLR2 induction by bacteria via a dual mechanism involving functional cooperation with NF-kappaB and MAPK phosphatase 1-dependent negative cross-talk with p38 MAPK. *J Biol Chem* **281:** 22397-22408.

Mitchell JA, Paul-Clark MJ, Clarke GW, McMaster SK, Cartwright N. **2007.** Critical role of toll-like receptors and nucleotide oligomerisation domain in the regulation of health and disease. *J Endocrinol* **193:** 323-330.

Mittelstadt PR, Ashwell JD. **2001.** Inhibition of AP-1 by the glucocorticoid-inducible protein GILZ. *J Biol Chem* **276:** 29603-29610.

Mullick AE, Tobias PS, Curtiss LK. **2005.** Modulation of atherosclerosis in mice by Toll-like receptor 2. *J Clin Invest* **115:** 3149-3156.

Musikacharoen T, Matsuguchi T, Kikuchi T, Yoshikai Y. **2001.** NF-kappa B and STAT5 play important roles in the regulation of mouse Toll-like receptor 2 gene expression. *J Immunol* **166:** 4516-4524.

Niu J, Kolattukudy PE. **2009.** Role of MCP-1 in cardiovascular disease: molecular mechanisms and clinical implications. *Clin Sci* **117:** 95-109.

Pajonk F, McBride WH. **2001.** The proteasome in cancer biology and treatment. *Radiat Res* **156:** 447-459.

Pearson G, Robinson F, Beers GT, Xu BE, Karandikar M, Berman K, Cobb MH. **2001.** Mitogen-activated protein (MAP) kinase pathways: regulation and physiological functions. *Endocr Rev* **22:** 153-183.

Perkins ND. **2007.** Integrating cell-signalling pathways with NF-kappaB and IKK function. *Nat Rev Mol Cell Biol* **8:** 49-62.

Popa C, Netea MG, van Riel PL, van der Meer JW, Stalenhoef AF. **2007.** The role of TNF-alpha in chronic inflammatory conditions, intermediary metabolism, and cardiovascular risk. *J Lipid Res* **48:** 751-762.

Pramanik R, Qi X, Borowicz S, Choubey D, Schultz RM, Han J, Chen G. **2003.** p38 isoforms have opposite effects on AP-1-dependent transcription through regulation of c-Jun. The determinant roles of the isoforms in the p38 MAPK signal specificity. *J Biol Chem* **278:** 4831-4839.

Puck TT. **1958.** Quantitative colonial growth of single mammalian cells. *Ann N Y Acad Sci* **71:** 1141-1142.

Pugin J, Ulevitch RJ, Tobias PS. **1995.** Tumor necrosis factor-alpha and interleukin-1 beta mediate human endothelial cell activation in blood at low endotoxin concentrations. *J Inflamm* **45:** 49-55.

Qin W, Shi Y, Zhao B, Yao C, Jin L, Ma J, Jin Y. **2010.** miR-24 regulates apoptosis by targeting the open reading frame (ORF) region of FAF1 in cancer cells. *PLoS ONE* **5:** e9429. http://www.plosone.org/article/info%3Adoi%2F10.1371%2Fjournal.pone.0009429. Accessed Feb 25, 2010.

Raingeaud J, Gupta S, Rogers JS, Dickens M, Han J, Ulevitch RJ, Davis RJ. **1995.** Pro-inflammatory cytokines and environmental stress cause p38 mitogen-

activated protein kinase activation by dual phosphorylation on tyrosine and threonine. *J Biol Chem* **270:** 7420-7426.

Regueiro V, Moranta D, Campos MA, Margareto J, Garmendia J, Bengoechea JA. **2009.** Klebsiella pneumoniae increases the levels of Toll-like receptors 2 and 4 in human airway epithelial cells. *Infect Immun* **77:** 714-724.

Remold-O'Donnell E. **1974.** Stimulation and desensitization of macrophage adenylate cyclase by prostaglandins and catecholamines. *J Biol Chem* **249:** 361-21.

Riccardi C, Bruscoli S, Ayroldi E, Agostini M, Migliorati G. **2001.** GILZ, a glucocorticoid hormone induced gene, modulates T lymphocytes activation and death through interaction with NF-kB. *Adv Exp Med Biol* **495:** 31-39.

Robinson EA, Yoshimura T, Leonard EJ, Tanaka S, Griffin PR, Shabanowitz J, Hunt DF, Appella E. **1989.** Complete amino acid sequence of a human monocyte chemoattractant, a putative mediator of cellular immune reactions. *Proc Natl Acad Sci U S A* **86:** 1850-1854.

Rollins BJ, Yoshimura T, Leonard EJ, Pober JS. **1990.** Cytokine-activated human endothelial cells synthesize and secrete a monocyte chemoattractant, MCP-1/JE. *Am J Pathol* **136:** 1229-1233.

Ross R. **1993.** The pathogenesis of atherosclerosis: a perspective for the 1990s. *Nature* **362:** 801-809.

Roux PP, Blenis J. **2004.** ERK and p38 MAPK-activated protein kinases: a family of protein kinases with diverse biological functions. *Microbiol Mol Biol Rev* **68:** 320-344.

Roy H, Bhardwaj S, Yla-Herttuala S. **2009.** Molecular genetics of atherosclerosis. *Hum Genet* **125:** 467-491.

Rozkova D, Horvath R, Bartunkova J, Spisek R. **2006.** Glucocorticoids severely impair differentiation and antigen presenting function of dendritic cells despite upregulation of Toll-like receptors. *Clin Immunol* **120:** 260-271.

Ruffini PA, Morandi P, Cabioglu N, Altundag K, Cristofanilli M. **2007.** Manipulating the chemokine-chemokine receptor network to treat cancer. *Cancer* **109:** 2392-2404.

Ruggeri ZM, Ware J. **1993.** von Willebrand factor. *FASEB J* **7:** 308-316.

Sakai A, Han J, Cato AC, Akira S, Li JD. **2004.** Glucocorticoids synergize with IL-1beta to induce TLR2 expression via MAP Kinase Phosphatase-1-dependent dual Inhibition of MAPK JNK and p38 in epithelial cells. *BMC Mol Biol* **5:** 2.

Satta N, Kruithof EK, Reber G, de Moerloose P. **2008.** Induction of TLR2 expression by inflammatory stimuli is required for endothelial cell responses to lipopeptides. *Mol Immunol* **46:** 145-157.

Schett G, Tohidast-Akrad M, Smolen JS, Schmid BJ, Steiner CW, Bitzan P, Zenz P, Redlich K, Xu Q, Steiner G. **2000.** Activation, differential localization, and regulation of the stress-activated protein kinases, extracellular signal-regulated kinase, c-JUN N-terminal kinase, and p38 mitogen-activated protein kinase, in synovial tissue and cells in rheumatoid arthritis. *Arthritis Rheum* **43:** 2501-2512.

Schoneveld AH, Oude Nijhuis MM, van Middelaar B, Laman JD, de Kleijn DP, Pasterkamp G. **2005.** Toll-like receptor 2 stimulation induces intimal hyperplasia and atherosclerotic lesion development. *Cardiovasc Res* **66:** 162-169.

Seliger HH, McElroy WD. **1964.** The colors of firefly bioluminescence: Enzyme configuration and species specifity. *Proc Natl Acad Sci U S A* **52:** 75-81.

Shaw G, Kamen R. **1986.** A conserved AU sequence from the 3' untranslated region of GM-CSF mRNA mediates selective mRNA degradation. *Cell* **46:** 659-667.

Shuang C, Wong MH, Schulte DJ, Arditi M, Michelsen KS. **2007.** Differential expression of Toll-like receptor 2 (TLR2) and responses to TLR2 ligands between human and murine vascular endothelial cells. *J Endotoxin Res* **13:** 281-296.

Shuto T, Imasato A, Jono H, Sakai A, Xu H, Watanabe T, Rixter DD, Kai H, Andalibi A, Linthicum F, Guan YL, Han J, Cato AC, Lim DJ, Akira S, Li JD. **2002.** Glucocorticoids synergistically enhance nontypeable Haemophilus influenzae-

induced Toll-like receptor 2 expression via a negative cross-talk with p38 MAP kinase. *J Biol Chem* **277:** 17263-17270.

Shuto T, Xu H, Wang B, Han J, Kai H, Gu XX, Murphy TF, Lim DJ, Li JD. **2001.** Activation of NF-kappa B by nontypeable Hemophilus influenzae is mediated by toll-like receptor 2-TAK1-dependent NIK-IKK alpha /beta-I kappa B alpha and MKK3/6-p38 MAP kinase signaling pathways in epithelial cells. *Proc Natl Acad Sci U S A* **98:** 8774-8779.

Sima AV, Stancu CS, Simionescu M. **2009.** Vascular endothelium in atherosclerosis. *Cell Tissue Res* **335:** 191-203.

Skoog T, Dichtl W, Boquist S, Skoglund-Andersson C, Karpe F, Tang R, Bond MG, de Faire U, Nilsson J, Eriksson P, Hamsten A. **2002.** Plasma tumour necrosis factor-alpha and early carotid atherosclerosis in healthy middle-aged men. *Eur Heart J* **23:** 376-383.

Soundararajan R, Wang J, Melters D, Pearce D. **2007.** Differential activities of glucocorticoid-induced leucine zipper protein isoforms. *J Biol Chem* **282:** 36303-36313.

Stein B, Yang MX, Young DB, Janknecht R, Hunter T, Murray BW, Barbosa MS. **1997.** p38-2, a novel mitogen-activated protein kinase with distinct properties. *J Biol Chem* **272:** 19509-19517.

Stewart CR, Stuart LM, Wilkinson K, van Gils JM, Deng J, Halle A, Rayner KJ, Boyer L, Zhong R, Frazier WA, Lacy-Hulbert A, Khoury JE, Golenbock DT, Moore KJ. **2010.** CD36 ligands promote sterile inflammation through assembly of a Toll-like receptor 4 and 6 heterodimer. *Nat Immunol* **11:** 155-161.

Sutcliffe AM, Clarke DL, Bradbury DA, Corbett LM, Patel JA, Knox AJ. **2009.** Transcriptional regulation of monocyte chemotactic protein-1 release by endothelin-1 in human airway smooth muscle cells involves NF-KB and AP-1. *Br J Pharmacol* **157:** 436-450.

Szmitko PE, Wang CH, Weisel RD, de Almeida JR, Anderson TJ, Verma S. **2003.** New markers of inflammation and endothelial cell activation: Part I. *Circulation* **108:** 1917-1923.

Takada Y, Aggarwal BB. **2004.** TNF activates Syk protein tyrosine kinase leading to TNF-induced MAPK activation, NF-kappaB activation, and apoptosis. *J Immunol* **173:** 1066-1077.

Takeuchi O, Sato S, Horiuchi T, Hoshino K, Takeda K, Dong Z, Modlin RL, Akira S. **2002.** Cutting edge: role of Toll-like receptor 1 in mediating immune response to microbial lipoproteins. *J Immunol* **169:** 10-14.

Tamandl D, Bahrami M, Wessner B, Weigel G, Ploder M, Furst W, Roth E, Boltz-Nitulescu G, Spittler A. **2003.** Modulation of toll-like receptor 4 expression on human monocytes by tumor necrosis factor and interleukin-6: tumor necrosis factor evokes lipopolysaccharide hyporesponsiveness, whereas interleukin-6 enhances lipopolysaccharide activity. *Shock* **20:** 224-229.

Tobias PS, Curtiss LK. **2008.** TLR2 in murine atherosclerosis. *Semin Immunopathol* **30:** 23-27.

Tomita N, Ogihara T, Morishita R. **2003.** Transcription factors as molecular targets: molecular mechanisms of decoy ODN and their design. *Curr Drug Targets* **4:** 603-608.

Triantafilou M, Gamper FG, Haston RM, Mouratis MA, Morath S, Hartung T, Triantafilou K. **2006.** Membrane sorting of toll-like receptor (TLR)-2/6 and TLR2/1 heterodimers at the cell surface determines heterotypic associations with CD36 and intracellular targeting. *J Biol Chem* **281:** 31002-31011.

Tsukagoshi H, Shimizu Y, Kawata T, Hisada T, Shimizu Y, Iwamae S, Ishizuka T, Iizuka K, Dobashi K, Mori M. **2001.** Atrial natriuretic peptide inhibits tumor necrosis factor-alpha production by interferon-gamma-activated macrophages via suppression of p38 mitogen-activated protein kinase and nuclear factor-kappa B activation. *Regul Pept* **99:** 21-29.

Ueberla K, Lu Y, Chung E, Haseltine WA. **1993.** The NF-kappa B p65 promoter. *J Acquir Immune Defic Syndr* **6:** 227-230.

Venugopal J. **2001.** Cardiac natriuretic peptides--hope or hype? *J Clin Pharm Ther* **26:** 15-31.

Vinson CR, Sigler PB, McKnight SL. **1989.** Scissors-grip model for DNA recognition by a family of leucine zipper proteins. *Science* **246:** 911-916.

Wada Y, Otu H, Wu S, Abid MR, Okada H, Libermann T, Kodama T, Shih SC, Minami T, Aird WC. **2005.** Preconditioning of primary human endothelial cells with inflammatory mediators alters the "set point" of the cell. *FASEB J* **19:** 1914-1916.

Wajant H, Pfizenmaier K, Scheurich P. **2003.** Tumor necrosis factor signaling. *Cell Death Differ* **10:** 45-65.

Wang CH, Tsao YP, Chen HJ, Chen HL, Wang HW, Chen SL. **2000.** Transcriptional repression of p21((Waf1/Cip1/Sdi1)) gene by c-jun through Sp1 site. *Biochem Biophys Res Commun* **270:** 303-310.

Wang T, Lafuse WP, Zwilling BS. **2001.** NFkappaB and Sp1 elements are necessary for maximal transcription of toll-like receptor 2 induced by Mycobacterium avium. *J Immunol* **167:** 6924-6932.

Wang XS, Diener K, Manthey CL, Wang S, Rosenzweig B, Bray J, Delaney J, Cole CN, Chan-Hui PY, Mantlo N, Lichenstein HS, Zukowski M, Yao Z. **1997.** Molecular cloning and characterization of a novel p38 mitogen-activated protein kinase. *J Biol Chem* **272:** 23668-23674.

Weber NC, Blumenthal SB, Hartung T, Vollmar AM, Kiemer AK. **2003.** ANP inhibits TNF-alpha-induced endothelial MCP-1 expression--involvement of p38 MAPK and MKP-1. *J Leukoc Biol* **74:** 932-941.

Young PR, McLaughlin MM, Kumar S, Kassis S, Doyle ML, McNulty D, Gallagher TF, Fisher S, McDonnell PC, Carr SA, Huddleston MJ, Seibel G, Porter TG, Livi GP, Adams JL, Lee JC. **1997.** Pyridinyl imidazole inhibitors of p38

mitogen-activated protein kinase bind in the ATP site. *J Biol Chem* **272:** 12116-12121.

Zhang C. **2008.** MicroRNomics: a newly emerging approach for disease biology. *Physiol Genomics* **33:** 139-147.

Zhang J, Shen B, Lin A. **2007.** Novel strategies for inhibition of the p38 MAPK pathway. *Trends Pharmacol Sci* **28:** 286-295.

Zhang XH, Lu X, Long XB, You XJ, Gao QX, Cui YH, Liu Z. **2009.** Chronic rhinosinusitis with and without nasal polyps is associated with decreased expression of glucocorticoid-induced leucine zipper. *Clin Exp Allergy* **39:** 647-654.

Zheng XL, Matsubara S, Diao C, Hollenberg MD, Wong NC. **2001.** Epidermal growth factor induction of apolipoprotein A-I is mediated by the Ras-MAP kinase cascade and Sp1. *J Biol Chem* **276:** 13822-13829.

Zhou X, Ferraris JD, Dmitrieva NI, Liu Y, Burg MB. **2008.** MKP-1 inhibits high NaCl-induced activation of p38 but does not inhibit the activation of TonEBP/OREBP: opposite roles of p38alpha and p38delta. *Proc Natl Acad Sci U S A* **105:** 5620-5625.

Publications

<u>Poster</u>

Ripoche N, **Längler K**, Diesel B, and Kiemer AK. 2008. Regulation of endothelial Toll-like receptor expression in inflammation. Poster presentation at the Annual Meeting of the Society for Microcirculation and Vascular Biology (GfMVB), Aachen.

<u>Original Publication</u>

Hirschfelder K, Diesel B, Huwer H, and Kiemer AK. 2010. Glucocorticoid-induced leucine zipper (GILZ) as a suppressor of endothelial TLR2 expression. *In preparation.*

Acknoledgements